

UC San Diego

UC San Diego Electronic Theses and Dissertations

Title

The Role of RFamide-Related Peptide 3 in Mammalian Reproduction

Permalink

<https://escholarship.org/uc/item/54k9w39q>

Author

Poling, Matthew C.

Publication Date

2015

Peer reviewed|Thesis/dissertation

UNIVERSITY OF CALIFORNIA, SAN DIEGO

The Role of RFamide-Related Peptide 3 in Mammalian Reproduction

A dissertation submitted in partial satisfaction of the requirements for the degree

Doctor of Philosophy

in

Biomedical Sciences

by

Matthew C. Poling

Committee in charge:

Professor Alexander S. Kauffman, Chair
Professor Djurdjica Coss
Professor Pamela L. Mellon
Professor Lisa Stowers
Professor Nicholas J. G. Webster

2015

Copyright
Matthew C. Poling, 2015
All rights reserved

The Dissertation of Matthew C. Poling is approved, and it is acceptable in quality and form for publication on microfilm and electronically:

Chair

University of California, San Diego

2015

DEDICATION

I dedicate this dissertation to my parents, Jeannette and Tom Poling, who have always praised and been patient with my academic endeavors. This thesis is also dedicated to Betty and Tom Jensen, for Betty initially encouraging me to engage in research as a teenager, and then for Tom convincing me to pursue a Ph.D.

EPIGRAPH

*Nobody said it was easy
No one ever said it would be this hard
Oh, take me back to the start
I was just guessing at numbers and figures
Pulling the puzzles apart
Questions of science, science and progress
Do not speak as loud as my heart*

“The Scientist” by Coldplay

TABLE OF CONTENTS

SIGNATURE PAGE	iii
DEDICATION	iv
EPIGRAPH	v
TABLE OF CONTENTS	vi
TABLE OF ABBREVIATIONS	vii
LIST OF FIGURES	ix
LIST OF TABLES	xi
ACKNOWLEDGMENTS	xii
VITA	xiv
ABSTRACT OF THE DISERTATION	xv
INTRODUCTION	1
CHAPTER 1: RFRP-3 suppresses LH secretion via central and peripheral effects; expression of Gpr147 and Gpr74 in the hypothalamus and pituitary	13
CHAPTER 2: Interactions between the RFRP-3 and kisspeptin systems	44
CHAPTER 3: Regulation of <i>Rfrp</i> expression by sex steroids	68
CHAPTER 4: Changes in <i>Rfrp</i> expression and neuronal activation with metabolic and glucocorticoid-mediated stressors	87
CHAPTER 5: <i>Rfrp</i> expression during postnatal development and the postnatal leptin surge	113
CONCLUSIONS	134
REFERENCES	138

LIST OF ABBREVIATIONS

3V	Third Ventricle
ANOVA	Analysis of variance
AR	Androgen Receptor
ARC	Arcuate Nucleus of the Hypothalamus
AVPV/PeN	Anteroventral-Periventricular Nucleus of the Hypothalamus
BAX	Bcl-2 associated protein X
cDNA	Complementary deoxyribonucleic acid
CORT	Corticosterone
CRH	Corticotrophin-Releasing Hormone
CT	Clock Time
DE	Diestrous
DHT	Dihydrotestosterone
DIG	Digoxigenin
DMN	Dorsal-Medial Nucleus of the Hypothalamus
DNA	Deoxyribonucleic acid
E ₂	Estradiol
ELISA	Enzyme-linked immunosorbent assay
ER α	Estrogen Receptor Alpha
ER β	Estrogen Receptor Beta
F	Female
FD	Food deprived/deprivation
FSH	Follicle-Stimulating Hormone
GDX	Gonadectomy
GDX + E ₂	Gonadectomy and estradiol replacement
GH	Growth Hormone
GnIH	Gonadotropin-Inhibiting Hormone
GnRH	Gonadotropin-Releasing Hormone
Gnrhr	GnRH receptor
Gpr147	G-protein coupled receptor 147
Gpr54 (Kiss1r)	G-protein coupled receptor 54 (Kiss1r)
Gpr74	G-protein coupled receptor 74
GR	Glucocorticoid Receptor
h	Hours
HE	High Expressing
HPG	Hypothalamic-Pituitary-Gonadal
iDTR	Inducible diphtheria toxin receptor
i.p.	Intraperitoneal
ICV	Intracerebralventricular
IHC	Immunohistochemistry
ir	Immunoreactivity
ISH	<i>in-situ</i> Hybridization
Kiss1	Kisspeptin
KNDy	Kisspeptin-Neurokinin B-Dynorphin
KO	Knockout
L	Ladder

LE	Low Expressing
LepRb	Leptin Receptor
LH	Luteinizing Hormone
M	Male
Mc4r	Melanocortin Receptor 4
mRNA	Messenger RNA
NKB (Tac2)	Neurokinin B (Tacykinin 2)
NPY	Neuropeptide Y
Ob	Obese
Oxt	Oxytocin
PCR	Polymerase Chain Reaction
PND	Postnatal Day
POA	Pre-Optic Area
PR	Progesterone Receptor
qPCR	Quantitative Polymerase Chain Reaction
RC	Rfrp-cre
RFamide	Arginine-Phenylalanine-amide
Rfrp	RFamide-related peptide
RFRP-1	RFamide-related Peptide 1
RFRP-3	RFamide-related Peptide 3
RIA	Radioimmunoassay
RNA	Ribonucleic acid
RT	Reverse transcriptase
s.c.	Subcutaneous
SEM	Standard Error of the Mean
SSC	Sodium citrate, sodium chloride
STAT	Signal transducer and activator of transcription
T	Testosterone
Tacr3	Tackinin Receptor 3
tdTom	Tandem-Dimer Tomato Protein
TRH	Thyrotropin-Releasing Hormone
VMN	Ventral-Medial Nucleus of the Hypothalamus
VO	Vaginal Opening
WT	Wildtype

LIST OF FIGURES

Figure 0.1	Cartoon representation of the hypothalamic-pituitary-gonadal axis and steroidal feedback	11
Figure 0.2	Cartoon representation of some of the inputs onto GnRH neurons	12
Figure 1.1	Effect of RFRP-3 on LH secretion in female mice	35
Figure 1.2	Effects of RFRP-3 on Oxytocin and Growth Hormone secretion	36
Figure 1.3	Expression of <i>Rfrp</i> in adult male and female mice by <i>in-situ</i> hybridization	37
Figure 1.4	Characterization of high expressing and low expressing <i>Rfrp</i> cells	38
Figure 1.5	<i>In-situ</i> hybridization for <i>Gpr147</i> and <i>Gpr74</i> in the brain of an adult male mouse	39
Figure 1.6	Low expression of RFamide receptors in GnRH neurons of mice, determined by double label <i>in-situ</i> hybridization	40
Figure 1.7	Expression of <i>Gpr147</i> in oxytocin neurons of female (diestrous) mice	41
Figure 1.8	Expression of <i>Gpr147</i> in corticotropin-releasing hormone neurons of female (diestrous) mice	42
Figure 1.9	Expression of <i>Gpr147</i> and <i>Gpr74</i> in mouse cell lines	43
Figure 2.1	Expression of <i>Gpr147</i> and <i>Gpr74</i> in AVPV/PeN <i>Kiss1</i> neurons	60
Figure 2.2	Expression of <i>Gpr147</i> in ARC <i>Tac2</i> neurons	61
Figure 2.3	Expression of <i>Gpr74</i> in ARC <i>Tac2</i> neurons	62
Figure 2.4	Representative photomicrograph of RFRP-3 immunoreactive fiber in apposition with ARC kisspeptin neuron in a female mouse	63
Figure 2.5	Expression of <i>Kiss1r</i> in <i>Rfrp</i> and GnRH neurons	64
Figure 2.6	Expression of <i>Tacr3</i> in <i>Rfrp</i> neurons	65
Figure 2.7	Immunohistochemistry for kisspeptin fibers and RFRP-3 cell bodies in the DMN	66
Figure 2.8	Expression <i>Tac2</i> in <i>Rfrp</i> neurons in the DMN by double label <i>in-situ</i> hybridization	67
Figure 3.1	Changes in <i>Rfrp</i> expression with E ₂ treatment	80
Figure 3.2	Changes in <i>Rfrp</i> expression with androgen treatment	81
Figure 3.3	Expression of ER α in <i>Rfrp</i> neurons by double label <i>in-situ</i> hybridization	82
Figure 3.4	Expression of AR in <i>Rfrp</i> neurons by double label <i>in-situ</i> hybridization	83

Figure 3.5	Serum LH of gonadectomized and estrogen replaced female and male mice	84
Figure 3.6	<i>In-situ</i> hybridization for <i>Rfrp</i> mRNA in the DMN during the LH surge	85
Figure 3.7	<i>In-situ</i> hybridization for <i>c-Fos</i> co-localization in <i>Rfrp</i> neurons during the time of the LH surge	86
Figure 4.1	Expression of hypothalamic energy balance genes in the dorsal-medial hypothalamus	106
Figure 4.2	<i>Rfrp</i> expression in obese (Ob) male and female gonadectomized mice	107
Figure 4.3	Effects of food deprivation on <i>Rfrp</i> expression and <i>Rfrp</i> neuron activation in gonadectomized (GDX) female mice	108
Figure 4.4	Effects of food deprivation on <i>Rfrp</i> expression and <i>Rfrp</i> neuron activation in intact male mice	109
Figure 4.5	Effects of immobilization restraint on <i>Rfrp</i> expression and <i>Rfrp</i> neuron activation in intact male mice	110
Figure 4.6	Effects of corticosterone injections on <i>Rfrp</i> expression and <i>Rfrp</i> neuron activation in intact male mice	111
Figure 4.7	Effects of corticosterone implants on <i>Rfrp</i> expression and neuron activation during the LH surge	112
Figure 5.1	Changes in <i>Rfrp</i> expression in male and female mice over postnatal development	127
Figure 5.2	Maturation of <i>Rfrp</i> neurons in BAX knockout mice	128
Figure 5.3	<i>Rfrp</i> expression over the first 16 days of postnatal life	129
Figure 5.4	Summary of changes in <i>Rfrp</i> expression over the first 16 days of postnatal life in female mice from single label <i>in-situ</i> hybridization	130
Figure 5.5	Long-form leptin receptor (LepRb) expression in some <i>Rfrp</i> neurons during postnatal life	131
Figure 5.6	<i>Rfrp</i> expression over postnatal life in female Obese (Ob) and wildtype (WT) littermates	132
Figure 5.7	Summary of changes in <i>Rfrp</i> expression on postnatal days (PND) 1, 6, 10, 12, and 16 in female Obese (Ob) and wildtype (WT) animals	133

LIST OF TABLES

Table 1.1	Probes used for <i>in-situ</i> hybridization	34
Table 1.2	Primers used for RT-PCR	34
Table 4.1	Summary of four double label <i>in-situ</i> hybridization assays for metabolic-related genes in the DMN co-expressed with <i>Rfrp</i> neurons	105

ACKNOWLEDGEMENTS

I would like to thank my advisor and mentor, Professor Alexander (Sasha) Kauffman, for his support and guidance throughout my thesis. Additionally, I would like to thank every member of the Kauffman lab, past and present, for his or her support, encouragement and training. Specifically Kristen Tolson, Shannon Stephens, Sheila Semaan, Josh Kim, Elena Lou and Melvin Rouse for their contributions to my projects and the jokes we've shared. I would like to thank the labs of Pamela Mellon, Mark Lawson, Djurdjica Coss, Varykina Thackray, Kellie Breen-Church, and Dave Natale for their contributions during group lab meeting, and allowing me to "borrow" emergency supplies. Furthermore, I would like to thank my thesis committee members, Pamela Mellon, Nicholas Webster, Djurdjica Coss and Lisa Stowers for their guidance and insight through the grad school process.

I would like to thank the UC San Diego Biomedical Sciences program for providing me with an amazing collection of faculty to learn from and fellow students to survive grad school with. Specifically, I'd like to thank Ayla Sessions, Alan West, Cara Bickers, Alex Liberman, Emily Witham, Jim Robinson, Polly Huang, Genevieve Ryan and Erica Pandolfi for emotional support during the grad school process.

My thesis work was jointly funded by National Institute of Health grants R01 HD065856, U54-HD012303, P30 DK063491, and National Science Foundation Grant IOS-1025893.

Portions of Chapters 1 and 3 have been published in *Endocrinology* (April 2012). The dissertation author was the primary investigator and author of this material. Josh Kim and Sangeeta Dhamija provided support with brain cyrosectioning and performing ISH. Alexander Kauffman supervised the project and provided advice.

Chapter 2 has been published in *Journal of Neuroendocrinology* (October 2013). The dissertation author was the primary investigator and author of this material. Janette Quennell and Greg Anderson provided the immunohistochemistry data and images. Alexander Kauffman supervised the project and provided advice.

Portions of Chapter 1, 4 and 5 have been published in *Neuroendocrinology* (November 2014). The dissertation author was the primary investigator and author of this material. Morris Sheih, Nagambika Munaganuru, and Elena Luo were undergraduates in the lab who assisted in cyrosectioning and performing ISH assays. Alexander Kauffman supervised the project and provided advice.

Portions of Chapters 3 and 4 are in preparation for publication. The dissertation author was the primary investigator and author of this material. Elena Luo assisted in animal preparation, tissue collection, cyrosectioning and performing ISH assays. Kellie Breen-Church and Alexander Kauffman supervised the project and provided advice.

VITA

2010 Bachelor of Sciences, University of California, San Diego

2015 Doctor of Philosophy, University of California, San Diego

PUBLICATIONS

Marcondes MCG, **Poling M**, Watry DD, Hall D, Fox HS. (2008). *In vivo* osteopontin-induced macrophage accumulation is dependent on CD44 expression. *Cellular Immunology*. 254: 56-62.

Semaan SJ, Murray EK, **Poling MC**, Dhamija S, Forger NG, and Kauffman AS. (2010). BAX-dependent and -independent regulation of Kiss1 neuron development in mice. *Endocrinology*. 151(12): 5807–5817.

Poling MC, Kauffman AS. (2012). Sexually-dimorphic testosterone secretion in prenatal and neonatal mice is independent of kisspeptin-Kiss1r and GnRH signaling. *Endocrinology*. 153(2): 782-793.

Poling MC, Kim J, Dhamija S, Kauffman AS. (2012). Development, sex steroid regulation, and phenotypic characterization of RFamide-Related Peptide (Rfrp) gene expression and RFamide receptors in the mouse hypothalamus. *Endocrinology*. 153(4): 1827-1840.

Rizwan MZ, **Poling MC**, Corr M, Comes P, Augustine R, Quennell J, Kauffman AS, Anderson GM. (2012). RFamide-related peptide-3 receptor gene expression in GnRH and kisspeptin neurons and GnRH-dependent mechanism of action. *Endocrinology*. 153(8): 3770-3779.

Poling MC, Kauffman AS. (2013). Organizational and activational effects of sex steroids on kisspeptin neuron development. *Frontiers in Neuroendocrinology*. 34(1): 3-17.

Poling MC, Quennell JH, Anderson GM, Kauffman AS. (2013). Kisspeptin neurons do not directly regulate RFRP-3 neurons but RFRP-3 may directly modulate a subset of hypothalamic kisspeptin cells in mice. *J. of Neuroendocrinology*. 25: 276-886.

Poling MC, Shieh MP, Munaganuru N, Luo EL, Kauffman AS. (2014). Examination of the influence of leptin and acute metabolic challenge on RFRP-3 neurons of mice in development and adulthood. *Neuroendocrinology*. 100(4): 317-333.

Russo KA, La JL, Stephens SB, **Poling MC**, Padgaonkar NA, Jennings KJ, Pekarski DJ, Kauffman AS, Kriegsfeld LJ. (2015). Circadian-Controlled Disinhibition of the Reproductive Axis and a Gated RFRP-3 Neuron Response in the Regulation of the Preovulatory Luteinizing Hormone Surge. *Endocrinology*. In press.

Poling MC, Luo EY, Kauffman AS. Sex differences in the activation of kisspeptin and RFRP-3 neurons may underlie the sexually dimorphic nature of the LH surge mechanism in mice. In preparation.

ABSTRACT OF THE DISSERTATION

The Role of RFamide-Related Peptide 3 in Mammalian Reproduction

by

Matthew C. Poling

Doctor of Philosophy in Biomedical Sciences

University of California, San Diego 2015

Professor Alexander S. Kauffman, Chair

Gonadotropin-releasing hormone (GnRH) secretion from the brain regulates reproductive function through its stimulation of the anterior pituitary and the subsequent release of gonadotropins and their stimulation of the gonads. RFamide-related peptide 3 (RFRP-3, gene name *Rfrp*) is known to be a potent suppressor of GnRH and gonadotropin secretion in adult rodents, but the role of this neuropeptide in normal reproductive function and the regulation of this peptide remain unclear. RFRP-3 was discovered as the mammalian ortholog of the avian

gonadotropin-inhibitory hormone; however, the role and importance of RFRP-3 in mammalian reproduction remains equivocal. The work presented herein investigates the role of RFRP-3 in various perturbations of the reproductive axis in mice in an effort to pinpoint where RFRP-3 fits into the greater network of reproductive control. First, general characterization of RFRP-3's effects on various hormones and neuropeptide systems were assayed demonstrating a potent suppression of luteinizing hormone secretion. Interconnections of the RFRP-3 and kisspeptin systems were also examined, and while RFRP-3 may regulate the kisspeptin neuronal network, this connection was found to not be reciprocal. Next, steroidal suppressive regulation of RFRP-3 neurons by estrogens and androgens was quantified, as well as changes in *Rfrp* expression in a model of the preovulatory LH surge. RFRP-3 was also examined in the context of stress, both metabolic and immobilization, which induced changes in the expression and activation of *Rfrp* neurons. Lastly, RFRP-3 neurons were investigated during development where drastic changes in *Rfrp* expression were found to occur. Collectively, these data provide a near exhaustive survey of the role of RFRP-3 in mouse reproduction.

INTRODUCTION

Overview of mammalian reproductive function

The propagation of a sexually reproducing species is fundamentally dependent on the merging of gametes, spermatozoa and oocytes from the male and female, respectively, during fertilization. This newly formed cell, termed a zygote, will begin to divide at an exponential rate, and in mammals will then implant into the uterine wall of its mother. After several weeks of gestation, this new organism will be physically separated from its mother at birth. After birth, infants are quite small compared to adults and require a considerable amount of time to fully mature into the adult state. During these immature stages, the reproductive system of the offspring is quiescent and incapable of producing offspring. It is not until the completion of the transitional developmental stage termed puberty that the individual can then reproduce.

A brain region called the hypothalamus controls the reproductive system and is responsible for initiating puberty. The hypothalamus is a region of the ventral diencephalon that is responsible for monitoring and modulating the workings of many body systems and behaviors, including hunger and thirst, body temperature, stress responses, growth, sleep, circadian rhythms, and reproduction. Feedback loops allow the brain to sense changes in these physiological systems and effect changes to maintain homeostasis. The reproductive is regulated in this way through the hypothalamic-pituitary-gonadal (HPG) axis (Figure 0.1). The HPG axis is a feedback loop in which specific biochemical signals (broadly referred to as hormones) are secreted from the hypothalamus into the hypophyseal portal vein. One of these main hypothalamic hormones, termed gonadotropin-releasing hormone (GnRH), then stimulates the pituitary gland to produce and secrete the gonadotropins, follicle-stimulating hormone (FSH) and luteinizing hormone (LH). These large, multi-subunit hormones are secreted into the general circulatory system where they travel to the gonads, located in the pelvis. The gonads, testes in males and ovaries in females, are specialized organs with a primary function of producing gametes for sexual reproduction, and a

secondary role of producing sex steroids for feedback and secondary sexual characteristics. The testes generate and mature spermatozoa, more commonly referred to as sperm, while the ovaries generate and mature oocytes, more commonly referred to as eggs. LH and FSH act on the gonads, stimulating them to synthesize and secrete sex steroid hormones, such as progesterone, testosterone, and estradiol. These sex steroids are released into the general circulation where they travel to several target tissues including the hypothalamus and pituitary. There they regulate the release of GnRH from the hypothalamus and therefore FSH and LH from the pituitary. The inhibitory action of these sex steroids on GnRH and FSH/LH completes a negative feedback loop and allows the hypothalamus to monitor and modulate the activity of the gonads.

Regulation of GnRH release

What appears to be a clean negative feedback loop in Figure 0.1 is actually exceedingly over-simplified. Our understanding of how the reproductive system is regulated at the neuronal level is incomplete. While GnRH is clearly an essential reproductive hormone secreted from the hypothalamus into hypophyseal portal vasculature, many upstream secretagogues for GnRH release remain poorly understood [reviewed heavily in (1)]. GnRH is secreted from a small population of scattered neurons, termed GnRH neurons, which are found along a continuum extending from the olfactory bulb to the medial preoptic area, and have projections that extend to the medial basal hypothalamus. GnRH neurons originate from the olfactory placode and migrate into the hypothalamus during embryonic development. Disruptions of GnRH neuron migration in humans presents as Kallman syndrome, and genetic mutations associated with this disease have helped scientists understand how GnRH neurons are developmentally regulated (2).

After this migratory phase is complete, the GnRH neurons remain functionally quiescent until the onset of puberty. Puberty is an extended developmental transition process between the infantile and adult reproductive states. Puberty is associated with the primary hallmarks of genital

and gonadal maturation and the development of secondary sexual characteristics. Depending on the species, puberty can take several days to years to reach completion, but common among all species is marked an increase in pulsatile GnRH release from the hypothalamus. During most of the infantile and juvenile phases of development the GnRH system is quiescent. However, based on mechanisms not clearly understood, when an individual reaches a sufficient age, the GnRH neuronal system becomes active, kickstarting the reproductive axis and allowing the pubertal transition to occur. In primates, these increases in GnRH pulses are primarily nocturnal and increase in frequency throughout pubertal development until adult-like levels are reached (3). In rodents, there is a similar increase in LH pulse frequency that is dictated by upstream pulsatile GnRH secretion (4,5). Based on these findings, changes in GnRH pulse frequency are considered the hallmark of puberty onset and the eventual attainment of reproductive competence.

While the secretion of GnRH is responsible for all subsequent reproductive function, GnRH neurons surprisingly lack many of the receptors responsible for sensing changes in the body's physiological status. GnRH neurons lack many sex steroid receptors (estrogen receptors alpha, androgen receptor, progesterone receptor,) receptors for nutritional sensing (leptin receptor, insulin receptors) and adrenal-corticotropic sensors (glucocorticoid receptors). Therefore, a collection of upstream interneurons must sense and transmit information on all these systems to the GnRH neurons to regulate reproductive function (Figure 0.2.) These interneuron populations can be stimulatory, promoting GnRH release, such as the neurons that release kisspeptin (6), α -melanocyte stimulating hormone (7), cocaine and amphetamine related transcript (8), norepinephrine (9) and the neurotransmitter GABA(10). Opposing these stimulatory circuits, inhibitory neuropeptides and transmitters can attenuate GnRH release, such as opioids β -endorphin and dynorphin (7), agouti related peptide (7), neuropeptide Y (7,11,12) and RFRP-3 (13). This long list of factors has been compiled from dozens of independent investigations, and therefore contradictions do exist. For example, in rodents, neuropeptide Y can

be inhibitory in gonadectomized animals but stimulatory when the animals are intact or when sex steroids are replaced (11,12). These various stimulatory and inhibitory systems are reviewed elsewhere (1,14-16).

RFamide peptides

During the 2000's, two new neuropeptides were introduced to the mammalian reproductive landscape. In 2003, kisspeptin and its receptor (Gpr54 or Kiss1r) were found to be essential for reproductive development and function in both mice and humans (17,18). Later in 2006, RFamide-related peptide 3 (RFRP-3) was determined to be the mammalian ortholog of gonadotropin-inhibiting hormone (abbreviated GnIH)*, a peptide characterized in Japanese quail that potently inhibits LH secretion from quail primary pituitary cells (19,20). Both kisspeptin and GnIH are from a family of neuropeptides called "RFamides" (21). The term RFamide refers to the conserved C-terminus of these peptides, which all end in the residues arginine (R) and phenylalanine (F) and with an amidation of the carboxyl group on phenylalanine. This RFamide motif is essential for ligand-receptor specificity and the biological activity of these peptides (22). The RFamide family consists of five genes that are conserved among vertebrate species: *Kiss1*, which codes for kisspeptin; *Rfrp* which codes for RFRP-1 and RFRP-3; *Npff*, which codes for neuropeptide FF and neuropeptide AF; *Prlh*, which codes for prolactin releasing peptide; and *Qrfp* which codes for pyroglutamylated RFamide peptide (21,22).

RFamide peptides signal through G-protein coupled receptors that are located on the surface of target cells. Activation of these receptors triggers a cascade of intracellular signals that modify the activity of the target cells. The RFamide motif that is present at the C-terminal end of

* The term "RFRP-3" and "GnIH" are sometimes used interchangeably to describe the same peptide. However, for clarity in this thesis, the term RFRP-3 will be used exclusively to describe the mammalian peptide, and matches with the official gene abbreviation, *Rfrp*. The term "GnIH" will be used to describe the avian peptide where appropriate.

the peptides helps ensure specificity for each ligand-receptor pair (23-26). In mammals, kisspeptin utilizes G-protein receptor 54 (Gpr54 or Kiss1r;), RFRP-1, RFRP-3, neuropeptide FF and neuropeptide AF utilize G-protein coupled receptor 147 and 74 (Gpr147 and Gpr74) with varying degrees of specificity, discussed below; prolactin-releasing peptide utilizes G-protein receptor 10 and pyroglutamylated RFamide peptide utilizes G-protein receptor 103. All of these receptors, with the exception of Gpr54, are G_i coupled G-protein coupled receptors and halt the catalytic activity of adenylyl cyclase and subsequent signaling (23,27,28). Gpr54, on the other hand, is G_q coupled, which allows for Ca²⁺ mobilization and changes in membrane conductivity (29). These highly related receptors are generally thought to be specific ligand-receptor pairs. However, crosstalk between the receptors and ligands has been demonstrated pharmacologically (26,30-32).

Arguably the most famous of these RFamides in reproduction is kisspeptin, due to its essential function in promoting reproductive development and function. This essential role was first reported in 2003 from the characterization of two consanguineous families with idiopathic hypogonadotropic hypogonadism (17,18). These families each carried recessive, inactivating mutations for KISS1R. Subsequently, various *Kiss1r* and *Kiss1* knockout (KO) mice were generated (18,33-37) and all of these mice lines phenocopied the absent puberty and hypogonadotropic hypogonadism. Patients with hypogonadotropic hypogonadism present with extremely low serum gonadotropins, nearly undetectable sex steroids, underdeveloped gonads, a failure of sexual development, and infertility. Moreover, female transgenic mice in which all of the *Kiss1* neurons have been ablated in adulthood via Cre-lox technology have impaired estrous cyclicity and are infertile, further supporting the importance of kisspeptin signaling in reproduction (38). Further experimentation in rodents, and subsequently, other species including humans, demonstrated that exogenous kisspeptin is able to induce a robust secretion of LH and FSH (34,39-42) and that this kisspeptin-induced stimulation of gonadotropins involves a GnRH-

dependent mechanism (6,43). Furthermore kisspeptin activates GnRH neurons, as determined by c-Fos induction in GnRH cells (a marker of neuronal activation) (39,43), increased firing of GnRH neurons in brain explants (44,45), and increased GnRH release *in situ* (34,46). These effects of kisspeptin on GnRH neurons are thought to be direct, as kisspeptin neuronal fibers have been shown to appose GnRH neuron somatas and/or axons (47-49) and the majority of GnRH neurons highly express *Kiss1r* (34,43,44). Moreover, ablation of *Kiss1r* from GnRH neurons alone reproduces the global reproductive phenotype (50). Despite this, some data suggests that kisspeptin may also act at the level of the pituitary, though this issue still remains controversial (51-54).

RFRP-3's role in reproductive and non-reproductive systems

RFRP-3 was first introduced to mammalian physiologists from studies in birds, where it is referred to as GnIH. In birds, GnIH is found in the paraventricular nucleus (19) and directly inhibits the release and expression of gonadotropins from the pituitary (55). Additionally, GnIH can inhibit GnRH-stimulated LH secretion in sparrows, presumably at the level of the pituitary where GnIH's receptor is expressed (56). However, GnIH immunoreactive fibers are found to appose avian GnRH neurons and the GnIH receptor is expressed avian GnRH neurons, supporting a direct action of GnIH on GnRH neurons in birds (57). The GnIH receptor in birds is also G-protein-coupled receptor and is orthogonal to the Gpr147 found in mammals and is expressed in the pituitary and several regions of the hypothalamus (58). At the peripheral level, GnIH treatment in birds decreases plasma testosterone concentration, induces testicular apoptosis, and decreases spermatogenic activity in adult male quail, suggesting either a direct action of GnIH at the testis or an upstream action at the pituitary via reduced gonadotropin secretion (55). In addition, GnIH treatment also reduced the testicular weight in immature birds, suggesting that GnIH may be involved in gonadal development (55). Taken together, GnIH acts as an

inhibitory neuropeptide and exerts multiple effects at all levels of the avian reproductive system, including the brain, pituitary, and gonads.

In rodents, GnIH is commonly referred to as RFRP-3 and was first characterized in mammals in as an inhibitory reproductive peptide in 2006 (20). However, two groups identified RFRP-3 in rodents in 2000 (59,60) prior to its association with avian GnIH. In all studies, *Rfrp* mRNA is expressed exclusively in the dorsal-medial nucleus of the hypothalamus (DMN) (59,60). This was confirmed via immunohistochemistry with antibodies against RFRP-3 (61) or an avian GnIH antibody (20). RFRP-3 immunoreactive fibers project to a variety of brain regions, including the preoptic area, median eminence, lateral hypothalamic area, paraventricular and arcuate nuclei (20,61-63), and come into apposition with GnRH neurons (20,64,65). While RFRP-3 immunoreactive fibers are observed in all these regions, it is still unknown what cell populations RFRP-3 may be acting on or what effect RFRP-3 may have on the neurons in these regions.

The functional role of RFRP-3 is still poorly understood. It is known that RFRP-3 has high affinity for Gpr147 (59,60). *Gpr147* mRNA is found in a number of brain regions (59,60), including several hypothalamic regions such as the preoptic area, paraventricular and arcuate nuclei (66). RFRP-3 appears to inhibit LH secretion through a central mechanism, as intracerebroventricular injections of RFRP-3 in rats will inhibit LH (64,67,68). Electrophysiology data in mice has shown that both RFRP-3 and avian GnIH treatment are able to inhibit GnRH neuronal firing and antagonize the stimulatory effects of kisspeptin on GnRH neurons (13,69). These data support a model in which RFRP-3 acts centrally to inhibit reproduction by directly or indirectly modulating GnRH secretion. Since it appears that RFRP-3's reproductive activity is restricted to the brain, determining the hypothalamic regions and cell types in which RFRP-3 acts directly to modulate reproductive function is an area of further investigation.

Because GnIH acts on the pituitary in birds, RFRP-3 is often assumed to also inhibit mammalian reproductive function at the pituitary directly, despite the lack of evidence to support this model. RFRP-3 immunoreactive terminals are found in the median eminence, where neuronal processes access the hypophyseal portal vasculature, but only in the internal and not external zones of the median eminence (20,61). Additionally, RFRP-3 neurons do not access the hypophyseal vasculature in rodents (70), and antagonizing Gpr147 in the pituitary is only effective at increasing LH secretion when GnRH signaling is intact (65). Studies have examined RFRP-3 action in pituitary cell lines, but failed to demonstrate the expression of Gpr147 *in vivo* (71).

It should also be noted that RFRP-3 has limited affinity for a second G-protein coupled receptor termed Gpr74 (24,60,72-75). RFRP-3's affinity for Gpr74 is several orders of magnitude less than its affinity for Gpr147, but still pharmacologically relevant. Therefore, it is possible that Gpr74 may account for several aspects of RFRP-3 biochemical activity, leading to uncertainty as to which receptor RFRP-3 is acting through *in vivo*.

In addition to modulating reproduction, RFRP-3 was recently identified as an orexigenic peptide, as it can increase food intake when injected into the brains of mice, rats, sheep, and monkeys (64,76,77). Electrophysiology data has shown that RFRP-3 can inhibit the firing of anorexigenic pro-opiomelanocortin neurons in slice preparation (78). A physiological role for RFRP-3 may be seated in energy balance circuits due to its expression in the DMN, a well-established feeding nucleus [reviewed in (79)]. Indeed, the DMN expresses a variety of energy balance genes, such as neuropeptide Y (80-82), leptin receptor (83) and melanocortin receptors (84), suggesting that neurons in this region, perhaps RFRP-3 neurons, could possibly receive and transmit energetic/metabolic cues. Within the hypothalamus, the DMN receives innervations from the arcuate nucleus (85) and sends projections to the preoptic area, amongst other nuclei (86,87), placing it in the center of both reproductive and energy balance circuits. However, it is unknown

if *Rfrp* neurons express metabolic-related receptors and are responsive to various energy balance signals.

In the last year, two transgenic and knockout animals have been developed to study RFRP-3 biology (88,89). The first is a transgenic rat, termed “EGFP-GnIH,” which labels RFRP-3 neurons with a fluorescent reporter (88). Initial studies examined decreases in RFRP-3, via the reporter, in old rats relative to young, as well as changes in neuronal activity with estrogen treatments. The second animal model developed is a Gpr147 knockout (KO) mouse, which is completely unresponsive to RFRP-3 injections (89). These Gpr147 KO mice do not have impaired fertility, and in fact have more pups per litter. There are only minor differences in LH secretion, that present primarily before puberty in males only. Interestingly, the suppressive effect of food deprivation on LH secretion appears to be dampened in Gpr147 KO mice, as LH levels remain high in the KO animals, but fall in wildtype animals after 12 hours of food deprivation (89). These higher LH levels in the KO animal after 12 hours of food deprivation suggest that Gpr147 is essential acute suppression of LH secretion during food deprivation. Further experimentation with these two animals models, as well as future models, will provide great insight into RFRP-3 biology.

Understanding RFRP-3’s role in adult reproduction, and possible roles in the development of reproductive neural connectivity, is important for our understanding of reproductive neuroendocrinology. There also remains the possibility that RFRP-3 is unnecessary for normal reproductive function but has essential roles in other physiological systems such as food intake, anxiety responses or temperature regulation. Most of the experiments presented are designed under the assumption RFRP-3 is acting to attenuate reproductive function, similar to GnIH’s role in birds. However, this does not limit the implications of the findings, as they will answer important physiological questions regardless of the experimental outcome. Therefore, this dissertation will address several primary research questions: RFRP-3’s interconnection with

known hypothalamic circuits (Chapters 1 and 2), the ability of *Rfrp* neurons to respond to physiological stimuli such as sex steroids, stress and nutritional changes (Chapters 3 and 4), and how *Rfrp* neurons change over development with regards to puberty (Chapter 5).

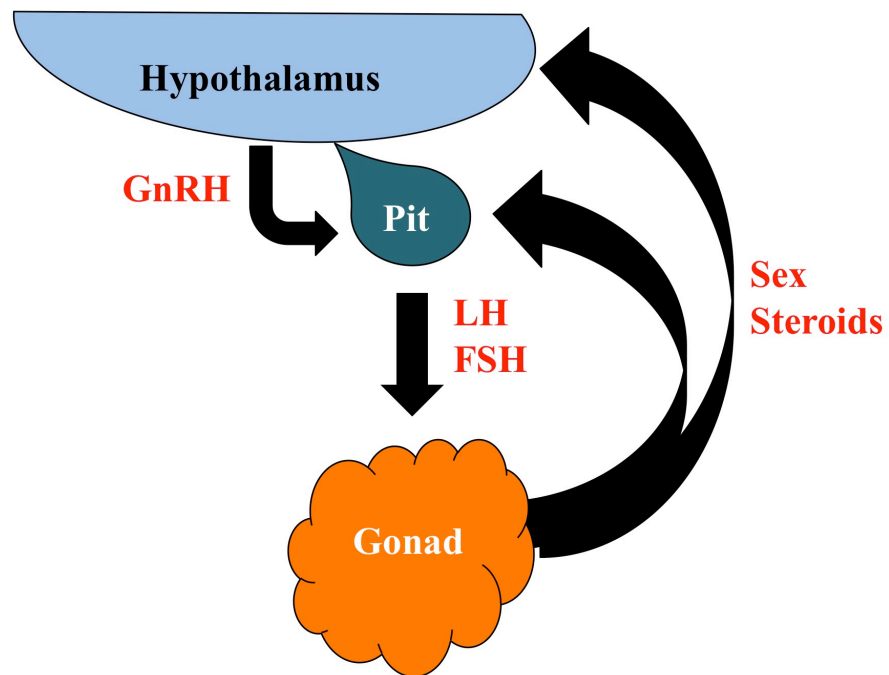


Figure 0.1 Cartoon representation of the hypothalamic-pituitary-gonadal axis and steroidal feedback. GnRH is released from the hypothalamus, which stimulates the pituitary to release gonadotropins, LH and FSH. These in turn stimulate the gonads. Gonadal sex steroids feedback onto the pituitary and hypothalamus and inhibit hormone production.

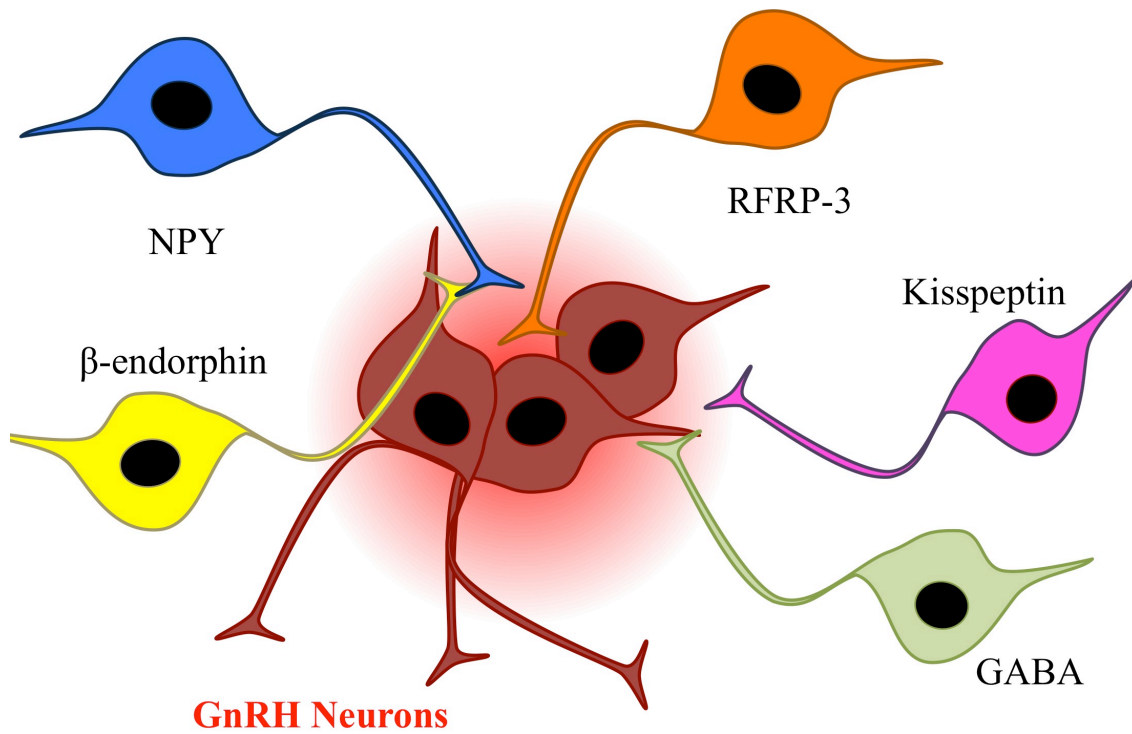


Figure 0.2 Cartoon representation of some of the inputs onto GnRH neurons. Various neuropeptide and neurotransmitter systems innervate and regulate GnRH secretion. RFRP-3, the focus of this thesis, is one of these regulatory peptides.

CHAPTER 1: RFRP-3 suppresses LH secretion via central and peripheral effects; expression of Gpr147 and Gpr74 in the hypothalamus and pituitary

Abstract

To begin assessing RFRP-3's role in mouse reproductive neuroendocrinology, a series of preliminary experiments were required to establish a tool set for this thesis. First, the mouse RFRP-3 peptide, which is similar but has structural differences, was examined for bioactivity in gonadectomized female mice in three routes of examination. RFRP-3 is able to suppress LH secretion when given intraperitoneally and intracerebroventricularly, but not when given subcutaneously. RFRP-3 is also able to stimulate oxytocin secretion, but is unable to stimulate growth hormone. Secondly, an *in-situ* hybridization protocol was developed to examine *Rfrp* mRNA expression in mouse hypothalamic tissue as well as to examine the co-expression of RFRP-3's receptors, *Gpr147* and *Gpr74*, in the mouse hypothalamus. *Rfrp* mRNA is found exclusively in the dorsal medial nucleus, but interestingly, appears to be distributed into two interspersed populations of cells. Looking at RFRP-3 receptors, low co-expression of *Gpr147* but no co-expression of *Gpr74* in GnRH neurons was found in both intact and gonadectomized males and females. Lastly, mouse cell lines were screened for *Gpr147* and *Gpr74* expression. The hypothalamic cell line GT1-7 expresses these receptors, but these receptors are absent pituitary cell line LβT-2. Interestingly, both receptors appear to be absent in the mouse pituitary. Thus, RFRP-3 may exert its effects on reproduction either directly, via Gpr147 in a subset of GnRH neurons, and/or indirectly, via upstream regulators of GnRH.

Introduction

RFamide-related peptide 3 has potent inhibitory actions on both GnRH neuronal activity and LH secretion in rodents (13,69,90). Encoded by the *Rfrp* gene, RFRP-3 is expressed in the dorsal-medial nucleus of the hypothalamus (DMN) (20,59,91,92). In rodents, RFRP-3-ir fibers project to several brain regions, including the paraventricular and arcuate nuclei, lateral hypothalamus, and the preoptic area, where some fibers appose GnRH neurons (20,61-63). Matching the presence of some RFRP-3-ir fibers in non-GnRH areas, RFRP-3 has also been shown to modulate anxiety, oxytocin, growth hormone, nociception, body temperature, and food intake (64,73,76,93-95), suggesting that RFRP-3 may have additional biological functions outside reproduction.

How RFRP-3 communicates with GnRH neurons is not clearly defined and the expression of RFRP-3 receptors specifically in GnRH neurons has not been well characterized in mammals. RFRP-3 binds Gpr147 with high affinity and Gpr74 at lower affinity (24,59,60,72-75), leading to uncertainty regarding which receptor(s) RFRP-3 acts through to inhibit GnRH/LH secretion. In male Siberian hamsters, Gpr147-ir was recently detected in ~80% of GnRH neurons (96), similar to findings in birds (57). In addition to studying GnRH *in-vivo*, GnRH neurobiology can be examined using immortalized cell line GT1-7 cells (97). These cells are a model of GnRH neurons and determining if they express either of RFRP-3's receptors is useful for concluding if they can be used to study RFRP-3 biology. However, whether similar Gpr147 (or Gpr74) co-expression levels exist in mice of either sex or mouse derived tools remains undetermined.

RFRP-3 may also act by directly inhibiting gonadotropin release from the pituitary. This direct inhibitory action of RFRP-3 has proven in birds (19,55) and sheep (98), but a direct action of RFRP-3 on the pituitary of mice remains unclear. In mice, RFRP-3 neurons do not have access to the hypophyseal vasculature (99), and to date, there are no reports of *Gpr147* or *Gpr74*

expression in the mouse pituitary. However, another group has shown effects of RFRP-3 on the pituitary gonadotrope cell line L β T-2 (100), which expressed *Gpr147* in their lab (71).

These series of experiments demonstrate 1) what effect murine RFRP-3 has on LH, oxytocin and growth hormone secretion in mice, 2) where *Rfrp* mRNA is expressed in the mouse, and identifies two sub-populations of *Rfrp*-expressing neurons interspersed within the DMN, and 3) whether GnRH neurons in male and females mice co-express either of the two RFRP-3 receptors, *Gpr147* and *Gpr74*, 4) *Gpr147* is expressed in two cell types in the paraventricular nucleus, 5) and finally *Gpr147* and *Gpr74* are expressed in the hypothalamic cell line GT1-7, but not in primary pituitaries or the L β T-2 pituitary gonadotrope cell line.

Materials and Methods

Animals, Gonadectomies, and Tissue Collection

Adult C57BL6 mice of both sexes were housed on a 12-12 light-dark cycle (lights off at 1800h) with food and water available *ad libitum*. For some experiments, mice were anesthetized and bilaterally gonadectomized (GDX) one week prior to sacrifice, as previously described (101,102). Silastic capsule (internal diameter 1.47 mm, external diameter 1.96 mm) packed with E₂ (4 mm, 1:4 with cholesterol) and placed subcutaneously. For *in-situ* hybridization studies, GDX mice, GDX with estrogen replacement (GDX + E₂) or gonadal-intact mice (females in diestrous, as determined by vaginal smears) were anesthetized with isoflurane and sacrificed by rapid decapitation. Brains were collected, frozen on dry ice, and stored at -80°C. Five coronal series of 20 μ m brain sections were cut on a cryostat, thaw-mounted onto Superfrost-plus slides, and stored at -80°C until use in *in-situ* hybridization. All experiments were conducted in accordance with the NIH Animal Care and Use Guidelines and with approval of the Animal Care and Use Committee of the University of California, San Diego.

Hormone Assays

Blood from adult animals was collected by retro-orbital bleed. Blood from juvenile animals was collected via trunk blood. Serum LH was measured by radioimmunoassay (UVA Ligand Core, range 0.04 – 37.4 ng/mL). Serum oxytocin was measured by an Oxytocin ELISA kit (Enzo Life Sciences, 15.6 – 1000 pg/mL). Serum growth hormone was measured by Growth Hormone Rat ELISA Kit (Life Technologies, 0.6 – 20 ng/mL).

Cloning and preparing in-situ hybridization probes.

All ISH cRNA probes, except for *Gnrh* and *c-Fos* [described previously (103)], were cloned from adult mouse hypothalamic cDNA into pBluscript II SK(-) transcription plasmid (Stratagene, CA), generally between HindIII and KpnI restriction sites, and antisense probes transcribed with T7 polymerase. To accomplish this, a male mouse was sacrificed, and its brain was frozen on dry ice. After freezing, the hypothalamus was dissected using razor blades and RNA was extracted using RNeasy RNA Lipid Extraction Kit (Qiagen). After RNA extraction, cDNA was generated using Omniscript Reverse Transcriptase Kit (Qiagen) with oligo dT primers. Portions of the genes of interest were amplified by PCR, and then amplified again in a nested reaction to add restriction sites. Amplicons with restriction sites were digested with appropriate restriction enzymes, along pBluscript II SK(-) plasmid overnight, and run on a 1% agarose gel, and purified with a Gel Extraction Kit (Qiagen). Digested inserts and plasmid were ligated with T4 ligase (Promega) at 4 °C for 72 hours. After ligation, the plasmids were transformed into *E. coli* (JM109 cells, Promega) and plated on lysogeny broth agar plates with ampicillin (50 mg/mL), X-gal (40 nM/plate), and isopropyl β -D-1-thiogalactopyranoside (40 nM/plate) and incubated overnight at 37 °C. White colonies, indicating positive clones, were selected and cultured overnight at 37 °C in 3 mL lysogeny broth with ampicillin (50 mg/mL) and plasmids were isolated via a High-Speed Mini-prep kit (Qiagen) and sequenced by Eurofins

sequencing services. Once the sequence was confirmed by alignment to the reference gene sequence (Serial Cloner 2.6.1) the clone of interest was cultured in 150 mL of lysogeny broth agar plates with ampicillin (50 mg/mL) overnight at 37 °C and the plasmid was purified with a High-Speed Maxi-prep kit (Qiagen).

20 µg of plasmid containing the template for ISH probes was linearized using the restriction enzyme on the opposite end of the T7 polymerase binding site (500 units/reaction) for 4 hours at 37 °C and purified using a phenol-chloroform-isoamyl alcohol protocol. 1.5 µg of purified, linearized plasmid is used as template for *in-vitro* transcription of the antisense ISH probe. The antisense probe is generated in using T7 polymerase (Thermo Scientific) in the presence of UTP- $\alpha^{33}\text{P}$ or DIG labeling kit (Roche) for 2 hours at 37 °C, DNase treated for 30 minutes at 37 °C and then all enzymes are quenched with 3 mM of ethylenediaminetetraacetic acid. Transcribed probes are purified using Probe Quant G50 micro columns (Amersham GE) and quantified using a scintillation counter.

A list of probes used in this thesis, including size, GenBank Accession number, and primary publication can be found in Table 1.1.

Single and double-label in-situ hybridization

Single-label ISH was performed as previously described (6,104-106). Briefly, slide-mounted sections were fixed in 4% paraformaldehyde, pretreated with acetic anhydride, rinsed in 2X SSC, delipidated in chloroform, dehydrated in ethanols, and air-dried. Radiolabeled (^{33}P) antisense riboprobes (0.04 pmol/ml) were combined with tRNA, heat-denatured, added to hybridization buffer, and applied to each slide (100 µl/slide). Slides were cover-slipped and placed in a 55°C humidity chamber overnight. The slides were then washed in 4X SSC and placed into RNase A treatment for 30 min at 37°C, then in RNase buffer without RNase A at 37°C for 30 min. After washing in 2X SSC at room temperature, slides were washed in 0.1X SSC

at 62°C for 1 hour, dehydrated in ethanols, and air-dried. Slides were then dipped in Kodak NTB emulsion, air-dried, and stored at 4°C for 3-4 days (depending on the assay) before being developed and cover-slipped. No staining was detected with sense probes.

Double-label ISH assays were performed similarly as above for single label ISH. However, after washing in 2X SSC at room temperature, slides were washed in 0.1X SSC at 62°C for 1 hour. Slides were then incubated in 2X SSC with 0.05% Triton X-100 containing 3% sheep serum for 75 min at room temperature and then incubated overnight at room temperature with anti-DIG antibody conjugated to alkaline phosphatase [(Roche) diluted 1:500 in Buffer 1 containing 1% NSS and 0.3% Triton X-100]. The next day, slides were washed with Buffer 1 and incubated with Vector Red alkaline phosphatase substrate (Vector Labs) for 1 h at room temperature. The slides were then air-dried, dipped in Kodak NTB emulsion, stored at 4°C, and developed and cover-slipped 9-11 days later.

ISH slides were analyzed with an automated image processing system (Dr. Don Clifton, University of Washington) by a person unaware of the treatment group of each slide (107). For single-label experiments, the software counted the number of ISH silver grain clusters representing single labels cells as well as the number of silver grains over each cell (which provides a semi-quantitative index of *Rfrp* mRNA expressed per cell) (106,108,109). Cells were considered positive when the number of silver grains in a cluster exceeded that of background by 3-fold. DIG-containing cells (*GnRH*, *Oxt* or *CRH* cells) were identified under fluorescence microscopy and the grain-counting software was used to quantify silver grains (representing *Gpr147*, *Gpr74*, *Gpr54*, mRNA) overlying each cell. Signal-to-background ratios for individual cells were calculated, and a cell was considered double-labeled if its ratio was > 4 for *Gpr147*, *Gpr74*, *Gpr54* in GnRH neurons. A cell was considered double label if signal-to-background ratio > 3 for *Gpr147* in *CRH* or *Oxt* co-expression assays.

Reverse Transcriptase PCR

GT1-7 and L β T-2 cells were generously provided by the Mellon lab. RNA from each cell line was extracted using QIAzol (Qiagen) following the manufacture's protocol. cDNA was generated using Omniscript Reverse Transcriptase (Qiagen) and then gene specific products were amplified using RedTaq (Sigma) and the primers listed in Table 1.2. PCR reactions were performed for 35 cycles. Control hypothalamus and pituitary samples were obtained from two adult male mice, frozen on dry ice immediately after sacrifice and then RNA was extracted using QIAzol as described above. RT-PCR products were run on a 2% agarose gel and visualized using ethidium bromide.

Statistical Analysis

All data are expressed as the mean \pm SEM for each group. In all experiments, differences were analyzed by Student's t-test or by 2-way ANOVA, followed by post-hoc comparisons for individual sex/treatment groups via Fisher's (protected) least significant difference. Statistical significance was set at $p < 0.05$. All analyses were performed in Statview 5.0.1 (SAS Institute, Cary, NC).

Experiment 1: Does RFRP-3 inhibit LH secretion in mice?

The conserved role of RFRP-3 in the inhibition of LH secretion is assumed to be true in mice but, surprisingly, data demonstrating this has not yet been reported. In order to test if the mouse RFRP-3 peptide is functionally able to suppress LH secretion in mice, as occurs with other RFRP-3 variants in other species, adult GDX female mice were injected i.p with either 100 ng or 500 ng of the murine RFRP-3 peptide (VNMEAGTRSHFPSLPQRF-NH₂, Genscript USA Inc.) dissolved in 100 μ L saline, or saline vehicle. 20 minutes after i.p. injection, blood was collected by retro-orbital bleed and the serum was assayed for LH (n = 7-8 per treatment group).

To date, the effect of subcutaneous (sc) injections of RFRP-3 has not been published. Since s.c. injections induce less stress on the mice and is methodically simpler, this route of administration may prove useful for future experiments. To test if RFRP-3 could be administered s.c., GDX female mice were injected with 1 μg or 5 μg of RFRP-3 dissolved in 100 μL of saline, or received a control injection of 100 μL of saline only. The mice were then bled 20 minutes later via retro-orbital bleed and the serum was assayed for LH (n = 5-6 per treatment group).

RFRP-3 can inhibit LH secretion in rats when administered via intracerebroventricular (ICV) injection. Briefly, the mouse is anesthetized and the top of the skull is shaved and sterilized and the location of bregma is determined by feeling for the fusion of the parietal and frontal bones using the tip of a 25^{5/8th}-gauge needle that is sheathed to allow only 3 mm of the tip of the needle to be exposed. This sheath will limit the depth in which the needle can penetrate the brain. Once bregma is found, the needle is moved 1 mm posterior and 2 mm lateral and pushed into the skull at a perpendicular angle. This needle is then removed and replaced with a Hamilton syringe with a 28-gauge needle that is sheathed to allow 3.5 mm of the needle tip to be exposed. This syringe is used to inject the 5 μL of RFRP-3 in saline, or saline vehicle over 1 minute. For the experiment, 5 nmol of RFRP-3 (in 5 μL of saline) was injected into GDX female mice and control GDX animals received 5 μL of saline without dissolved RFRP-3. Animals were bled retro-orbitally 20 minutes after injection and serum was assayed for LH (n = 5-6 per treatment group).

Experiment 2: Does RFRP-3 modulate oxytocin and growth hormone secretion in mice?

Central injections of RFRP-3 have been shown to stimulate oxytocin and growth hormone secretion in rats (64,95), in addition to suppressing LH secretion. However, this result has not been reproduced in mice. In order to test if the mouse RFRP-3 peptide is functionally able to stimulate oxytocin or GH secretion in mice, 50 pmol of the murine RFRP-3 peptide dissolved

in 5 μ L saline, or saline vehicle, was injected into the ventricles using the feed-hand ICV method described above. 25 minutes after ICV injection, blood was collected by retro-orbital bleed and the serum was assayed for oxytocin or growth hormone (n = 7-8 per treatment group).

Experiment 3: Where is RFRP-3 expressed in the hypothalamus?

Other investigators have previously published the expression of *Rfrp* mRNA in the mouse hypothalamus (59,60). However, to further investigate *Rfrp* a new ISH probe was developed to determine the distribution and intensity of *Rfrp* expression and for quantification in subsequent experiments. ³³P-labeled anti-sense probes of the mouse *Rfrp* mRNA were hybridized to hypothalamic section of intact adult male and female (diestrous) mice and exposed these slides to photographic emulsion. After developing the slides, silver grain distribution and intensity were quantified (n = two animals per sex).

Experiment 4: Where are Gpr147 and Gpr74 expressed in the hypothalamus?

The distributions of the RFRP-3 receptors, Gpr147 and Gpr74, have been described loosely in rats (23,59,110) and only a few times in mice using receptor autoradiography (110,111). Detailed characterization of the distribution of either of these receptors via ISH has yet to be reported. Using single label ISH, the distribution of these two receptors in the hypothalamus and adjacent structures of adult intact males and females (diestrous) were examined to determine where *Gpr147* or *Gpr74* mRNAs were highly expressed (n = two animals per sex)

Experiment 5: Assessment of co-expression of RFRP-3 receptors, Gpr147 and Gpr74, in GnRH, neurons

While *Grp147* and *Gpr74* are not highly expressed in the areas where GnRH neurons are found, RFRP-3's inhibition of GnRH neurons is likely mediated through one of the two receptors.

This experiment tested whether either receptor is co-expressed in GnRH neurons. Double-label ISH for *Gpr147* or *Gpr74* mRNA in GnRH neurons was performed on brain tissue from intact males and females (diestrous) (n = 5-7 animals per sex). For comparison, a group of 3 diestrous female mice were examined for co-expression of *Gpr54* (kisspeptin receptor) in GnRH neurons. To determine if RFRP-3 receptor levels in GnRH neurons change depending on the sex steroid milieu, co-expression of *Gpr147* and *Gpr74* in GnRH neurons of GDX males and females was also measured.

Experiment 6: Assessment of co-expression of Gpr147 in neuronal populations of the paraventricular nucleus

Gpr147 mRNA was found to be highest in the paraventricular nucleus (PVN) of the hypothalamus (Experiment 4). Since RFRP-3 has been shown to stimulate oxytocin secretion (Experiment 3) *Gpr147* expression in oxytocin neurons of the mouse PVN was also measured. Double label ISH was performed on intact males and females (diestrous) (n = 4-6 animals per sex).

Data from collaborators suggest the RFRP-3 induces anxiety behavior in mice, possibly by stimulating the hypothalamic-pituitary-adrenal axis, by stimulating corticotropin-releasing hormone (CRH) (G. M. Anderson, personal communication). Therefore, double label ISH was performed to determine if *Gpr147* was expressed in CRH neurons of the mouse PVN. This was performed on intact females (diestrous) as well as GDX + E₂ treated female mice (n = 4-6 animals per sex).

Experiment 7: Gpr147 and Gpr74 expression in mouse cell lines

To determine if *Gpr147* or *Gpr74* are expressed in mouse hypothalamic (GT1-7) or pituitary gonadotrope (LβT-2) cell lines, RNA was extracted from these two cell lines and

independently assayed for *Gpr147* or *Gpr74* expressing by RT-PCR. These PCR products were run on 2% gel and visualized. RNA from non-neuronal 3T3 cells (112) were also screened as a negative control and RNA from a male mouse hypothalamus served as positive control. 16S ribosomal RNA served as a loading control.

Results

Experiment 1: The murine RFRP-3 peptide inhibits LH secretion in adult female mice

To determine if peripherally administered murine RFRP-3 peptide can suppress LH secretion in mice, as occurs with other RFRP-3 variants in other species, 100 ng or 500 ng of RFRP-3 or saline was injected i.p. in adult GDX female mice. Both the 100 ng and 500 ng doses of murine RFRP-3 were able to significantly suppress LH secretion, to nearly 70% of saline-treated control levels (Figure 1.1A, $p < 0.05$). There was no difference in the efficacy of the two doses of murine RFRP-3 on LH suppression.

In addition to peripheral administration via i.p. injection, RFRP-3 was also injected s.c. using a 1 μ g or 5 μ g dose. However, this dose was ineffective at suppressing LH secretion in GDX female mice after 20 minutes (Figure 1.1B). Further experiments using 1 μ g doses and a 40 minute time courses were also ineffective at suppressing LH secretion in GDX female mice (*data not shown*).

Lastly, RFRP-3 was administered centrally via ICV injection. A 5 nmol dose significantly suppressed of LH secretion 20 minutes after injection in GDX female mice (Figure 1.1C, $p < 0.05$). This dose was had similar to efficacy as the i.p. treatment in suppressing LH to nearly 70% of saline-treated control levels.

Experiment 2: Murine RFRP-3 can induce oxytocin secretion but has no effect on growth hormone secretion

A single ICV injection of RFRP-3 (5 nmol or 50 pmol) was administered to intact female mice and after 20 minutes blood was collected and the serum was measured for oxytocin and growth hormone. The 50 pmol dose of RFRP-3 significantly increased oxytocin secretion in female mice (Figure 1.2A, $p < 0.05$) 20 minutes after injection, similar to the results seen in rats (95). However, growth hormone secretion was not modified by RFRP-3 injection after 20 minutes (Figure 1.2B).

Experiment 3: Neuroanatomical expression of Rfrp mRNA in the mouse hypothalamus

An *in-situ* hybridization probe was designed against the published *Rfrp* mRNA sequence. Hybridization of this probe to mouse hypothalamic tissue yielded discrete cells located exclusively in the area immediately adjacent and in dorsal medial nucleus of the hypothalamus. This staining pattern mimics what has been previously shown in mice and rats (20,59). Sexual dimorphisms are common in many reproductive neuropeptides (113), however neither the total number of *Rfrp*-expressing cells, nor the relative amount of *Rfrp* mRNA per cell, nor the total amount of *Rfrp* mRNA in the DMN was significantly different between adult males and females (Figure 1.3).

In analyzing *Rfrp* expression in this experiment, two obvious sub-populations of *Rfrp*-expressing cells interspersed with each other in the DMN: one set of cells expressed extremely high levels of *Rfrp* mRNA and another set expressed much lower *Rfrp* levels (~ 3-fold lower; Fig 1.4A-B). These two *Rfrp* subpopulations, termed high-expressing (HE) and low-expressing (LE) cells, were analyzed separately in adult mice to determine if a sex difference exists in either cell-type. In each sex, there were many more LE cells than HE cells. However, there were no sex

differences in either the number of LE or HE *Rfrp* cells or in the relative mRNA content of either cell type (Figures 1.4C-D). Also, examining the rostral-caudal distribution of LE and HE *Rfrp* neurons in the DMN found no noticeable differences in the anatomical distribution of either *Rfrp* sub-population: both HE and LE *Rfrp* cells are present throughout the DMN, with no preferential localization (*data not shown*).

Experiment 4: Gpr147 and Gpr74 are expressed in the hypothalamus

Single label *in-situ* hybridization for *Gpr147* or *Gpr74* demonstrated that the receptors for RFRP-3 are found in numerous brain regions. Notably, *Gpr147* is expressed in the arcuate, dorsal medial and paraventricular nuclei of the hypothalamus, as well as the superior colliculus, and dorsal septum. The highest expression of *Gpr147* is seen in the dorsal septum and paraventricular nucleus (Figure 1.5A). *Gpr74* expression is distributed throughout a number of brain regions, but high expression was observed suprachiasmatic nucleus of the hypothalamus, nucleus accumbens and the highest expression seen in and thalamic nucleus of reunion (Figure 1.5B). These patterns of staining match with previously published findings (60,110,111).

Experiment 5: Gpr147 is weakly expressed in a subset of GnRH neurons, whereas Gpr74 is not readily co-expressed in GnRH neurons

Gpr147 and/or *Gpr74* likely mediate RFRP-3's inhibitory actions on GnRH neurons, but the expression of either of these receptors in GnRH neurons of mice of either sex has not been demonstrated. Double-label ISH was used to determine that *Gpr147* mRNA is present at low levels in ~ 15% of GnRH neurons (Figure 1.6A,D). There were no significant differences in *Gpr147*/GnRH co-expression between males and females or between hormonal conditions (Figure 1.6D). *Gpr74* was weakly expressed in only ~ 3% of GnRH neurons (Figure 1.6B). There

were no significant differences in *Gpr74*/GnRH co-expression between the sexes or between hormone treatments (Figure 1.6E). In stark contrast to *Gpr147* and *Gpr74*, *Gpr54* (kisspeptin receptor) was highly co-expressed in the majority of GnRH neurons of adult female mice, with \geq 85% of GnRH neurons expressing *Gpr54* (Figure 1.6C,F), consistent with previous reports (39,43).

Experiment 6: Gpr147 is expressed in Oxytocin and CRH neurons

In experiment 2, RFRP-3 was able to stimulate oxytocin secretion in female mice. And *Gpr147* is highly expressed in the PVN suggesting that RFRP-3 may directly signal in oxytocin neurons. To test this, double-label in-situ hybridization for *Gpr147* in *Oxt* neurons in the PVN was performed on adult diestrous female and intact male mice (n = 5 animals per group). Nearly one half of *Oxt* neurons co-expressed *Gpr147* in adult female mice (Fig. 1.7A-D). On average, 44% of *Oxt* neurons expressed *Gpr147* in diestrous females, while *Gpr147* was detected in approximately 40% of *Oxt* neurons in male mice (Fig. 1.7E). This percent co-expression of *Gpr147* in oxytocin neurons was not significantly different between sexes.

Since *Gpr147* is highly expressed in the PVN and experiments from collaborators suggested that RFRP-3 may regulate CRH secretion, it was hypothesized that RFRP-3 may directly signal in CRH neurons. To test this, double-label in-situ hybridization for *Gpr147* in *CRH* neurons in the PVN was performed in adult diestrous female mice, as well as in GDX + E₂ mice (n = 5 animals per group) was performed. Approximately one third of *CRH*-expressing neurons co-expressed *Gpr147* in adult female mice (Fig. 1.8A-D). On average, 31% of *CRH* neurons expressed *Gpr147* in diestrous females, while *Gpr147* was detected in approximately 40% of *CRH* neurons in OVX + E₂ females (Fig. 1.8D). This percent co-expression of *Gpr147* in *CRH* neurons was not significantly different between treatment groups.

Experiment 7: Expression of Gpr147 and Gpr74 in cell lines and primary pituitary

RT-PCR reactions were performed to screen for *Gpr147* and *Gpr74* expression in the GnRH cell line, GT1-7, and the pituitary gonadotrope cell line, L β T-2. A weak *Gpr147* product was visible in both GT1-7 cell samples, while *Gpr74* appears to be more highly expressed in the same samples (Figure 1.9A). Neither receptor was present in 3T3 cells. When examining L β T-2 cells, no products for *Gpr147* or *Gpr74* were successfully amplified, but the GnRH receptor (*Gnrhr*) was successfully amplified from both the cell line and primary pituitaries (Figure 1.9B). Interestingly, *Gpr147* and *Gpr74* could not be amplified from primary pituitary RNA (Figure 1.9B), even though both genes had been assumed in the literature to be expressed in this tissue. As seen with the GT1-7 experiment, *Gpr147* and *Gpr74* could not be amplified from 3T3 cells. Both gene products were successfully amplified from hypothalamic RNA (Figure 1.9B). 16S ribosomal RNA served as a loading control.

Discussion

RFRP-3 has emerged as a potent regulator of GnRH and gonadotropin release, but the function and regulation of *Rfrp* neurons in mice has not been thoroughly examined. This is the first documentation that the murine RFRP-3 peptide can be used in mice, to elicit changes in secretion of multiple hormones and through various routes of administration. As well, this is the first documentation of two subpopulations of *Rfrp*-producing neurons in the DMN with significant differences in their *Rfrp* mRNA levels. It is also demonstrated that unlike some neural populations, these two *Rfrp* subpopulations, as well as the total *Rfrp* population, are not sexually dimorphic. Lastly, this is the first demonstration that *Gpr147* is expressed in small subset of GnRH neurons in mice of both sexes, whereas *Gpr74* is not readily co-expressed in GnRH cells,

suggesting that any direct effects of RFRP-3 on GnRH neurons likely occur via Gpr174 (or another yet-to-be-identified receptor).

Despite the reported effect of the rat variant of RFRP-3 to inhibit LH secretion in many species, including rodents (rats and hamsters), the effect of the murine variant of RFRP-3 on LH has not been reported in any species, including mice themselves. As the RFRP-3 field moves towards transgenic and knockout animals (88,89), mouse models will become increasingly important and affirming our understanding of murine RFRP-3 pharmacology and physiology is essential. The present finding of markedly suppressed LH secretion 20 min after peripheral injection of 2 doses of murine RFRP-3 in adult female mice matches previous results found in rat, hamster, and sheep using the rat RFRP-3 peptide (20,67,70,98,114). Until just recently, RFRP-3 of any variant had surprisingly never been administered to mice. León et al. reported that a truncated rat RFRP-3 peptide given via intracerebroventricular injection modestly decreased serum LH (by ~ 25%) in wildtype GDX female mice (89). That reduction in LH was considerably less than the suppressive effects of peripheral murine RFRP-3 observed in the present study, in which there is a ~ 70% decrease in serum LH after peripheral murine RFRP-3 injections at 2 different doses. Besides potential species differences in RFRP-3 peptide efficacy, the difference in magnitude of effect might be due to dosing or the route of administration, as peripheral RFRP-3 can act directly on both the pituitary and hypothalamus. Interestingly, the 100 ng and 500 ng doses were equally effective in suppressing LH secretion, suggesting that the suppressive effect of RFRP-3 may max out near the 100 ng dose. As in this experiment RFRP-3 was administered peripherally, it cannot be discerned at what level(s) of the HPG axis the lowered LH secretion is attributable to. However, most data in rodents suggests that RFRP-3's effects on LH are induced in the brain, via diminished GnRH signaling, rather than at the pituitary (65). This is in agreement with data presented here that intracerebroventricular injections of RFRP-3 can equally able to suppress LH secretion, suggesting that RFRP-3 can act at the level of the hypothalamus.

Subcutaneous injections of RFRP-3 were ineffective at suppressing LH, although it remains unclear if this is a mechanistic difference in the peptides metabolism or drawback with proper dosing in the subcutaneous route.

Oxytocin secretion was significantly increased after RFRP-3 injection in mice, in agreement with previous reports in rats (95). These findings are supported by the a finding a of noticeable degree of co-expression of *Gpr147* with *Oxt* neurons of the mouse PVN. Oxytocin is an important behavioral and lactational hormone in rodents. Studies from collaborators have concluded that RFRP-3 neurons form a conduit between the site of action of prolactin, another lactation hormone, and the stress axis. As shown here, 30-50% of CRH neurons were found to express RFRP-3 receptor mRNA and be apposed by RFRP-3 fibers (*data not shown*). RFRP-3 neurons were found to respond directly to prolactin, and lactation reduced *Rfrp* mRNA levels in a prolactin-dependent manner (G. Anderson, personal communication). Collectively based on these findings, RFRP-3 may prove to have a role in mediating stress behaviors and/or lactational behavior changes in rodents.

RFRP-3 has previously been shown to increase growth hormone secretion in rats treated with with 3.75 nmol and 7 nmol doses of RFRP-3 (95), but a similar dose of mouse RFRP-3 used here was ineffective in stimulating growth hormone secretion. Possible explanations for this discrepancy could be decreased sensitivity of growth hormone release to RFRP-3, and higher doses of the peptide may be effective at inducing secretion, or that RFRP-3's stimulation of somatotrophs is a rat specific response, as these findings have not been repeated in other species to date.

These studies were the first to show the distribution and neuroanatomical location of *Rfrp* mRNA in mice. Furthermore, previous RFRP-3 studies examined either just one sex or male and females separately (66,115-117) and this is the first study to directly assess possible sex differences in the mammalian RFRP-3 system. Focusing on *Rfrp* gene expression, there are no

major differences in *Rfrp* cell number or mRNA levels between adult males and females. This is in sharp contrast to some other RFamide systems, like kisspeptin, which are robustly sexually dimorphic (104). Although a previous study in hamsters proposed that RFRP-3 neurons are involved in the sexually-dimorphic LH surge in female rodents (63), the absence of *Rfrp* sex differences in this present study suggests that RFRP-3 may not be a key component of the sexually-dimorphic aspect of the positive feedback mechanism (however, see chapter 3).

This is the first study to identify subsets of *Rfrp* cells in the DMN, with the finding of high *Rfrp*-expressing and low *Rfrp*-expressing cells being interspersed in the same area. The presence of these *Rfrp* subpopulations, and their differential development and hormonal regulation, discussed below, was likely missed in previous studies which used either qPCR analysis of homogenized brain tissue or fluorescent immunohistochemistry, which may not be sensitive enough to easily distinguish differences in staining levels between individual RFRP-3 cells. This current finding demonstrates obvious differences in the number, development, and hormonal regulation of HE and LE cells (Chapters 3 and 5), and in some cases, these subpopulation differences are obscured when examining the entire *Rfrp* population as a whole. Importantly, similar HE and LE cells are apparent in published *Rfrp* staining in sheep (though this was not addressed) (118), as well as some other neuropeptides in the DMN, such as TRH (119). Whether the HE and LE *Rfrp* cells have different or overlapping functions remains to be determined.

RFRP-3 has agonist activity for both Gpr74 and Gpr147 (24,60,72-74), and the antagonist RF-9, which stimulates LH secretion, can antagonize either receptor (68,120). It is demonstrated here for the first time that *Gpr147* is significantly co-expressed in GnRH neurons, whereas *Gpr74* is virtually non-existent in GnRH cells. However, the degree of *Gpr147/GnRH* co-expression was low, being detectable in only small subset of GnRH neurons in either sex, regardless of the hormonal milieu. This contrasts with the kisspeptin receptor, which is co-

expressed in the vast majority of GnRH cells. This *Gpr147* data disagree with another report in male Siberian hamsters, in which *Gpr147-ir* was observed in ~ 80% of GnRH neurons (96). However, only ~ 25% of GnRH neurons in mice are inhibited electrical firing by RFRP-3 (13), matching the present co-expression data. Whether the discrepancy in co-expression between this mouse data and the hamster data reflects species or technical differences (*in-situ* hybridization versus immunohistochemistry) is unknown, though preliminary findings from another group have observed similar low co-expression levels in mice (99). If *Gpr147* is indeed only lowly-expressed in mouse GnRH cells, some of RFRP-3 inhibitory actions may be achieved indirectly via other upstream GnRH-regulating pathways.

Cell lines have proved to be powerful models for understanding molecular mechanisms of hormone signaling. GnRH and gonadotrope cell lines have been developed, but their relevance to studying RFRP-3 biology is unclear since expression of RFRP-3's receptors is unknown. RT-PCR revealed that *Gpr147* and *Gpr74* are expressed in GT1-7 cells, a GnRH cell line, but not in L β T-2 cells. With regards to GT1-7 cells, there is conflicting evidence regarding the functional effectiveness of RFRP-3. One set of experiments from our collaborators have shown that RFRP-3 is able to inhibit the stimulatory effects of Forskolin on *c-Fos* induction (C. Glidewell-Kenney, personal communication) while other investigators have had difficulty detecting any effect of RFRP-3 treatment on GT1-7 cells (N. Gojska, personal communication) and have developed new cell lines to test (121). L β T-2 cells appear to lack *Gpr147* and *Gpr74*, in agreement with the present results from primary pituitary, which is an unexpected finding since these receptors are in avian pituitaries. Expression of *Gpr147* and *Gpr74* in the mouse pituitary is assumed, but no report has actually demonstrated this to be true. In fact, the only known report to examine *Gpr147* mRNA in the rodent pituitary (although, in female rats) found it at near undetectable levels (66). *Gpr147* mRNA was detected in L β T-2 used by Son et al. (122) but gene expression in cell lines is known to vary between investigators and treatment. Most recently, a new report has demonstrated

an induction of both *Gpr147* and *Gpr74* in both GT1-7 and L β T-2 after GnRH stimulation (123). Therefore, this might possibly explain why neither gene could be amplified from unstimulated cells in the present study.

In summary, this chapter determined that murine RFRP-3 is able to suppress LH secretion in gonadectomized female mice, both peripherally and centrally. Moreover, *Rfrp* expression in mice is not sexually dimorphic, but there are two subpopulations of *Rfrp*-expressing neurons in the DMN, present in both sexes. Also, many GnRH cells lack RFRP-3 receptors, suggesting that RFRP-3 directly regulates only a subset of GnRH cells (via *Gpr147*) and/or that some of RFRP-3's actions on GnRH neurons are achieved indirectly. And lastly, GnRH cell lines, but not pituitary cell lines, express RFRP-3's receptors, matching what is seen *in-vivo*, and supporting an indirect mechanism for LH suppression.

Portions of this chapter are published in *Endocrinology* (April 2012). The dissertation author was the primary investigator and author of this material. Josh Kim and Sangeeta Dhamija provided support with brain cyrosectioning and performing ISH. Alexander Kauffman supervised the project and provided advice.

Portions of this chapter are published in *Neuroendocrinology* (November 2014). The dissertation author was the primary investigator and author of this material. Morris Sheih, Nagambika Munaganuru, and Elena Luo were undergraduates in the lab who assisted in cyrosectioning and performing ISH. Alexander Kauffman supervised the project and provided advice.

Table 1.1 Probes used for *in-situ* hybridization

Gene Name	Length	Bases	GenBank Accession	Reference
<i>AR</i>	312	2001-2312	NM_013476	(124)
<i>c-Fos</i>	1352	285-1637	NM_022197	(103)
<i>CRH</i>	373	10-382	NM_205769	
<i>ERα</i>	820	1165-1982	NM_007956	(124)
<i>GnRH</i>	370	120-490	NM_008145	(103)
<i>Gpr147</i>	485	246-724	NM_001177511	(124)
<i>Gpr54/Kiss1r</i>	650	2276-2879	NM_053244	(124)
<i>Gpr74</i>	426	62-487	NM_133192	(124)
<i>GR</i>	960	416-1386	NM_008173	
<i>Kiss1</i>	409	76-486	NM_178260	(6)
<i>LepRb</i>	534	3379-3912	NM_146146	(125)
<i>Mc4r</i>	887	589-1442	NM_016977	(126)
<i>NPY</i>	462	7-468	NM_0223456	(126)
<i>Oxt</i>	297	146-443	NM_011025	
<i>Rfrp</i>	488	52-538	NM_021892	(124)
<i>Tac2</i>	265	350-612	NM_009312	(108,127)
<i>Tacr3</i>	398	286-691	NM_021382	(126)
<i>TRH</i>	265	308-572	NM_009426	(119)

Table 1.2 Primers used for RT-PCR

Primer	Primer Sequence (5'-3')
Gpr147 Fwd	ATG TTC ATC CTC AAC CTG GCT GTC
Gpr147 Rev	ATG CGG GCG TAC ATG ACC ACG ATG A
Gpr74 Fwd	CTC TCT CCA GGT GAA CAC TGG
Gpr74 Rev	CAC CAG CCC ACT GAT CTT GC
Gnrhr Fwd	GCC CCT TGC TGT ACA AAG C
Gnrhr Rev	CCG TCT GCT AGG TAG ATC ATC C
16S Fwd	CAC TGC AAA TGA GGA AAT GG
16S Rev	TGA GAT GGA CTG TCG GAT GGC

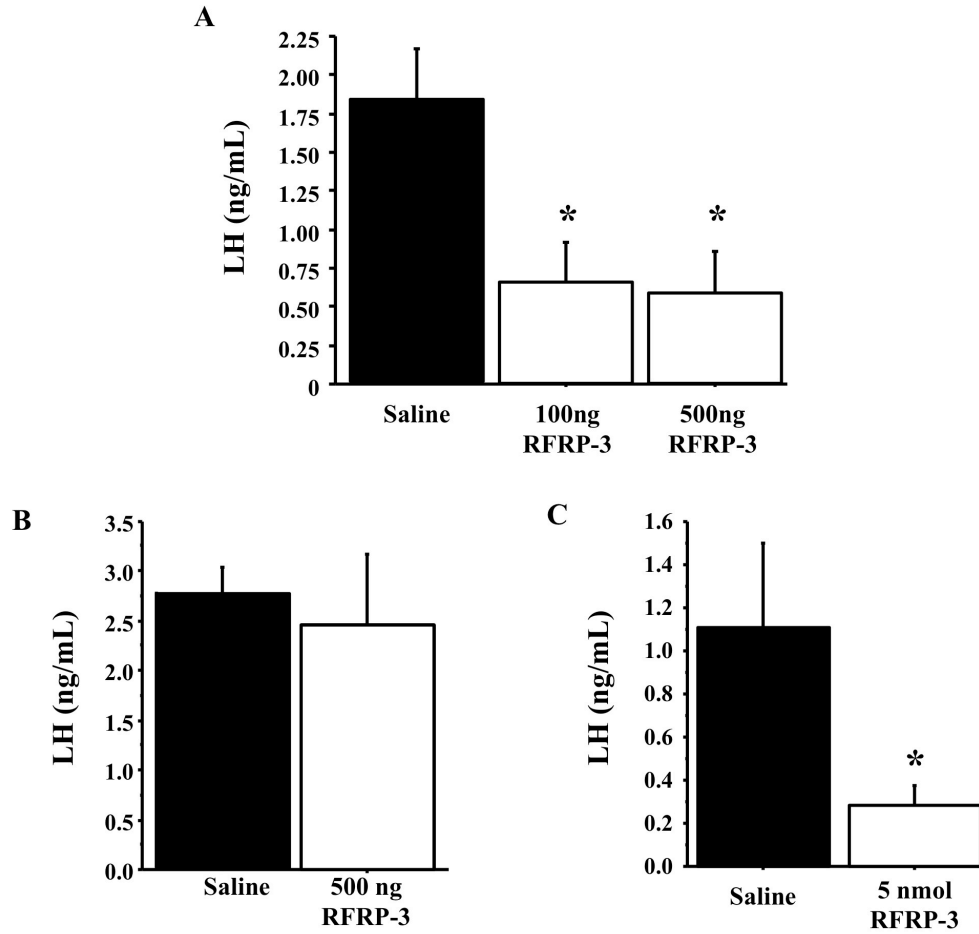


Figure 1.1 Effect of RFRP-3 on LH secretion in female mice. Blood samples were collected 20 minutes after RFRP-3 or saline injection for all three experiments. **[A]** Intraparenteral injections of RFRP-3 (100 ng or 500 ng) or saline into OVX female mice. **[B]** Subcutaneous injections of RFRP-3 (1 μ g or 5 μ g) or saline into OVX female mice. **[C]** Intracerebroventricular injections of RFRP-3 (5 nmol) or saline into OVX female mice.

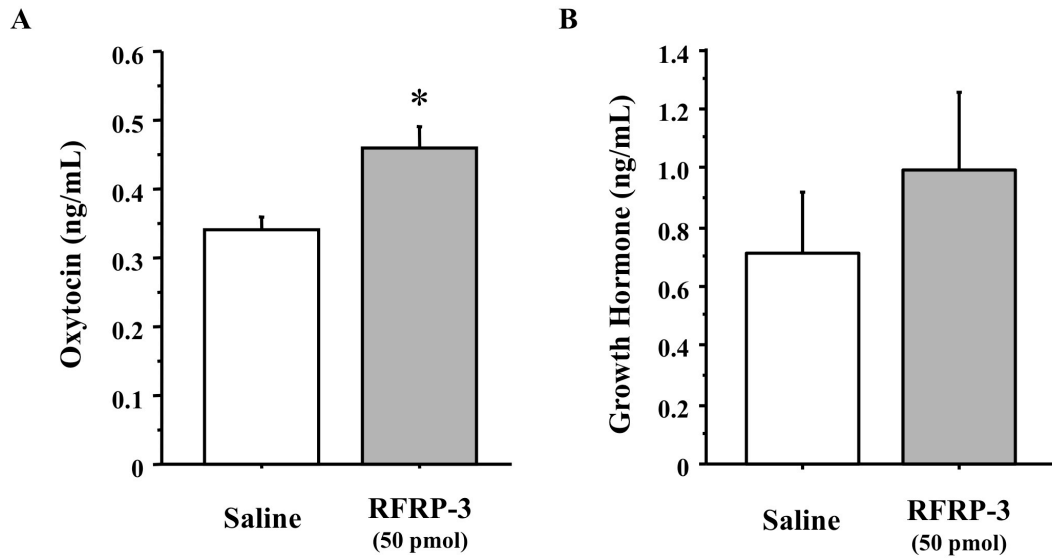


Figure 1.2 Effects of RFRP-3 on Oxytocin and Growth Hormone secretion in female mice. **[A]** Increases in serum oxytocin after intracerebroventricular injection of 50 pmol of RFRP-3 or saline. **[B]** No changes in growth hormone secretion after intracerebroventricular injection of 50 pmol of RFRP-3 or saline.

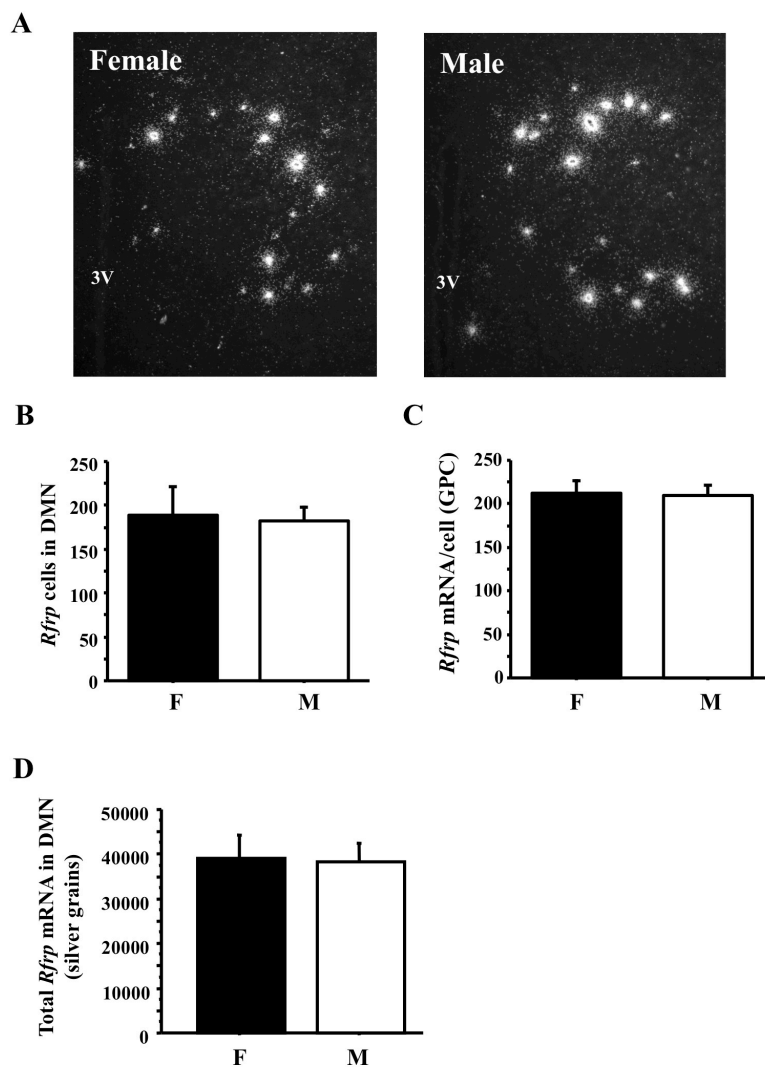


Figure 1.3 Expression of *Rfrp* in adult male and female mice by *in-situ* hybridization. **[A]** Representative low-power photomicrograph of *Rfrp* expression in adult female (diestrous) and male mouse. 3V, third ventricle **[B]** Total number of *Rfrp* cells in the DMN is not significantly different between adult female and male mice. **[C]** Mean *Rfrp* mRNA/cell (determined by silver grains per cell [GPC]) and **[D]** total *Rfrp* mRNA in DMN (total silver grains in the DMN) are not significantly different between adult females and males.

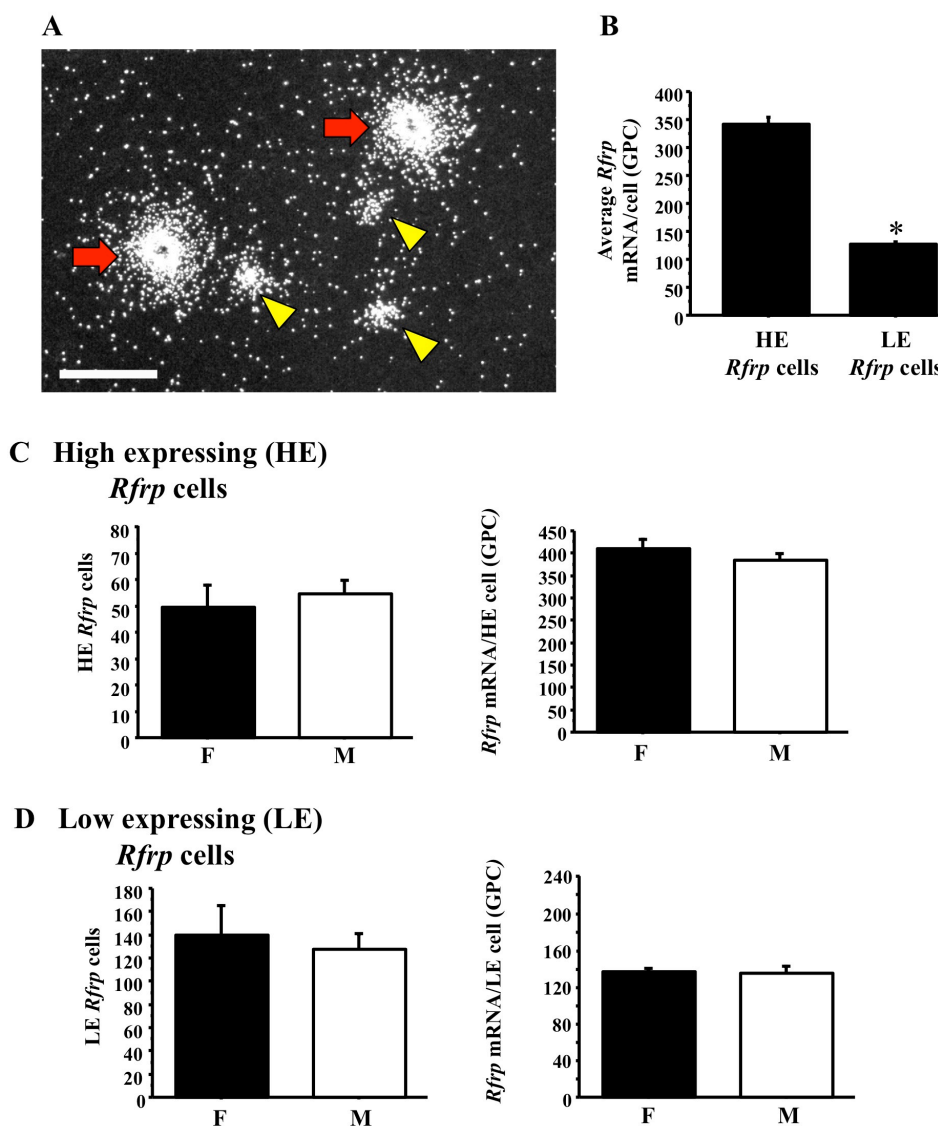


Figure 1.4 Characterization of high expressing and low expressing *Rfrp* cells in the DMN. **[A]** Representative photomicrograph of high-expressing (HE, red arrows) and low-expressing (LE, yellow arrowheads) *Rfrp* cells in an adult male. Note that the central dark void observed in some high-expressing *Rfrp* cells is actually an extremely dense clustering of silver grains that prevents transillumination under dark field, as determined under bright field microscopy (*data not shown*). Scale bar = 50 μ m. **[B]** Average *Rfrp* mRNA/cell (determined by silver grains) between HE and LE population from a representative adult male. The two *Rfrp* sub-populations have significantly different ($p < 0.05$) amounts of *Rfrp* mRNA (silver grains per cell, GPC). **[C]** Mean number of HE *Rfrp* cells in adult females and males and *Rfrp* mRNA/HE cell as determined by silver grains/HE cell. Neither measure was significantly different between sexes. **[D]** Mean number of LE *Rfrp* cells in adult females and males and mRNA/cell as determined by grains/cell of LE cells. Neither measure was significantly different between sexes.

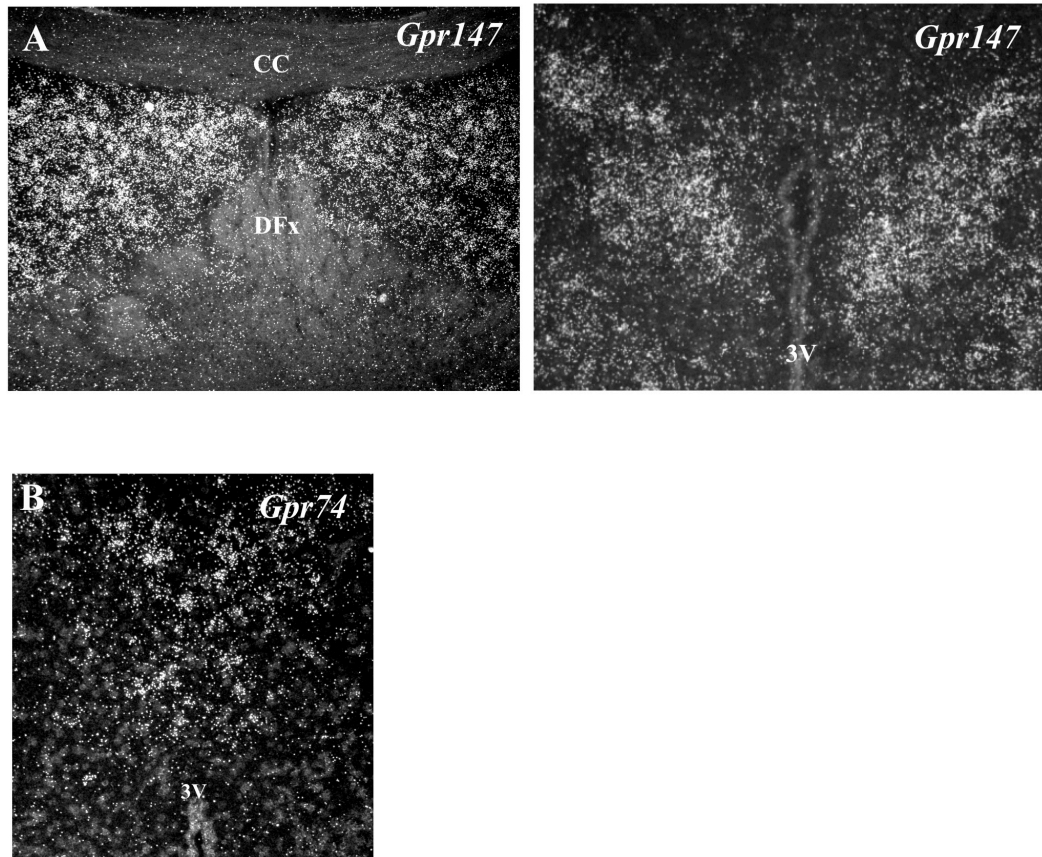


Figure 1.5 *In-situ* hybridization for *Gpr147* and *Gpr74* in the brain of an adult male mouse. **[A]** *Gpr147* is expressed the highest in the dorsal septum (right) and paraventricular nucleus (left). Cc, corpus callosum; Dfx, dorsal fornix; 3V, third ventricle **[B]** *Gpr74* expression is prevalent in the mouse brain, but highest expression can be found in thalamic nucleus of reunion.

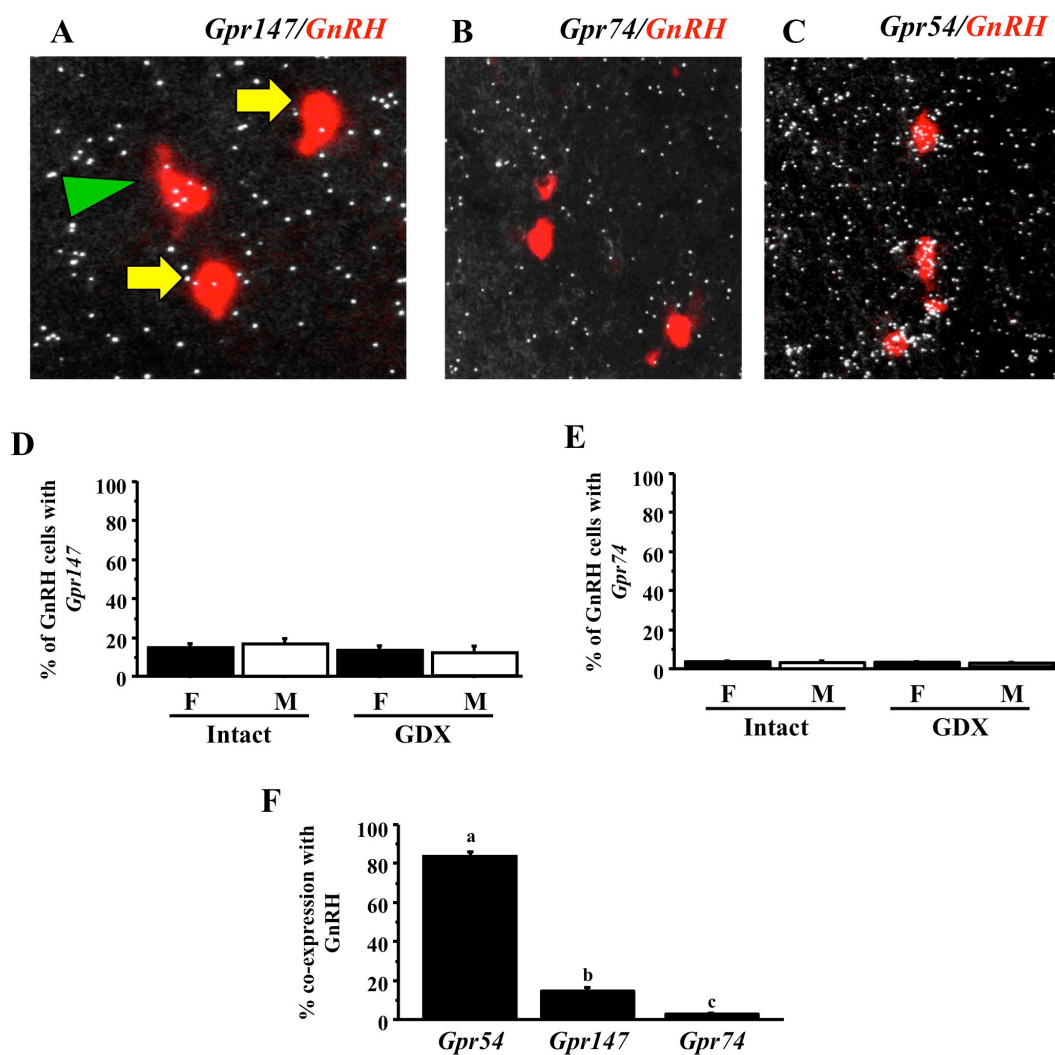


Figure 1.6 Low expression of RFamide receptors in GnRH neurons of mice, determined by double label *in-situ* hybridization. **[A]** Representative photomicrographs of *Gpr147* mRNA (silver grains) in a GnRH neuron (red fluorescence; indicated by blue arrowhead) from a male mouse. GnRH neurons not co-expressing *Gpr147* are indicated with yellow arrows. **[B]** Representative photomicrograph of GnRH neurons (red fluorescence) and *Gpr74* mRNA (silver grains) in a female mouse. **[C]** Representative photomicrograph of GnRH neurons (red fluorescence) and *Gpr54* mRNA (silver grains) in a female mouse. All GnRH neurons pictured have significant co-expression of *Gpr54* mRNA. **[D]** Quantification of the percent co-expression of *Gpr147* in GnRH neurons in intact and gonadectomized (GDX) females (F) and males (M). There were no significant differences between any groups. **[E]** Quantification of the percent co-expression of *Gpr74* in GnRH neurons in intact and gonadectomized females and males. There were no significant differences between any groups. **[F]** Comparison of the percent co-expression of *Gpr54*, *Gpr147* and *Gpr74* in GnRH neurons of intact (diestrous) females.

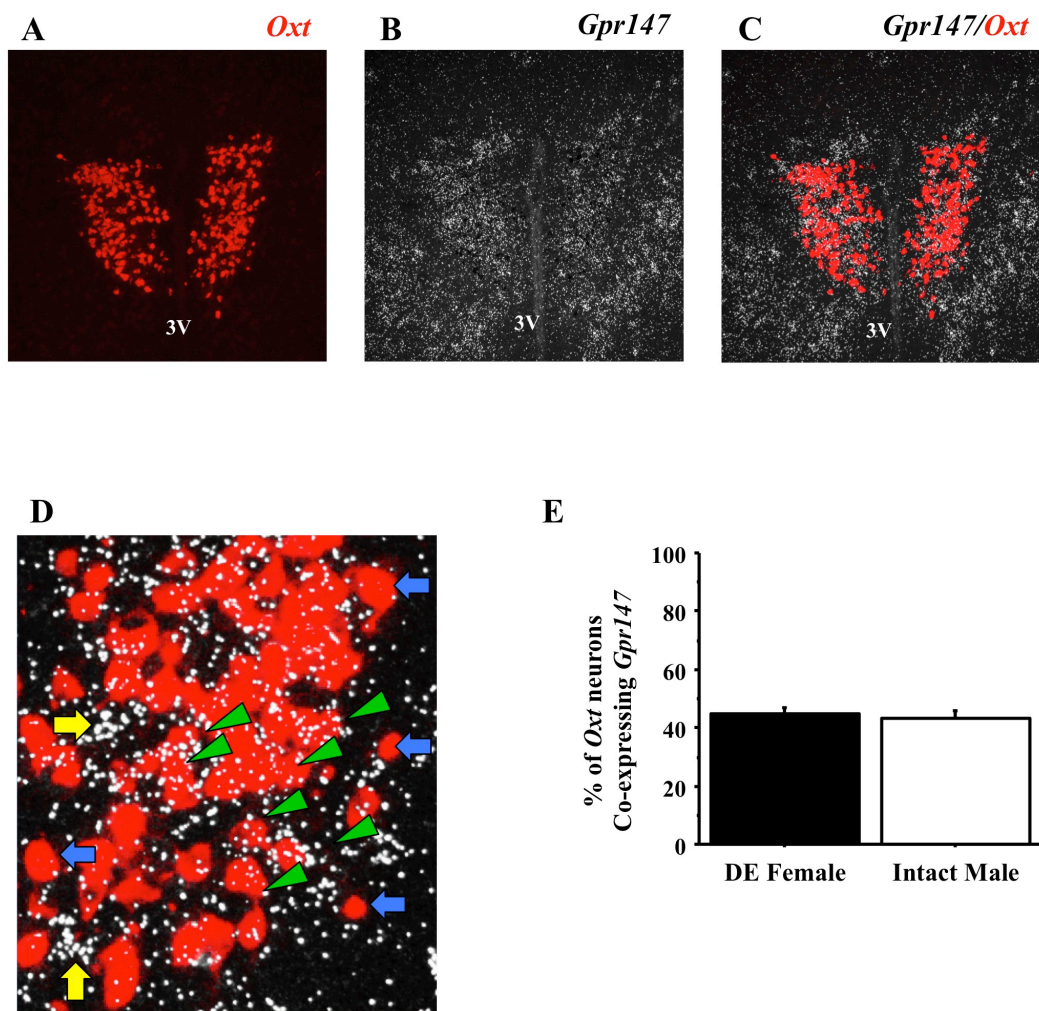


Figure 1.7 Expression of *Gpr147* in oxytocin neurons of female (diestrus) mice. **[A]** *Oxt* mRNA (red fluorescence) in the hypothalamus of a female mouse, 3V, third ventricle. **[B]** *Gpr147* mRNA (silver grains) of the same tissue slice as [A]. **[C]** Merge overlay showing co-expression of *Gpr147* in *Oxt* neurons. **[D]** High power photomicrograph of *Gpr147* co-expression with *Oxt*. Green arrowheads indicate double-labeled *Gpr147/Oxt* neurons, blue arrows indicate *Oxt* neurons that do not express *Gpr147*, and yellow arrows indicate neurons that express *Gpr147* only. **[E]** Quantification of the percent co-expression of *Gpr147* in oxytocin neurons in intact females and males. There were no significant differences between groups.

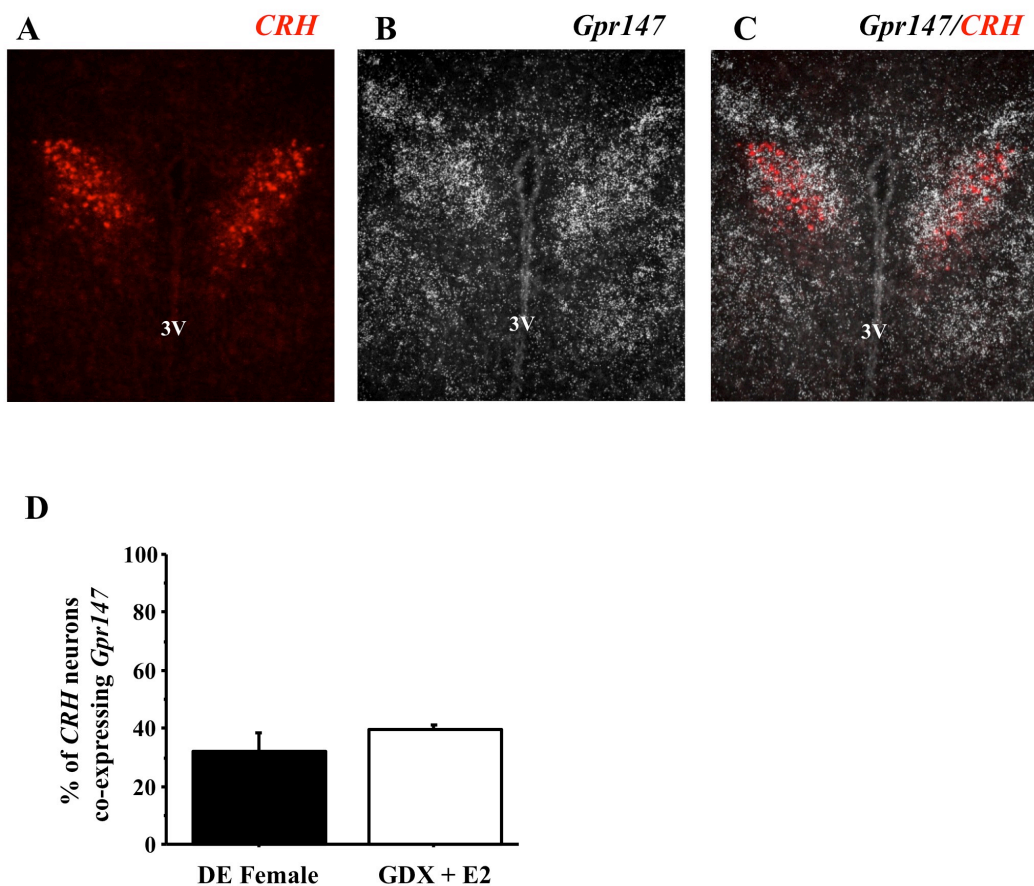


Figure 1.8 Expression of *Gpr147* in corticotropin-releasing hormone neurons of female (diestrous) mice. [A] *CRH* mRNA (red fluorescence) in the hypothalamus of a female mouse, 3V, third ventricle. [B] *Gpr147* mRNA (silver grains) of the same tissue slice as [A]. [C] Merge overlay showing co-expression of *Gpr147* in *CRH* neurons. [D] Quantification of the percent co-expression of *Gpr147* in corticotropin-releasing hormone neurons in intact females (diestrous) and ovariectomized and estrogen replaced (OVX + E). There were no significant differences between any groups.

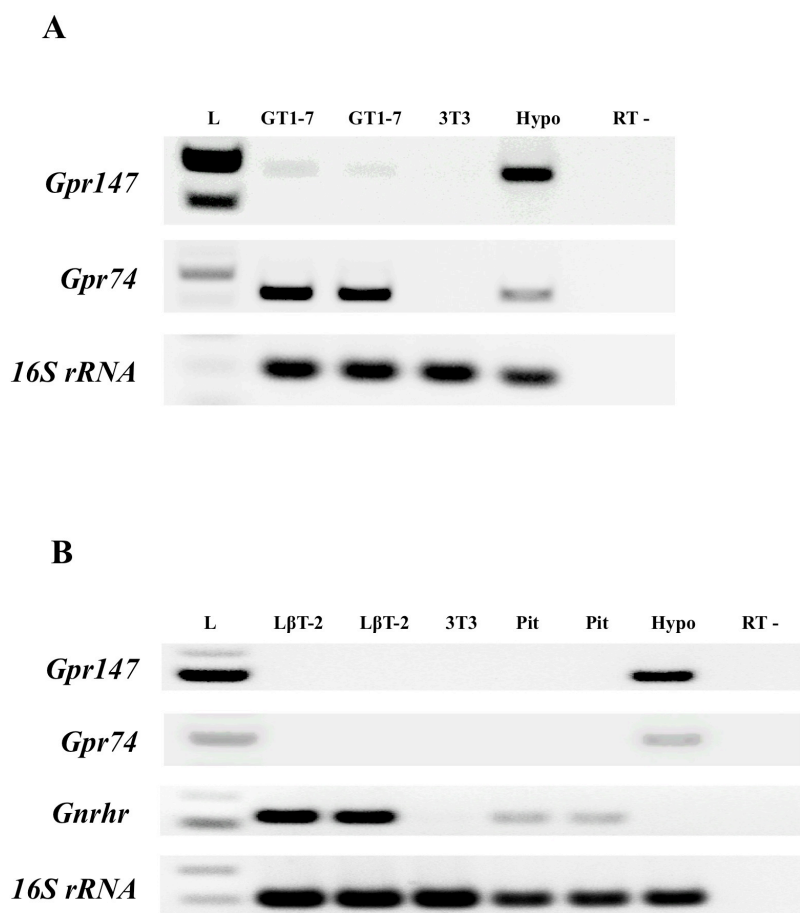


Figure 1.9 Expression of *Gpr147* and *Gpr74* in mouse cell lines. **[A]** RT-PCR was performed for *Gpr147* and *Gpr74* mRNAs in GT1-7 cell line. A weak product is visible for *Gpr147* mRNA while *Gpr74* is more predominantly expressed. The non-neuronal 3T3 cell line does not express either receptor. cDNA from hypothalamus (Hypo) serves as positive control. RT- = hypothalamic cDNA reaction without reverse transcriptase, L = ladder **[B]** RT-PCR was performed for *Gpr147* and *Gpr74* mRNAs in LβT-2 cell line. No product is seen for either receptor in the pituitary cell line or primary pituitary cells (pit). RT-PCR for the GnRH receptor (*Gnrhr*) serves as positive control for LβT-2 and pituitary samples. The non-neuronal 3T3 cell line does not express either receptor. cDNA from hypothalamus (Hypo) serves as positive control. RT- = hypothalamic cDNA reaction without reverse transcriptase, L = ladder. In both experiments, 16S ribosomal RNA served as a loading control.

CHAPTER 2: Interactions between the RFRP-3 and kisspeptin systems

Abstract

The neuropeptides kisspeptin (encoded by *Kiss1*) and RFamide-related peptide-3 (also known as GnIH; encoded by *Rfrp*) are potent stimulators and inhibitors, respectively, of reproduction. Whether kisspeptin or RFRP-3 might act directly on each other's neuronal populations to indirectly modulate reproductive status is unknown. To begin to examine such possible interconnectivity of the kisspeptin and RFRP-3 systems, double label *in-situ* hybridization (ISH) for RFRP-3's receptors, *Gpr147* and *Gpr74*, in hypothalamic *Kiss1* neurons of adult male and female mice, as well as double-label ISH for kisspeptin's receptor, *Kiss1r*, in *Rfrp*-expressing neurons of the hypothalamic dorsal-medial nucleus (DMN) was performed. Only a very small proportion (5-10%) of *Kiss1* neurons of the anteroventral periventricular region expressed *Gpr147* or *Gpr74* in either sex, whereas higher co-expression (21-25%) existed in *Kiss1* neurons in the arcuate nucleus. Thus, RFRP-3 could signal to a small, primarily arcuate, subset of *Kiss1* neurons. Next, the possibility of kisspeptin innervation of RFRP-3 neurons was addressed. In contrast to the former situation, no *Rfrp* neurons co-expressed *Kiss1r* in either sex, and *Tacr3*, the receptor for neurokinin B (NKB; a neuropeptide co-expressed with arcuate kisspeptin neurons) was found in < 10% of *Rfrp* neurons. Moreover, kisspeptin-immunoreactive fibers did not appose RFRP-3-immunoreactive cells in either sex, further excluding the likelihood that kisspeptin neurons directly communicate to RFRP-3 neurons. Lastly, despite abundant NKB in the DMN region where RFRP-3 soma reside, NKB was not co-expressed in the majority of *Rfrp* neurons. These results suggest that RFRP-3 may modulate a small proportion of kisspeptin-producing neurons in mice, particularly in the arcuate nucleus, whereas kisspeptin neurons are unlikely to have any direct reciprocal actions on RFRP-3 neurons.

Introduction

Neuropeptides of the arginine-phenylalanine-amide (RFamide) family have been demonstrated to have potent modulatory effects on a variety of physiological functions, including reproduction (21). Two members of this family, kisspeptin (encoded by *Kiss1*) and RFamide-related peptide 3 (RFRP-3, encoded by *Rfrp*), have been shown to regulate mammalian reproductive function through central mechanisms, but have opposing effects on the reproductive axis in mice, with kisspeptin stimulating and RFRP-3 inhibiting reproduction, respectively.

The kisspeptin system, which includes kisspeptin and its receptor, *Kiss1r* (formerly known as *Gpr54*), is considered stimulatory and essential for reproductive function. Human patients or rodents lacking functional *Kiss1* or *Kiss1r* genes suffer from impaired puberty and hypogonadotropic hypogonadism, presenting with low levels of gonadotropins and sex steroids, underdeveloped gonads, impaired sexual development, and infertility (17,18,33,34). Exogenous kisspeptin administration potently stimulates the secretion of luteinizing hormone (LH) and follicle stimulating hormone (34,39-42), working centrally through a gonadotropin-releasing hormone (GnRH)-dependent mechanism (6,43). Kisspeptin can directly activate GnRH neurons, as determined via c-Fos induction (a marker of neuronal activation) in GnRH cells (39,43) and stimulation of electrical firing of GnRH neurons in brain explants (44,45). Anatomical support for a direct kisspeptin effect on GnRH cells includes the presence of kisspeptin neuronal fibers appositions on GnRH neurons (47-49) and high *Kiss1r* expression in the majority of GnRH neurons (34,43,44). Within the rodent brain, kisspeptin/*Kiss1* mRNA somata are found in two primary populations: the rostral hypothalamic continuum of the anteroventral periventricular nucleus and neighboring rostral periventricular nucleus (AVPV/PeN), and the arcuate nucleus (ARC) (6,47). In the ARC, kisspeptin neurons highly co-express both neurokinin B (NKB,

encoded by the *Tac2* gene) (127) and dynorphin, giving rise to the terminology KNDy neurons, but exact roles of these co-transmitters are still being elucidated.

In contrast to kisspeptin, RFRP-3 has potent inhibitory actions on both GnRH neuronal activity and LH secretion in most rodent species (13,69,90). RFRP-3 is produced from a precursor peptide encoded by the *Rfrp* gene (59) and is the mammalian ortholog of avian gonadotropin-inhibiting hormone (GnIH) (19,20). Through immunohistochemical assessment, RFRP-3-immunoreactive (ir) cells are found exclusively in the dorsal-medial nucleus of the hypothalamus (DMN) of rodents (20,61), mirroring the selective expression of *Rfrp* mRNA in this region, as determined by *in-situ* hybridization (ISH) (60,124). In rodents, some GnRH neurons are contacted by RFRP-3 axonal fibers (20,64,65) and a subset of GnRH neurons express Gpr147, a high affinity receptor for RFRP-3 (65,124). In addition, RFRP-3 can bind to a second G-protein coupled receptor, Gpr74, with lower affinity (59,60), but this receptor is not expressed in GnRH neurons (26), and its relevance for the reproductive actions of RFRP-3 is currently unknown.

While both kisspeptin and RFRP-3 appear to modulate the reproductive axis in part by direct effects on GnRH, it is possible that these two neuropeptides may also influence reproductive status via indirect pathways. To this end, it is currently unclear if there is modulatory cross-talk between these two neuropeptide populations. In addition to projecting to some GnRH cells, RFRP-3-ir fibers also project to a variety of brain regions that do not have GnRH neurons, including the AVPV, lateral hypothalamic area, paraventricular nucleus, and ARC (20,61,63-65), and appositions of RFRP-3 fibers on some kisspeptin cells in the AVPV/PeN have been observed in female mice (65). Moreover, RFRP-3's receptors, Gpr147 and Gpr74 are also expressed in several hypothalamic non-GnRH regions, including the periventricular nucleus, paraventricular nucleus, and ARC (65,66,71,124). Additionally, RFRP-3 has been functionally shown to inhibit the electrical firing of some ARC kisspeptin neurons (78), suggesting that

RFRP-3 may in fact be able to directly regulate this kisspeptin population. However, whether ARC kisspeptin neurons actually express RFRP-3 receptors in animals of either sex has not been addressed. Likewise, the possibility of kisspeptin neurons regulating RFRP-3 neurons, either through kisspeptin itself or one of its co-transmitters, such as NKB, has not yet been explored. Indeed, kisspeptin fibers have been observed in the DMN, and some *Kiss1r* expression has also been reported in this area (128), as has *Tacr3* (the receptor for NKB, a co-transmitter of ARC kisspeptin neurons) (129). Thus, there may be unilateral or bilateral communication between the RFRP-3 and kisspeptin populations to fine-tune each other's actions on the reproductive axis, but this has not yet been thoroughly examined.

To begin to address the possible anatomical interconnectivity of the kisspeptin and RFRP-3 systems, double-label ISH and immunocytochemistry were used to determine 1) if one or both of RFRP-3's receptors are expressed in *Kiss1* cells of either the AVPV/PeN or the ARC of males and females, 2) if the kisspeptin or NKB receptors are co-expressed with *Rfrp* neurons in the DMN, 3) if kisspeptin axonal fibers are found apposing RFRP-3 cells in the DMN, and lastly, 4) if *Rfrp* neurons co-express *Tac2* (the gene encoding NKB) which is also known to be highly expressed in the DMN.

Materials and Methods

Animals, Gonadectomies, and Tissue Collection

Adult C57BL6 mice of both sexes were housed on a 12-12 light-dark cycle (lights off at 1800 h) with food and water available *ad libitum*. For some experiments, mice were anesthetized and bilaterally gonadectomized (GDX) one week prior to sacrifice, as previously described (101,102). For *in-situ* hybridization studies, GDX mice or gonadal-intact mice (females in diestrus, as determined by vaginal smears) were anesthetized with isoflurane and sacrificed by

rapid decapitation. Brains were collected, frozen on dry ice, and stored at -80°C. Five coronal series of 20 µm brain sections were cut on a cryostat, thaw-mounted onto Superfrost-plus slides, and stored at -80°C until use in *in-situ* hybridization. For immunohistochemistry experiments, gonadal-intact male and GDX male and female mice were perfused with 4% paraformaldehyde in 0.1 M phosphate buffer for brain collection. Coronal (30 µm thick) sections throughout the caudal hypothalamus, containing the ARC and DMN, were cut from each brain on a sliding microtome with a freezing stage. For all experiments, each group consisted of 4-6 animals. All experiments were conducted in accordance with the NIH Animal Care and Use Guidelines and with approval of the Animal Care and Use Committee of the University of California, San Diego and the University of Otago Animal Ethics Committee.

Double-label In-Situ Hybridization (ISH)

Double-label ISH assays and riboprobes were performed as described in Chapter 1. For double-label assays studying ARC KNDy cells, *Tac2* was used as a designator for KNDy neurons, as pilot studies indicated that *Tac2* expression per cell was stronger than *Kiss1*, allowing for better detection with the fluorescent DIG probe. Radio-labeled (³³P) antisense *Gpr147*, *Gpr74*, *Kiss1r*, *Tac2*, or *Tacr3* and DIG- labeled *Rfrp*, *Kiss1*, *Tac2* or *Gnrh* riboprobes (Roche digoxigenin labeling kit, 1:500) were combined with tRNA, denatured by boiling, and dissolved together in hybridization buffer.

Immunohistochemistry for kisspeptin and RFRP-3 in the DMN and ARC

For dual label immunohistochemistry of kisspeptin and RFRP-3, all steps were separated by four 10 minute washes in 50 mM tris-buffered saline containing 0.5% Triton X-100 (TBS-TX). After blocking in TBS-TX containing 1% BSA and 1% normal donkey serum, sections were incubated overnight at 4 °C in sheep anti-mouse kisspeptin-52 (AC053, kindly provided by Dr

Alain Caraty, National Institute for Agronomic Research, France; 1:2000 dilution), and rabbit anti-sparrow GnIH (PAC 123/124, kindly provided by Dr George Bentley, University of California, Berkeley; 1:5000) in blocking solution. Sections were then incubated for 2 hours at room temperature in biotinylated donkey anti-sheep (1:500 dilution; Jackson ImmunoResearch) and Alexa Fluor 488 donkey anti-rabbit (1:500 dilution; Molecular Probes, Life Technologies). Following this, sections were incubated for 1 hour in Alexa Fluor 568-streptavidin (1:500 dilution; Molecular Probes). Staining was observed with a Zeiss LSM 710 confocal microscope using a 63 X objective lens and laser excitation lines and filters for 488 nm or 543 nm. Stacks of images, collected at intervals of 600 nm, were analyzed offline using ImageJ software (National Institutes of Health). In the DMN, twenty RPRP-3 cell bodies were visualized per mouse and all kisspeptin-ir contacts recorded. In the ARC, 29-50 kisspeptin cell bodies were visualized per mouse and all RFRP-3 contacts were recorded. Contacts were defined as no black pixel between the fiber and the soma. Omission of any of the primary antibodies resulted in complete absence of staining.

Statistical Analysis

All data are expressed as the mean \pm SEM for each group. In all experiments, differences were analyzed by Student's t-test or by 2-way ANOVA, followed by post-hoc comparisons for individual sex/treatment groups via Fisher's (protected) least significant difference. Statistical significance was set at $p < 0.05$. All analyses were performed in Statview 5.0.1 (SAS Institute, Cary, NC).

Results

Experiment 1: Only a small proportion of AVPV Kiss1 neurons express Gpr147 or Gpr74

This lab previously reported that 12-15% of *Kiss1* neurons in the AVPV/PeN of female mice express *Gpr147*, both in ovary-intact (diestrous) and estradiol-treated conditions (65). However, it is unknown if a similar proportion of AVPV/PeN *Kiss1* neurons in male mice express *Gpr147*. Additionally, the co-expression of *Gpr74* with *Kiss1* in the AVPV/PeN in either sex has not previously been determined. In the present experiment, double-label ISH determined co-expression of *Gpr147* or *Gpr74* mRNA in *Kiss1* neurons in the AVPV/PeN of gonadally-intact female (diestrous) and male mice. Such co-expression was not also examined in GDX mice, as *Kiss1* expression is nearly undetectable in the AVPV/PeN in the GDX state (101). As expected, there was a pronounced sex difference in the number of detectable AVPV/PeN *Kiss1* neurons, with females having several fold more *Kiss1* neurons than males (*data not shown*) (104). In terms of RFRP-3 receptors, there is an overall low abundance of both *Gpr147* and *Gpr74* expression in the AVPV/PeN region, unlike other regions such as the paraventricular nucleus and thalamus where *Gpr147* and *Gpr74* mRNAs, respectively, were more highly expressed. In agreement with previous studies (65), quantitatively, only 12% of AVPV/PeN *Kiss1* neurons expressed *Gpr147* in females, and a similar proportion was observed in males (Figure 2.1). An even smaller proportion (5-6%) of AVPV/PeN *Kiss1* neurons co-expressed *Gpr74* in either sex. There were no statistical differences between the sexes for co-expression of either RFRP-3 receptor with *Kiss1* in the AVPV/PeN. The relative amount of *Gpr147* or *Gpr74* mRNA per *Kiss1* cell, reflected by the number of silver grains in each *Kiss1* cell, also did not differ between sexes (*data not shown*).

Experiment 2: A moderate proportion of KNDy neurons in the ARC express Gpr147 or Gpr74 and receive contacts from RFRP-3 fibers

The ARC *Kiss1* population highly co-expresses *Tac2* (which encodes NK1) and is referred to as the KNDy neuron population. Here, it was determined if either *Gpr147* or *Gpr74* is co-expressed in ARC KNDy neurons of adult male and female mice. *Gpr147* mRNA was moderately expressed in approximately 21% and 25% of KNDy neurons in gonadally-intact female (diestrus) and male mice, respectively (Figure 2.2A-C). Similar levels of *Gpr147* co-expression were found in GDX mice of both sexes (Figure 2.2). Like *Gpr147*, 21-22% of ARC KNDy neurons in gonadally-intact male and female mice co-expressed *Gpr74* mRNA (Figure 2.3A-C). For both assays, GDX mice had considerably more KNDy neurons than gonadally-intact mice ($p < 0.05$; *data not shown*), as expected due to known stimulatory effects of GDX on KNDy cells in rodents (130,131). There were no statistical differences between sexes or gonadal states in the degree of *Gpr147* or *Gpr74* co-expression in ARC KNDy neurons and no group differences were observed in the relative amount of receptor mRNA per KNDy neuron (silver grains per double-labeled cell). The co-expression for the two RFRP-3 receptors within KNDy neurons was evenly dispersed throughout the ARC and not noticeably different between in any anatomical sub-region within the KNDy neuron population.

To further examine possible RFRP-3 neuron to kisspeptin neuron interactions, double-label IHC was used to assess potential RFRP-3 fiber contacts on kisspeptin neurons in the ARC of female mice. For this analysis, GDX females were used, as this gonadal state allows for identification of kisspeptin cell bodies in the ARC, unlike gonadally-intact mice in which the dense kisspeptin fiber network obscures cell bodies. Supporting the receptor co-expression data above, RFRP-3 fibers were found to appose a moderate proportion of ARC kisspeptin cells. Quantification determined that ~35% of kisspeptin soma in the ARC received RFRP-3 fiber contacts (Figure 2.4).

Experiment 3: Rfrp neurons do not highly express Kiss1r or Tacr3 or receive axonal contacts from kisspeptin neurons

Experiments 1 and 2 indicated that a small population of kisspeptin neurons in the AVPV/PeN, and more so in the ARC, could be responsive to RFRP-3 signaling. A reciprocal relationship might also exist: could kisspeptin neurons also act on *Rfrp* neurons? To address this, double label ISH determined the degree of *Kiss1r* co-expression in *Rfrp* neurons and also to which kisspeptin fibers contact RFRP-3 neurons in the DMN. Double label ISH for *Kiss1r* in *Rfrp* neurons in adult male and female mice revealed that essentially all *Rfrp* neurons (> 99%) lacked *Kiss1r* (Figure 2.5A). In fact, *Kiss1r* was surprisingly absent from the DMN, despite previous ISH data demonstrating high expression of *Kiss1r* in this nucleus (128). As a positive control, pronounced *Kiss1r* mRNA expression was observed in the habenula, a known region of *Kiss1r* expression (*data not shown*). To ensure that lack of *Kiss1r* in *Rfrp* neurons was not due to technical reasons, a second set of slides from the rostral hypothalamus of adult females was concurrently assayed for *Kiss1r* expression in *Gnrh* neurons (Figure 2.5C, D) along with *Kiss1r* in *Rfrp* neurons. Whereas > 85% of GnRH neurons expressed *Kiss1r*, no *Rfrp* neurons expressed *Kiss1r* (Figure 2.5C, D), consistent with the previous assay.

In the ARC, kisspeptin neurons co-express NKB, which could potentially be used by ARC KNDy neurons to communicate with RFRP-3 neurons via *Tacr3* signaling. Indeed, *Tacr3* (the NKB receptor) is highly expressed in the DMN region, along with NKB fibers (129,132), but it is unknown if this specifically includes RFRP-3 neurons. Using double-label ISH for *Tacr3* and *Rfrp*, a robust staining for both mRNAs in the DMN of mice of both sexes was found (Figure 2.6A,B). However, quantitative analysis determined that *Tacr3* mRNA was absent in most *Rfrp* neurons. Less than 10% of *Rfrp* neurons expressed *Tacr3* in gonadally-intact males and females (Figure 2.6C), and similar low co-expression levels were quantified in GDX mice of both sexes, with *Tacr3* being detected in only ~ 8% of *Rfrp* neurons (Figure 2.6C). There were no statistical

differences between sexes or gonadal state in the proportion of cells expressing *Tacr3* or the relative *Tacr3* mRNA level per *Rfrp* cell.

In a complementary experiment, double-label IHC to assessed potential kisspeptin fibers contacts, which could arise from either the AVPV/PeN kisspeptin population and/or ARC kisspeptin/NKB (KNDy) cells, on RFRP-3 neurons in the DMN. Matching the receptor co-expression data, virtually no RFRP-3 cells were observed with contacts from kisspeptin fibers (Figure 2.7A). Quantification of the staining revealed that, on average, just 4% of RFRP-3-immunoreactive cells received apparent contacts from kisspeptin-containing fibers in gonadally-intact adult male mice (Figure 2.7B). Similar results were observed in GDX males, with only ~3% of RFRP-3 cells receiving kisspeptin fiber appositions (Figure 2.7B). There were no statistical differences in the degree of kisspeptin-RFRP-3 contacts between intact and GDX mice.

Experiment 4: Is NKB a co-neuropeptide with RFRP-3?

Tac2 mRNA, which codes for NKB, is known to be highly expressed in the DMN (133), but its co-expression in RFRP-3 neurons is unknown. Double-label ISH to determined if *Rfrp* neurons are in fact the same or an overlapping population of DMN cells as those expressing *Tac2*. However, despite strong expression of both genes in the DMN region, *Rfrp* and *Tac2* neurons in the DMN are mostly distinct populations, with relatively low levels of co-expression (Figure 2.8A, B). Quantitatively, approximately 12% of *Rfrp* neurons co-express *Tac2* in adult mice of both sexes (Figure 2.8C) under both gonadal-intact and GDX conditions. There were no statistical differences in the proportion of *Rfrp* neurons co-expressing *Tac2* between sexes or treatment group and there were no differences in the grains per cell representing *Tac2* mRNA levels in the double-labeled cells (Figure 2.8C). The degree of reciprocal co-localization of DMN *Tac2* neurons expressing *Rfrp* was not quantified. However, it was noted that significantly more total

Tac2 neurons than *Rfrp* neurons were in the DMN region, indicating that the proportion of *Tac2* cells co-expressing *Rfrp* would be notably lower than the 12% of *Rfrp* neurons found to co-express *Tac2*.

Discussion

Despite the potent and reciprocal activities of kisspeptin and RFRP-3 on the reproductive axis, comprehensive interconnectivity of these two neuropeptide systems has not been thoroughly investigated. Here, it was determined if the receptors for RFRP-3, Gpr147 and Gpr74, were expressed in either population of hypothalamic kisspeptin neurons and whether kisspeptin's receptor, or that for NKB, was expressed in RFRP-3 cells. The majority of AVPV/PeN *Kiss1* neurons do not express either of the receptors known to mediate the actions of RFRP-3, whereas a moderate percentage of kisspeptin cells in the ARC do co-express RFRP-3 receptors. Conversely, *Kiss1r* (kisspeptin receptor) was absent in virtually all *Rfrp* neurons and almost no RFRP-3 neurons receive appositions from kisspeptin axonal fibers. Moreover, *Tacr3*, the receptor for ARC kisspeptin's co-transmitter NKB, was not highly expressed in most RFRP-3 cells. Overall, the anatomical data suggest that the kisspeptin and RFRP-3 neuronal systems likely act independently on the GnRH-pituitary axis and may only have notable communication with each other at the level of RFRP-3 signaling to ARC kisspeptin cells.

The various mechanisms by which RFRP-3 neurons might regulate the reproductive axis are not fully elucidated. A good part of RFRP-3's reproductive modulation appears to occur through the inhibition of GnRH release, and antagonizing the GnRH receptor abolishes the stimulatory effect of an RFRP-3 antagonist, RF9, on LH secretion (65). These data suggest that RFRP-3 provides an inhibitory tone upstream of GnRH signaling, since blockade of RFRP-3 signaling is only effective at stimulating LH when GnRH signaling pathways are functional.

However, using several different techniques, there is only low to moderate co-expression of the RFRP-3 receptors, Gpr147 and Gpr74, in GnRH neurons, with a majority of GnRH cells not expressing either receptor (65,124), matching the finding that only a subset of GnRH neurons changing their firing rate after RFRP-3 treatment (13). The ability of RFRP-3 to inhibit GnRH and LH despite a majority of GnRH cells not expressing RFRP-3 receptors could indicate that some RFRP-3-mediated inhibition on GnRH may occur indirectly. While the possibility of RFRP-3 acting on the pituitary has been hypothesized, RFRP-3 neurons of rodents are not hypophysiotropic, since they are unable take up peripherally administered retrograde tracers (70). These data exclude the possibility of RFRP-3 acting directly on the pituitary of rodents, which differs from the ovine model, where RFRP-3 can be measured in portal blood (134).

Given that only a subset of GnRH neurons expresses RFRP-3 receptors, it can be speculated that RFRP-3 may also regulate the GnRH axis through an intermediate neuropeptide population(s), such as kisspeptin neurons. Kisspeptin is a potent stimulator of GnRH release (6), but the “upstream” circuitry that regulates the synthesis and secretion of kisspeptin is poorly understood. Thus, it is hypothesized that RFRP-3 may be an upstream factor that negatively modulates kisspeptin neurons to thereby reduce GnRH activation. This possibility was supported by data indicating that RFRP-3 fibers appose some AVPV/PeN kisspeptin neurons in female mice (65) and are also present in the ARC where kisspeptin neurons also reside (20,61,63). However, based on the present findings, it appears that a large majority of kisspeptin neurons, in both the AVPV/PeN and the ARC, are lacking receptors for RFRP-3. This was especially apparent in the AVPV/PeN, suggesting that kisspeptin neurons in that nucleus are unlikely to be significantly regulated by direct RFRP-3 signaling. In the ARC, however, a moderate proportion (~20-25%) of kisspeptin cells co-expressed Gpr147 or Gpr74, and nearly 35% of ARC kisspeptin neurons receive RFRP-3 fibers, indicating that there could be some functional regulation of kisspeptin neurons by RFRP-3 in this specific brain region. Even so, it is not clear what the functional

significance of such communication would be, given the lack of RFRP-3 receptors and fibers contacts in such a large proportion of these ARC KNDy cells. Since triple labeling experiments could not be performed, it is unknown if the same ARC kisspeptin cells that express Gpr147 also express Gpr74, or if different kisspeptin cells express each of the two RFRP-3 receptors. If the latter scenario, then not only would a larger proportion of ARC kisspeptin cells than are observed (20-25%) actually be responsive to RFRP-3 signals, but also the differing affinities of RFRP-3 for these receptor subtypes might enable graded or differing responses of different kisspeptin cells to the same RFRP-3 stimulus. Whereas the maximum percent of ARC kisspeptin neurons directly modulated by RFRP-3 signaling is likely capped at one third, due to the proportion of KNDy neurons with RFRP-3 fibers appositions and RFRP-3 receptors, it remains possible that such RFRP-3 signaling may still affect the entire KNDy population indirectly via the reciprocally interconnected nature of the KNDy neuron network. Of note, *Tac2* expression was used to represent KNDy neurons, since nearly all *Tac2* neurons (> 95%) co-express *Kiss1* in the ARC of mice (A.S. Kauffman, unpublished observation). Thus, *Tac2* expression in the mouse ARC faithfully reflects *Kiss1* expressing neurons.

One interesting possible role for RFRP-3-kisspeptin interactions that has been hypothesized is the regulation of the preovulatory GnRH/LH surge, an event driven by kisspeptin and suppressed by RFRP-3 (90,135). RFRP-3 neuronal activity declines at the time of the LH surge (63), as does the hypothalamic concentration of RFRP-3 peptide (M.Z. Rizwan and G.M. Anderson, unpublished data). It is conceivable that this decline reduces inhibitory RFRP-3 tone on kisspeptin neurons, allowing increased kisspeptin drive to trigger the GnRH/LH surge (48). Such speculation would be consistent with previous reports of RFRP-3 causing suppression of cellular activity as well as reduced kisspeptin neuronal firing rate in the AVPV (13,90), a key brain region implicated in the LH surge event. However, this is less consistent with the present finding of minimal RFRP-3 receptors in AVPV kisspeptin neurons. Indeed, most RFRP-3

receptors in kisspeptin neurons were located in the ARC rather than the AVPV, and the former brain region is not implicated in the LH surge in rodents. Thus, the findings suggest that any effects of RFRP-3 on AVPV kisspeptin neurons to govern the LH surge would likely be indirect on those neurons.

Initial ISH studies targeting *Kiss1r* suggested it was highly expressed in the DMN (128), and kisspeptin fibers have been observed in the DMN (136), supporting the possibility that kisspeptin signaling may interface with RFRP-3 neurons. The present results, however, strongly exclude the possibility of kisspeptin acting on RFRP-3 neurons through *Kiss1r*, as no *Rfrp* neurons expressed the mRNA for this receptor. Moreover, contrary to the initial report (128), there is no evidence of significant *Kiss1r* mRNA in the DMN area, at least under the conditions examined. This was not due to poor sensitivity of the *Kiss1r* ISH, since there was high *Kiss1r* expression in GnRH neurons and other brain regions, as expected. To complement this receptor expression data, kisspeptin-containing fibers apposed RFRP-3 cells was also determined. In agreement with the ISH data, these immunohistochemistry results also excluded the likelihood of kisspeptin neurons targeting RFRP-3 neurons, as virtually all RFRP-3 neurons were devoid of kisspeptin fibers appositions. Importantly, these fibers apposition data also indicate that, due to the lack of physical connectivity, it is highly unlikely that kisspeptin neurons utilize other co-neuropeptides, such NKB or dynorphin, to act directly on *Rfrp* neurons. This was supported by the finding that *Tacr3*, the receptor for NKB (a co-transmitter with kisspeptin from ARC cells), was absent in the vast majority of *Rfrp* neurons, despite robust *Tacr3* expression elsewhere nearby in the DMN. Any NKB interaction on the small subset of RFRP-3 neurons expressing *Tacr3* would likely arise from non-ARC NKB neurons, since almost no kisspeptin fibers appose RFRP-3 neurons (ARC KNDy neuron fibers would contain kisspeptin as well as NKB).

Most hypothalamic neuropeptide populations tend to produce more than one neuropeptide or neurotransmitter. Yet, the potential co-transmitters that may also be expressed in and released by RFRP-3 neurons are unknown. The present study also examined if NKB was co-expressed with RFRP-3, as many neurons in the DMN highly express *Tac2*. However, despite a little degree of overlap, *Tac2* was not expressed in the large majority of *Rfrp* neurons. These data suggest that the RFRP-3 and NKB neuronal populations residing in the DMN are, for the most part, distinct and separate neuropeptide populations. Thus, it presently remains unknown if RFRP-3 neurons also highly secrete additional co-transmitters or not.

In summary, the data presented here exclude the likelihood of RFRP-3 acting on any sizable proportion of kisspeptin neurons in the AVPV/PeN in either sex, but suggest that RFRP-3 may potentially provide some direct regulation to a moderate subset of ARC KNDy cells. Additionally, the possibility of a reciprocal action of kisspeptin or NKB on RFRP-3 neurons was strongly excluded, as no *Rfrp* neurons express *Kiss1r* and virtually no RFRP-3-ir neurons receive kisspeptin appositions or express *Tacr3*. Lastly, the majority of *Rfrp* neurons lack *Tac2*, indicating that NKB is not co-expressed with RFRP-3 and that these are likely two separate neuronal populations in the DMN. These data demonstrate that kisspeptin is acting independently of, and in parallel with, the RFRP-3 system to govern the reproductive axis, whereas some effects of RFRP-3 on reproduction may potentially be derived via actions on a subset of ARC kisspeptin cells. Whether RFRP-3 also acts elsewhere in the brain to indirectly modulate reproduction remains unexplored, but could possibly include other regions such as paraventricular nucleus, lateral hypothalamus, thalamus, and amygdala where RFRP-3 fibers have been reported (61) and where *Gpr147* or *Gpr74* mRNAs are notably expressed (110).

Portions of this chapter are published in *Journal of Neuroendocrinology* (October 2013). The dissertation author was the primary investigator and author of this material. Josh Kim and Sangeeta Dhamija provided support with brain cyrosectioning and performing ISH. Alexander Kauffman supervised the project and provided advice.

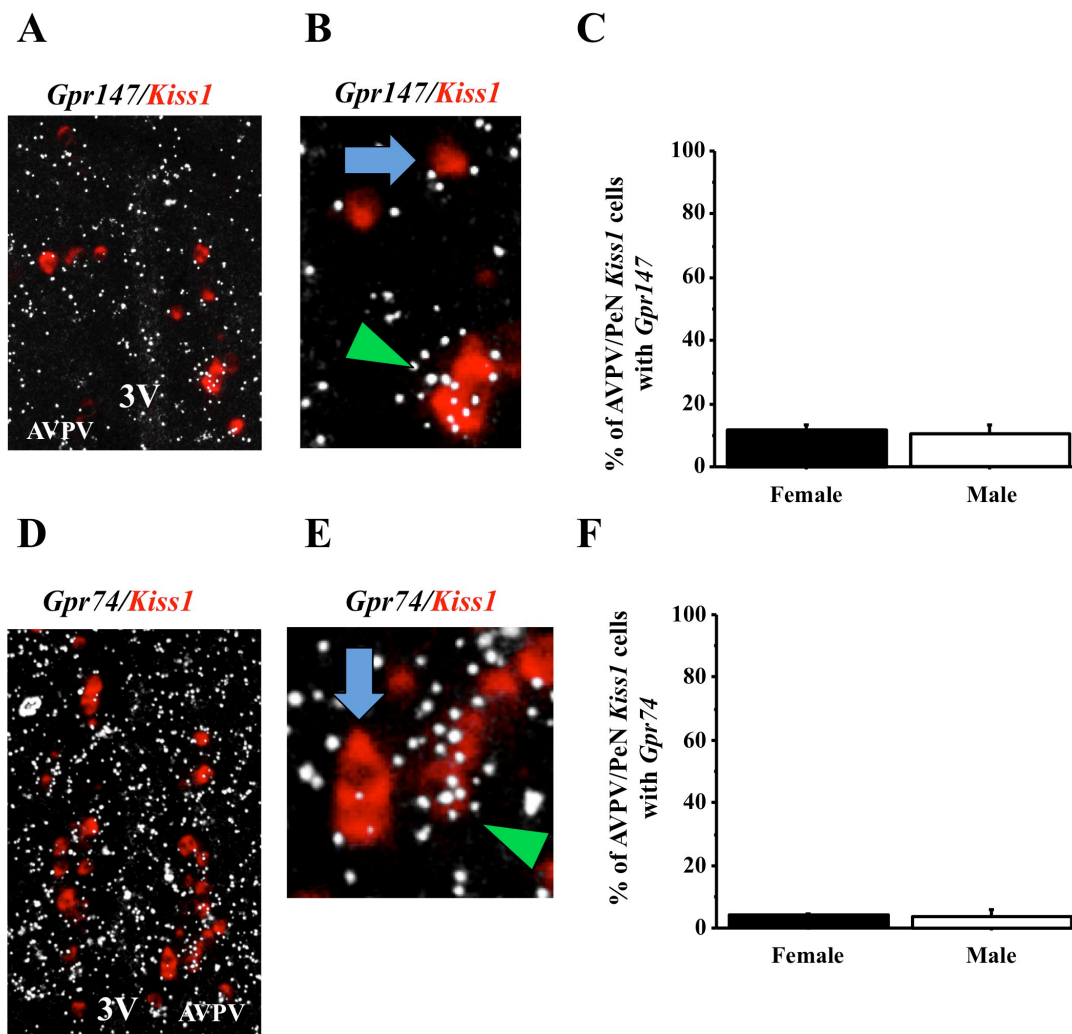


Figure 2.1. Expression of *Gpr147* and *Gpr74* in AVPV/PeN *Kiss1* neurons by double label *in-situ* hybridization. **[A]** Representative photomicrographs of double label *in-situ* hybridization of *Kiss1* (red fluorescence) and *Gpr147* (silver grains) in an intact male. 3V, third ventricle **[B]** *Kiss1* neurons co-expressing *Gpr147* (green arrowhead) and *Kiss1* neurons with no co-expression of *Gpr147* (blue arrows). **[C]** Quantification of the percent co-expression of *Gpr147* in *Kiss1* neurons between gonadally-intact females (F) and males (M). There were no significant differences in co-expression between any of the groups. **[D]** Representative photomicrographs of double label *in-situ* hybridization of *Kiss1* (red fluorescence) and *Gpr74* (silver grains) in a diestrous female. **[E]** *Kiss1* neurons co-expressing *Gpr74* (green arrowhead) and *Kiss1* neurons with no co-expression of *Gpr147* (blue arrows). **[F]** Quantification of the percent co-expression of *Gpr147* in *Kiss1* neurons between gonadally-intact females (F) and males (M). There were no statistical differences between the sex or gonadal state.

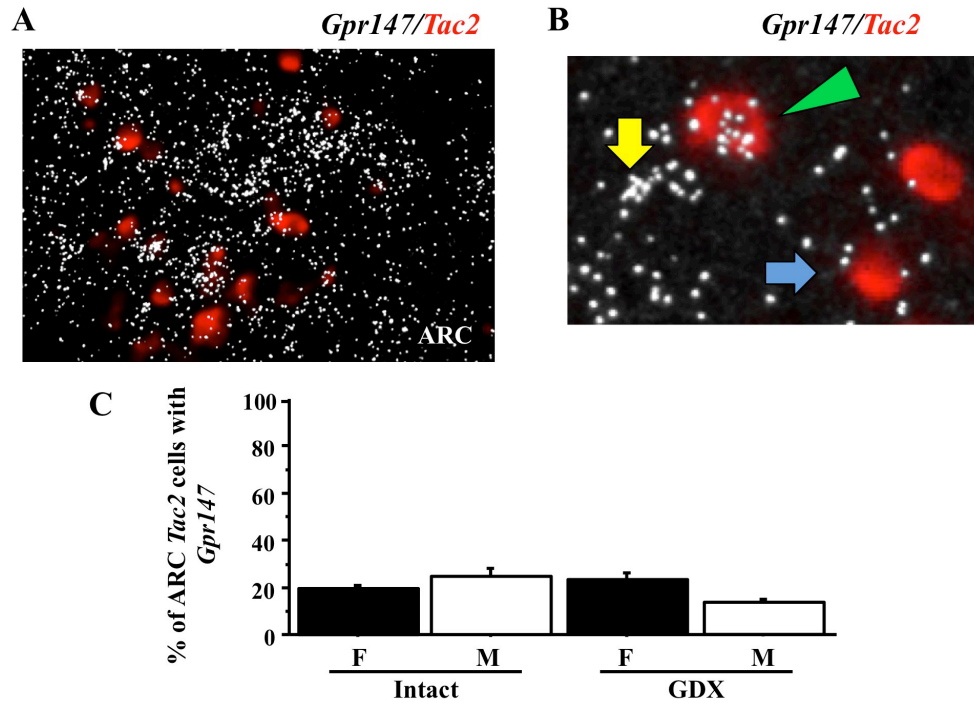


Figure 2.2. Expression of *Gpr147* in ARC *Tac2* neurons by double label *in-situ* hybridization. **[A]** Representative photomicrographs of double label *in-situ* hybridization of *Tac2* (red fluorescence) and *Gpr147* (silver grains) in a diestrous female. **[B]** *Tac2* neurons co-expressing *Gpr147* (green arrowhead) and *Tac2* neurons with no co-expression of *Gpr147* (blue arrows). **[C]** Quantification of the percent co-expression of *Gpr147* in *Tac2* neurons between gonadally-intact females (F) and males (M) and gonadectomized (GDX) M and F. There were no significant differences in co-expression between any of the groups.

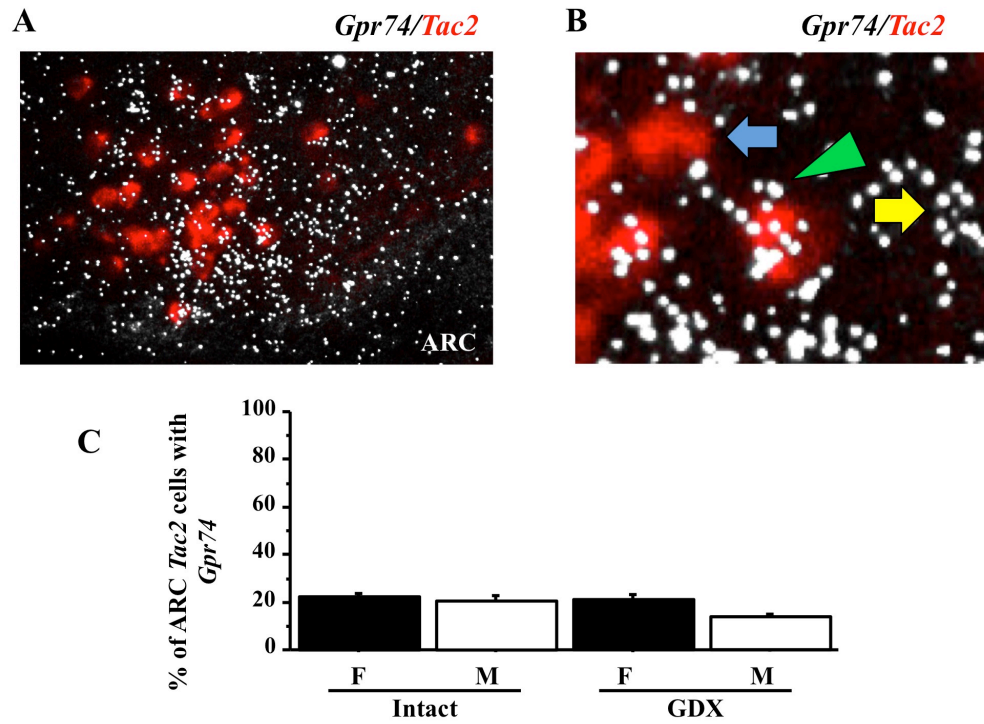


Figure 2.3. Expression of *Gpr74* in ARC *Tac2* neurons by double label *in-situ* hybridization. [A] Representative photomicrographs of double label *in-situ* hybridization of *Tac2* (red fluorescence) and *Gpr74* (silver grains) in a diestrous female. [B] *Tac2* neurons co-expressing *Gpr74* (green arrowhead) and a *Gpr74* neuron that is not expressing *Tac2* (yellow arrow). [C] Quantification of the percent co-expression of *Gpr147* in *Tac2* neurons between gonadally-intact females (F) and males (M) and gonadectomized (GDX) M and F. These experimental groups were not statistically different.

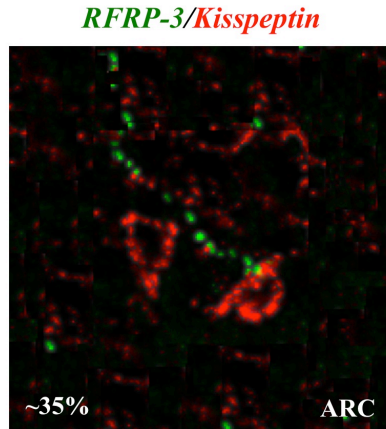


Figure 2.4. Representative photomicrograph of RFRP-3 immunoreactive fiber (green fluorescence) in apposition with ARC kisspeptin neuron (red fluorescence) in a female mouse. Immunohistochemical analysis revealed RFRP-3 contacts with ~ 35% of kisspeptin cell bodies in the ARC of GDX female mice. Figure is a collapsed stack of several confocal optical sections.

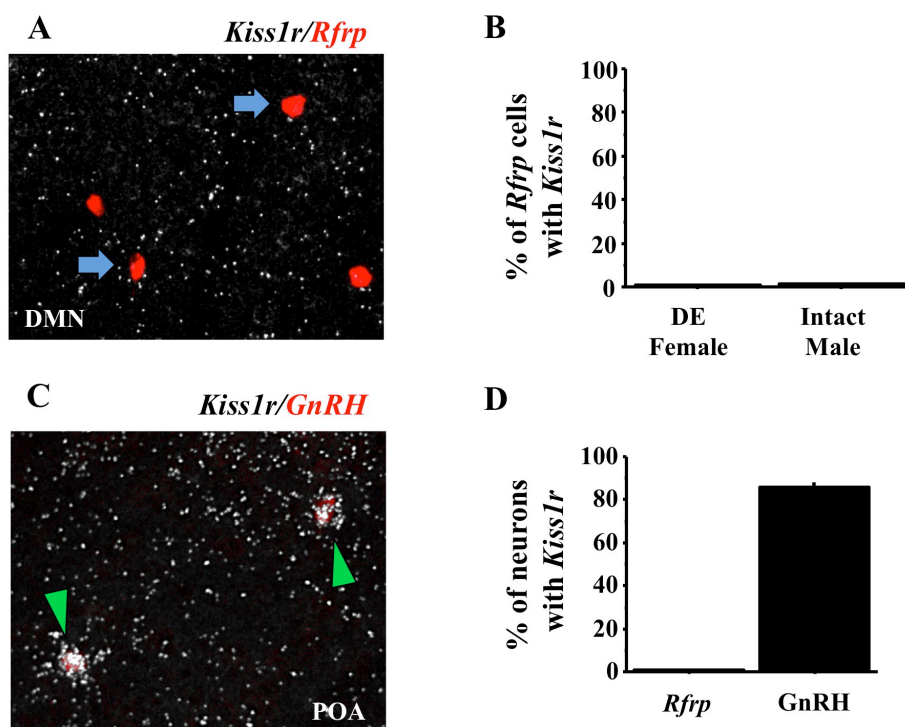


Figure 2.5. Expression of *Kiss1r* in *Rfrp* and GnRH neurons by double label *in-situ* hybridization. [A] Representative photomicrographs of double label *in-situ* hybridization of *Rfrp* (red fluorescence) and *Kiss1r* (silver grains) in the DMN of a diestrous female. *Rfrp* neurons lacking *Kiss1r* are marked with blue arrows [B] Quantification of the percent co-expression of *Kiss1r* in *Rfrp* neurons between gonadally-intact females and males. There were no significant differences in co-expression between sexes. [C] Representative photomicrographs of double label *in-situ* hybridization of *Kiss1r* (silver grains) and GnRH (red fluorescence) in the preoptic area (POA) of an intact male. Green arrowheads identify double-labeled cells [D] Quantification of the percent co-expression of *Kiss1r* in *Rfrp* or GnRH neurons in diestrous females and intact males (percentages averaged across all animals).

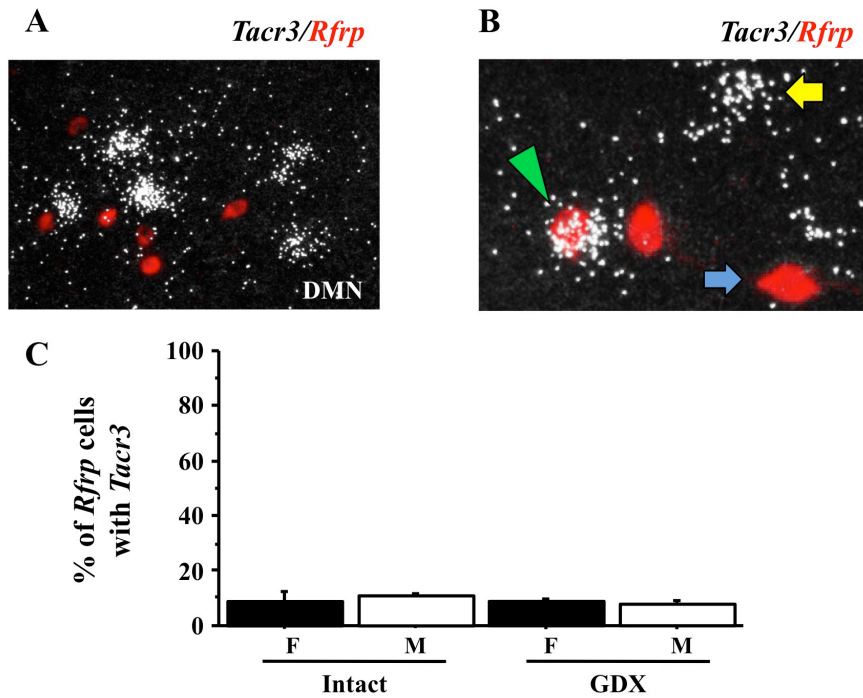


Figure 2.6. Expression of *Tacr3* in *Rfrp* by double label *in-situ* hybridization. **[A]** Representative photomicrographs of double label *in-situ* hybridization of *Rfrp* (red fluorescence) and *Tacr3* (silver grains) in the DMN of an intact male mouse. **[B]** *Rfrp* neurons co-expressing *Tacr3* (green arrowhead) and a cell expressing *Tacr3* without *Rfrp* (yellow arrow). **[C]** Quantification of the percent co-expression of *Tacr3* in *Rfrp* neurons between gonadally-intact females (F) and males (M) and gonadectomized (GDX) M and F. There were no significant differences in co-expression between any of the groups.

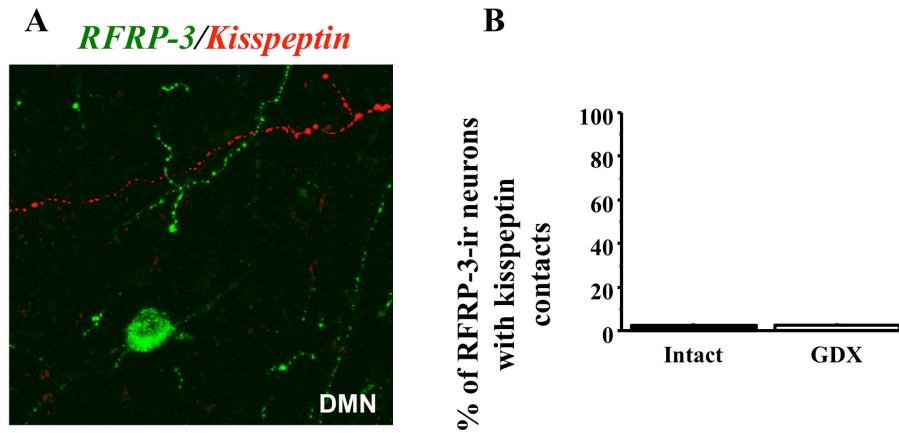


Figure 2.7. Immunohistochemistry for kisspeptin fibers and RFRP-3 cell bodies in the DMN. **[A]** Immunohistochemistry of an RFRP-3 cell body and fibers (green fluorescence) and a kisspeptin fiber (red fluorescence) in the DMN of a gonadally-intact male. **[B]** Quantification of the percent of RFRP-3 neurons receiving contacts from kisspeptin fibers in the DMN of intact and gonadectomized (GDX) male mice. Almost no RFRP-3 cells were contacted and there was no statistical difference between gonadal states.

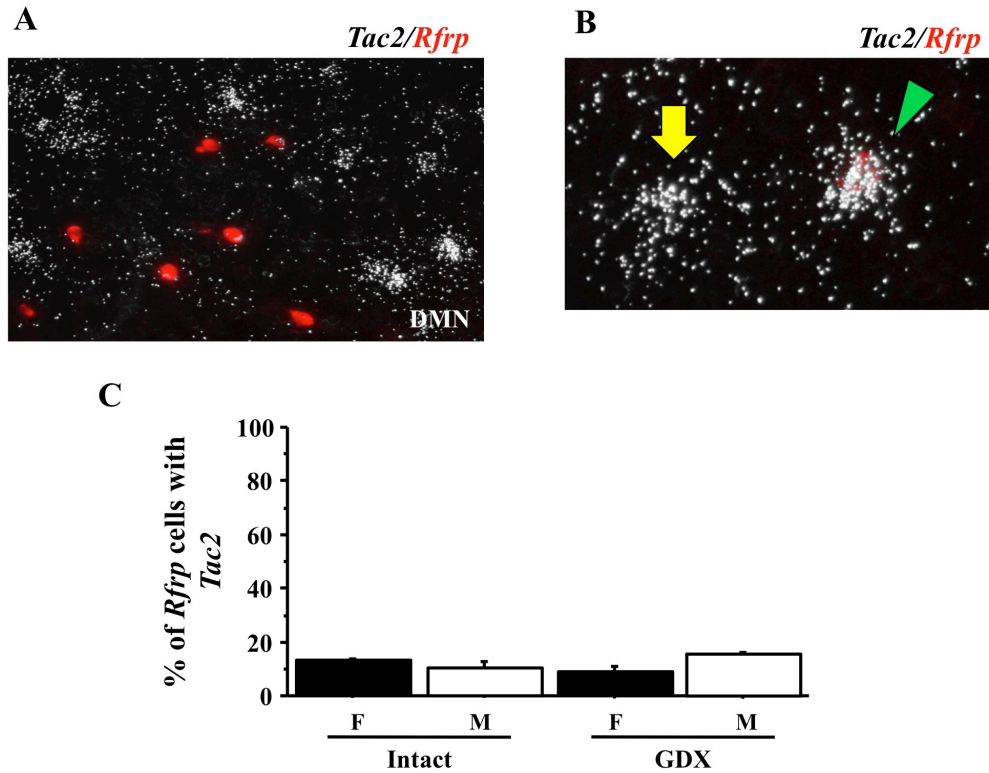


Figure 2.8. Expression *Tac2* in *Rfrp* neurons in the DMN by double label *in-situ* hybridization. [A] Representative photomicrographs of double label *in-situ* hybridization of *Rfrp* (red fluorescence) and *Tac2* (silver grains) in a diestrous female. [B] *Rfrp* neurons co-expressing *Tac2* (green arrowhead) and a *Tac2* neuron that is not expressing *Rfrp* (yellow arrow). [C] Quantification of the percent co-expression of *Gpr147* in *Tac2* neurons between gonadally-intact females (F) and males (M) and gonadectomized (GDX) M and F. These experimental groups.

CHAPTER 3: Regulation of *Rfrp* expression by sex steroids

Abstract

RFRP-3's suppressive effects on the reproductive axis may be a mechanism in which sex steroids, testosterone and estradiol, feedback and regulate GnRH release. If sex steroids regulated RFRP-3 neurons, then *Rfrp* expression would likely be modulated by changes in these sex steroids and RFRP-3 neurons would have the appropriate sex steroid receptors to sense these changes. Using single *in-situ* hybridization, in adult mice, estradiol and testosterone moderately repress *Rfrp* expression in both high expressing and low expressing cells, while the non-aromatizable androgen dihydrotestosterone has no effect. Using double-label ISH, it was determined that ~25% of *Rfrp* neurons co-express estrogen receptor alpha in each sex, whereas *Rfrp* cells do not readily express androgen receptor in either sex, regardless of hormonal milieu. Given RFRP-3 inhibitory effects on reproduction, this suppression by estradiol and testosterone suggests that RFRP-3 may not be apart of the negative feedback loop. However, these outcomes suggest RFRP-3 may have a role the sex steroid positive feedback loop that occurs during ovulation. *In-situ* hybridization was performed for *Rfrp* mRNA under LH surge like conditions, and no changes in *Rfrp* expression were found at any time point. Interestingly, there was a significant suppression in *c-Fos* co-expression in *Rfrp* neurons of females around the time of lights off, when the LH surge is at its peak. This suppression of *c-Fos* co-expression was not observed in male mice, suggesting female, sex steroid positive feedback specific mechanism. These experiments provide insight into the sex steroid regulation of *Rfrp* expression.

Introduction

Sex steroids regulate many neuropeptide systems, but contradictory outcomes currently exist regarding the roles of these hormones in regulating *Rfrp* neurons. Estradiol (E_2) treatment had no effect on total *Rfrp* mRNA levels in female rats (66) but decreased total *Rfrp* expression in female mice (137). Further clouding the issue, another study in female rats reported that E_2 treatment increases total *Rfrp* mRNA levels (117). Likewise, the degree of co-expression of sex steroid receptors in RFRP-3 neurons is currently not well characterized. In female hamsters, ~40% of RFRP-3 immunoreactive neurons co-express estrogen receptor alpha ($ER\alpha$) (20), but in female mice, only 20% of *Rfrp* neurons co-express $ER\alpha$ (137). At present, no studies have examined the effects of E_2 on, or the degree of $ER\alpha$ co-expression in, RFRP-3 neurons of male rodents. Furthermore, the regulation of *Rfrp* specifically by androgen pathways has not yet been examined in either sex of any species, nor has the co-expression of androgen receptors (AR) in *Rfrp* neurons been quantified.

Ovulation in female mammals is gated at the neuroendocrine level by an estradiol-mediated positive feedback LH surge. This release of LH is controlled by GnRH neurons, and when estradiol levels are high, and only in the late afternoon, there is an increase in GnRH neuron activity and pulse frequency that induces a surge in LH (135). The mechanism that promotes this switch from positive to negative feedback remains unclear, however it is clear that this event is circadian gated and dependent on estrogen (138,139). RFRP-3 neurons show decreased immunoreactivity and decreased c-Fos co-expression during the late afternoon of proestrus, coinciding with the endogenous LH surge (63). This is also supported by the fact that high estradiol levels, which are present during the LH surge, suppress *Rfrp* mRNA expression in both sexes (124). Furthermore, this decrease in RFRP-3 neuron activity aligns with increased GnRH neuron activity seen during an LH surge (63), suggesting that the increase in GnRH neuronal

activation could be due to an attenuation of RFRP-3 suppressive effects. However, RFRP-3's involvement during the sexually dimorphic LH surge remains unexplored in mice.

These experiment set to determine 1) whether sex steroids, including estradiol and androgens, can affect *Rfrp* neurons in both sexes, 2) whether any sex steroid effects are direct by assessing whether *Rfrp* neurons co-express either ER α and/or AR in both sexes, 3) if *Rfrp* expression or neuronal activation are suppressed prior or during the LH surge.

Materials and Methods

Animals, Gonadectomies, Tissue Collection, and in-situ hybridization

For experiments 1 and 2, adult mice were anesthetized with isoflurane, bilaterally gonadectomized (GDX), and implanted subcutaneously with a SILASTIC capsule (internal diameter 1.47 mm, external diameter 1.96 mm) packed with E₂ (4 mm, 1:4 with cholesterol), testosterone (T, 6 mm), or DHT (8 mm), or received no implant. These implants have been shown previously to produce elevated physiological levels of hormone (87.9 ± 10.0 pg/mL for E₂; 11.1 ± 0.8 ng/mL for T; 2.8 ± 0.7 ng/mL for DHT) (101,102) and to significantly change gene expression of other neuropeptides in adult mice (101,102,106,109). One week after GDX, animals were anesthetized with isoflurane and rapidly decapitated. Brains were collected, frozen on dry ice, and stored at -80°C.

For experiment 3, adult C57BL6 mice were housed on a 12-12 light-dark cycle (lights off at 1700h) with food and water and a running wheel available *ad libitum*. All mice were anesthetized with isoflurane and bilaterally gonadectomized and subcutaneously implanted with a SILASTIC capsule (inner diameter = 0.20 cm, outer diameter = 0.318 cm) capsules containing either 0.625 μ g (for females) or 0.885 μ g (for males) of 17- β E₂ dissolved in sesame oil (105,140). This treatment produces constant E₂ levels of 20–30 pg/ml, similar to female mouse

proestrus levels (105,140,141). Pilot experiments determined males required a higher dose of $17\text{-}\beta$ E_2 to produce the 20-30 pg/mL of serum E_2 , likely due to increased body weight (*data not shown*). Under this hormonal milieu, female mice demonstrate a daily circadian-timed LH surge around the time of lights off. After three days of recovery, animals were anesthetized with isoflurane and sacrificed by rapid decapitation. Brains were collected, frozen on dry ice, and stored at -80°C .

For all experiments, five coronal series of 20 μm brain sections were cut on a cryostat, thaw-mounted onto Superfrost-plus slides, and stored at -80°C until use in *in-situ* hybridization. *In-situ* hybridization was performed for *Rfrp* (single label) or *Rfrp* and *ER α* , or *Rfrp* and *AR*, or *Rfrp* and *c-Fos* (double labels) as described in Chapter 1. Signal-to-background ratios for individual cells were calculated, and a cell was considered double-labeled if its ratio was > 4 for *ER α* and *AR* co-expression *Rfrp* experiments. A cell was considered double label if signal-to-background ratio > 3 for *c-Fos* and *Rfrp* co-expression experiments.

All experiments were conducted in accordance with the NIH Animal Care and Use Guidelines and with approval of the Animal Care and Use Committee of the University of California, San Diego.

Statistical Analysis

All data are expressed as the mean \pm SEM for each group. In all experiments, differences were analyzed by Student's t-test or by 2-way ANOVA, followed by post-hoc comparisons for individual sex/treatment groups or time points via Fisher's (protected) least significant difference. Statistical significance was set at $p < 0.05$. All analyses were performed in Statview 5.0.1 (SAS Institute, Cary, NC).

Experiment 1: Evaluation of the regulatory effects of E₂ and androgens on Rfrp expression in adult gonadectomized males and females

The effects of E₂ on *Rfrp*-expressing cells are unclear and not fully characterized. Moreover, the effects of E₂ on *Rfrp* have not yet been examined in males, nor have the effects of non-aromatizable androgens (DHT) on *Rfrp* neurons been examined yet in any species. The first experiment examined whether *Rfrp* expression differs between GDX mice of each sex with and without E₂ replacement. Adult male and female mice were GDX and implanted with steady-state E₂ (or nothing). Brains were collected one week later and assayed for *Rfrp* expression via ISH (n = 6 animals/group). The next experiment tested whether *Rfrp* expression is regulated by androgens. Adult GDX males were given implants containing E₂, T, or non-aromatizable DHT, or received no implant. One week later, brains were collected and assayed for *Rfrp* expression using ISH (n = 6 animals/group).

Experiment 2: Co-expression of sex steroid receptors in Rfrp neurons in males and females

If sex steroids act directly on *Rfrp* neurons, then sex steroid receptors should be co-expressed in *Rfrp* cells. Brains from gonadally-intact males and females (diestrous), as well as GDX + E₂ males and females, were assayed for co-expression of ER α in *Rfrp* neurons using double-label ISH. In a separate experiment, alternate sections from the same gonadally-intact and E₂-treated groups were assayed for AR co-expression in *Rfrp* neurons by double-label ISH (n = 6-7 animals/group/assay).

Experiment 3: Changes in Rfrp expression and Rfrp neuron activation during the LH surge

E₂ appears to have a suppressive effect on *Rfrp* expression. This mechanism may be a part of the female-only LH surge positive feedback loop, in which *Rfrp* neurons are suppressed,

in either *Rfrp* expression and/or *c-Fos* induction, to reduce RFRP-3 inhibitory tone on GnRH neurons. This removal of RFRP-3's inhibition would allow the LH surge to escalate without the damping effects of RFRP-3 on LH secretion. To test this hypothesis, adult male and female mice were gonadectomized and estrogen replaced (see Chapter 3 *Animals, Gonadectomies, and Tissue Collection* subheading). Two days after recovery, brains were collected and processed ISH and serum was collected to measure LH and confirm E_2 levels. Animals were sacrificed at five time points; clock time (CT) 4 and CT12, corresponding to the baseline and peak LH surge levels, as well as CT10.5 and CT13.5, gating 90 minutes on either side of the peak of the LH surge, and CT18 which is after the LH surge and when LH levels and neuronal activity would return to baseline values ($n = 7-11$ animals/sex/time point). Clock time nomenclature is used for this experiment to standardize the time points to circadian time, which defines lights-off as CT12.

Results

Experiment 1: Rfrp expression is moderately regulated by E_2 in both sexes and unaffected by DHT

This experiment tested if *Rfrp* expression or cell number is altered by E_2 or androgens in adult mice of either sex. There is no significant difference in the total number of *Rfrp* neurons between GDX and GDX + E_2 animals in either sex. However, E_2 treatment significantly decreased the overall relative amount of *Rfrp* mRNA/cell, as well as the total amount of *Rfrp* mRNA in the DMN, in both males and females ($p < 0.05$, Figure 3.1).

When *Rfrp* cells were subdivided into HE and LE cells, both the number of HE cells and the amount of *Rfrp* mRNA/HE cell were significantly reduced by E_2 treatment in both sexes (Figure 3.1C, $p < 0.05$). E_2 also significantly reduced the relative amount of *Rfrp* mRNA/cell of

LE cells in both sexes (Figure 3.1D, $p < 0.05$), but had no effect on LE cell number. No sex differences in *Rfrp* expression were detected in GDX or GDX + E₂ animals for any measures.

Like E₂, androgens can influence gene expression, either by acting through AR or acting via ER after aromatization to E₂. Therefore the effects of T or DHT *Rfrp* expression was tested in adult males. The inhibitory effect of E₂ on *Rfrp* levels observed above was reproduced in this assay, with E₂ having no effect on total cell number but significantly reducing the relative amount of *Rfrp* mRNA per cell ($p < 0.05$, Figure 3.2). Likewise, T treatment did not change *Rfrp* cell number but induced a small, but significant, reduction in the relative amount of *Rfrp* mRNA/cell and total *Rfrp* mRNA levels ($p < 0.05$ relative to GDX controls, Figure 3.2). In contrast, DHT treatment had no effect on either the total number of *Rfrp* cells, the relative amount of *Rfrp* mRNA per cell, or total *Rfrp* levels (Figure 3.2).

When examining just HE cells, both E₂ and T significantly reduced the number of HE cells and relative amount of *Rfrp* mRNA/HE cell (Figure 3.2C, $p < 0.05$ compared to GDX controls), whereas DHT had no effect on either measure. LE cell numbers were not changed by any hormone treatment, though E₂ (but not T or DHT) significantly reduced relative *Rfrp* mRNA/cell of LE cells (Figure 3.2D, $p < 0.05$). Thus, unlike E₂, DHT had no effect on any *Rfrp* measure.

Experiment 2: A small proportion of Rfrp neurons co-express ER α in both sexes but virtually no Rfrp cells co-express AR

Only two studies have examined ER α co-expression in *Rfrp* cells of female rodents, but the results were not similar, leaving the issue unresolved. Additionally, ER α /*Rfrp* co-expression in males has not been determined, nor have co-expression levels of AR in *Rfrp* cells been reported in either sex. It was determined that ER α mRNA is expressed in ~25% of *Rfrp* neurons,

and the degree of co-expression does not significantly differ between sexes or hormonal treatments (Figure 3.3A-C). The number of *ERα* silver grains in *Rfrp* cells was low, with only ~9 silver grains per cell, suggesting that *ERα* is only weakly expressed in these cells. In contrast, high *ERα* expression in the arcuate nucleus of the same animals was observed (Figure 7B). Unlike *ERα*, *AR* mRNA was virtually undetectable in *Rfrp* cells, with < 3% of *Rfrp* neurons co-expressing *AR* in both sexes (Figure 3.3D-F). High *AR* expression was readily detected in the same animals elsewhere in the brain, such as the ventromedial nucleus (Figure 3.3E).

Experiment 3: Temporal Rfrp expression in the DMN of GDX + E₂ replaced female and male mice

The GDX + E₂ paradigm used in experiment 3 is intended to induce an LH surge in female, but not male mice, around the time of lights off. In order to confirm this, serum LH and E₂ values were measured in all animals. In the female mice, serum LH values were near undetectable at CT4 and increased significantly at CT10.5 and CT12, and then fell back to near undetectable levels at CT13.5 and CT18. Males showed no circadian changes in serum LH (Figure 3.4). Circulating E₂, which originates from the implanted capsule, was not different between sexes or time points (*data not shown*).

It was hypothesized that RFRP-3 expression or neuronal activity is inhibited prior to an LH surge, to allow increased GnRH release and subsequent LH secretion. To test this, GDX + E₂ were examined via single label and double label ISH for *Rfrp* mRNA. Using single label ISH, there were no differences in the number of *Rfrp* neurons or the amount of *Rfrp* mRNA detected in the hypothalamus at any time point in either sex (Figure 3.5A-C). Conversely, there was a significant decrease in *c-Fos* co-expression in *Rfrp* neurons in female mice during the height of, and immediately after, the LH surge, as determined by double label ISH (Figure 3.6A-B). Male

mice, however, showed no circadian changes in *c-Fos* co-expression, which remained constant throughout the day (Figure 3.6C-D).

Discussion

Given RFRP-3's potent inhibitory effects on LH secretion, it seemed plausible that sex steroids may regulate *Rfrp* mRNA as a mechanism of positive or negative feedback. Therefore, using single label ISH, it was determined that in both sexes, E₂ has a moderate inhibitory effect on *Rfrp* expression whereas non-aromatizable androgens have no effect on *Rfrp* expression, supported by a relative lack of AR in *Rfrp* cells. Some of the inhibitory effects of E₂ may be achieved by direct action in *Rfrp* cells, because a small proportion of *Rfrp* neurons co-express *ERα* in both sexes. When examining sex steroid positive feedback during the preovulatory LH surge, there were no significant differences in *Rfrp* expression at any time point in either sex. However, *Rfrp* neuronal activation, as measured by *c-Fos* co-expression, was significantly diminished, around lights off, during the height of the LH surge in female mice. Conversely, *c-Fos* co-expression remained unchanged in male mice at all time points. In concert, these data demonstrate that *Rfrp* is suppressed by sex steroids, which may play into the regulation of the LH surge.

Previous reports have examined E₂ regulation of *Rfrp* in only females, and with inconsistent results (117,137). The present experiment shows that E₂ moderately represses *Rfrp* expression in mice of both sexes, including reducing expression levels in both LE and HE cells. Although E₂ also reduced HE, but not LE, cell number, a similar decrease in LE cell number may have been masked by some 'original' HE cells reducing their *Rfrp* expression levels to become LE cells. The purpose of the E₂-mediated repression of *Rfrp* is unclear but does not support a role for RFRP-3 in E₂-mediated negative feedback, since such a model would predict that E₂

upregulates *Rfrp* to increase inhibition of GnRH. Such E₂-induced repression of *Rfrp* could possibly relate to reducing RFRP-3-mediated inhibition of GnRH during the LH surge, though it's unclear why E₂ would act similarly in males (who lack positive feedback). Alternatively, E₂ may regulate RFRP-3's involvement in other non-reproductive functions, such as temperature or energy homeostasis (64,76,93), or cognitive behaviors (95,142).

Only ~ 25% of *Rfrp* neurons co-express ER α mRNA in both males and females, regardless of the sex steroid milieu, consistent with ~ 20% co-expression detected previously in female mice by immunohistochemistry (137). E₂'s inhibitory effects on *Rfrp* expression may therefore be mediated directly in only a small subset of *Rfrp* neurons, or conversely, E₂ may regulate other "upstream" circuits that signal to *Rfrp* neurons. Whether or not ER α co-expression is restricted to just HE or LE cells is unknown, though both subpopulations were affected by E₂ treatment.

The role of androgens in regulating *Rfrp* in mice has not been previously assessed. In contrast to E₂ and T, DHT had no discernable effect on *Rfrp* cell number or mRNA levels, suggesting that androgen-signaling pathways are not important regulators of RFRP-3 neurons. This conclusion is supported by the finding of virtually no co-expression of *AR* in *Rfrp* cells of either sex.

Since the first experiment found that *Rfrp* is suppressed by high levels of E₂ rather than being upregulated as was expected, it was next hypothesized that E₂ suppressed *Rfrp* expression in a mechanism of removing inhibition on the reproductive axis during the LH surge. When given exogenously, RFRP-3 is able to blunt the LH surge and activation of GnRH neurons during the LH surge in rats (90), and in Syrian hamsters, the number of RFRP-3 immunoreactive cell bodies is significantly lower during the height of the LH surge, returning to diestrous levels as the surge diminishes (63). However, in the present study, in E₂-treated female mice, there appear to be no

significant changes in *Rfrp* mRNA expression during the LH surge, nor are there any changes in similarly-treated male mice. The activation of *Rfrp* neurons, as measured by *c-Fos* co-expression, did decrease during the LH surge in female mice, similar to the pattern seen in the Syrian hamsters (63). Interestingly, both studies show that the peak of the LH surge precedes the majority of inhibition in *Rfrp* neuron activation, opposite of what would be expected. If the removal of RFRP-3 secretion was necessary for an LH surge to occur, it stands to reason that *Rfrp* neuron activation would be inhibited prior to the LH surge, not after the climax. However, both the data presented here and in Gibson et al. (63) show an inhibition of *Rfrp* neuron activation after the majority of the LH surge is completed. Therefore, it is possible that the inhibition of *Rfrp* neuron activation presented here is a secondary effect of the overall changes in neuronal activity that occurs during the LH surge. This inhibition of activity may allow LH secretion to continue throughout the surge but is not necessary for triggering surge onset.

The suppression in *Rfrp* neuron activation in E₂-treated mice is sexually dimorphic, as the *Rfrp* neurons of male mice showed no changes in *c-Fos* co-expression between any circadian time points. To date, this is the only known sex difference in *Rfrp* neurons, as previous investigations into sex differences in *Rfrp* neurons have yielded no significant effects of sex (20,124,126,143). This novel sex difference may be intrinsic to the *Rfrp* neuron itself, or *Rfrp* neurons in female mice may receive sexually dimorphic inputs from other brain regions. The DMN is generally not considered a sexually dimorphic nucleus (113,144), so an intrinsic sex difference in *Rfrp* neurons seems unlikely but remains possible. The knowledge of *Rfrp* neuron afferents is currently limited, but further investigation may yield novel supporting sexually dimorphic inputs to *Rfrp* neurons, explaining this difference in neuronal activation.

In summary, this chapter demonstrated that 1) *Rfrp* expression is suppressed by E₂ and T, but not DHT, suggesting an estrogen receptor mechanism 2) *ERα* is present in some *Rfrp* neurons

but *AR* from all *Rfrp* neurons, and 3) *Rfrp* neuronal activation is suppressed during the height of LH surge in females and this estradiol effect, in combination with circadian gating, possibly promotes the LH surge.

Portions of this chapter are published in *Endocrinology* (April 2012). The dissertation author was the primary investigator and author of this material. Josh Kim and Sangeeta Dhamija provided support with brain cyrosectioning and performing ISH. Alexander Kauffman supervised the project and provided advice.

Portions of this chapter are in preparation for publication. The dissertation author was the primary investigator and author of this material. Elena Luo assisted in animal preparation, tissue collection, cyrosectioning and performing ISH assays. Alexander Kauffman supervised the project and provided advice.

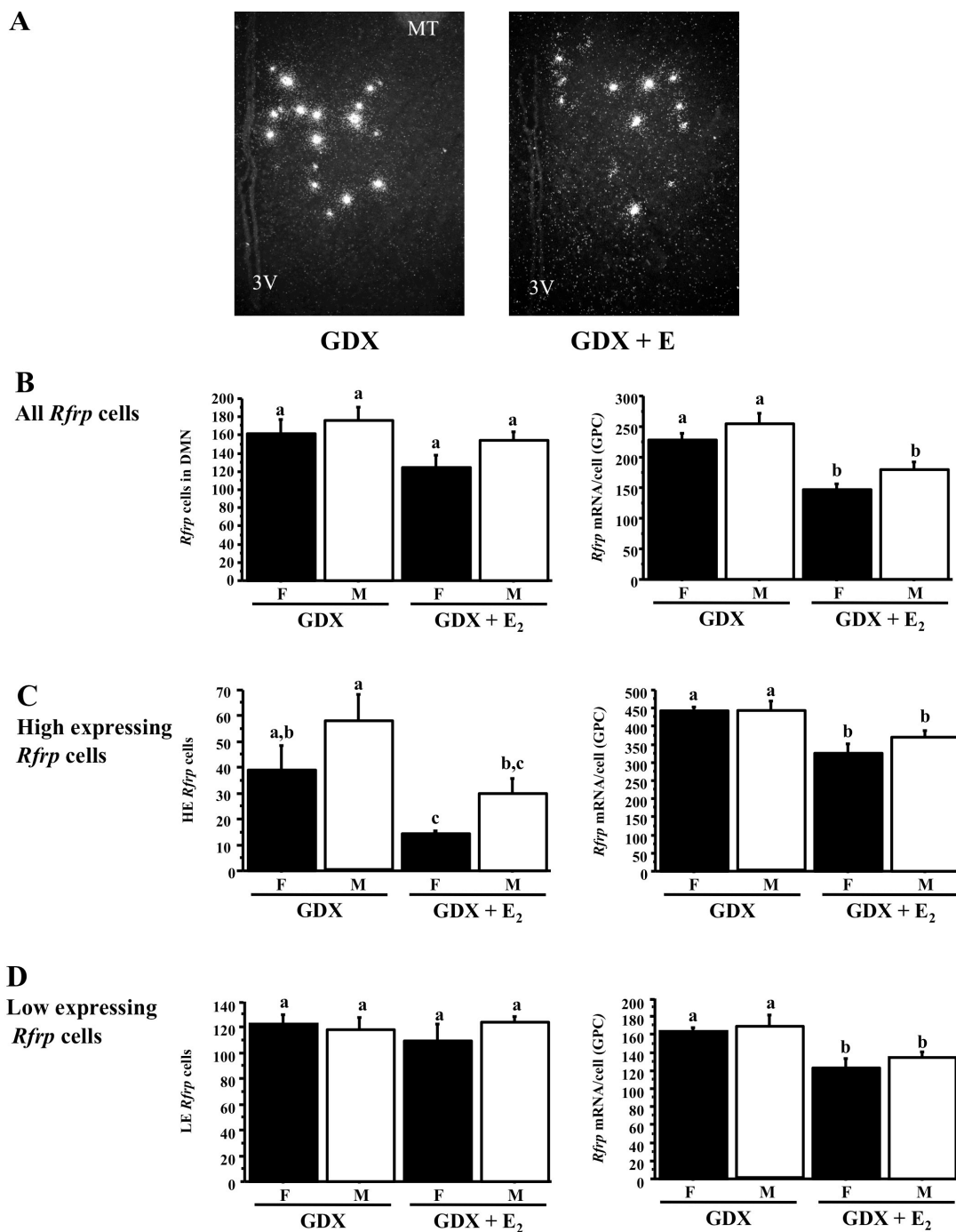


Figure 3.1. Changes in *Rfrp* expression with E₂ treatment. **[A]** Photomicrographs of *Rfrp* expression in gonadectomized (GDX) and gonadectomized with E₂-replaced (GDX + E₂) adult females. 3V, third ventricle. **[B]** Mean changes in the total number of *Rfrp* cells and *Rfrp* mRNA/cell of all cells in GDX and GDX + E₂ males (M) and females (F). **[C]** Mean changes in the high-expressing (HE) *Rfrp* cells. **[D]** Mean changes in the low-expressing (LE) *Rfrp* cells in GDX and GDX + E₂ M and F. Different letters designate significantly different groups ($p < 0.05$).

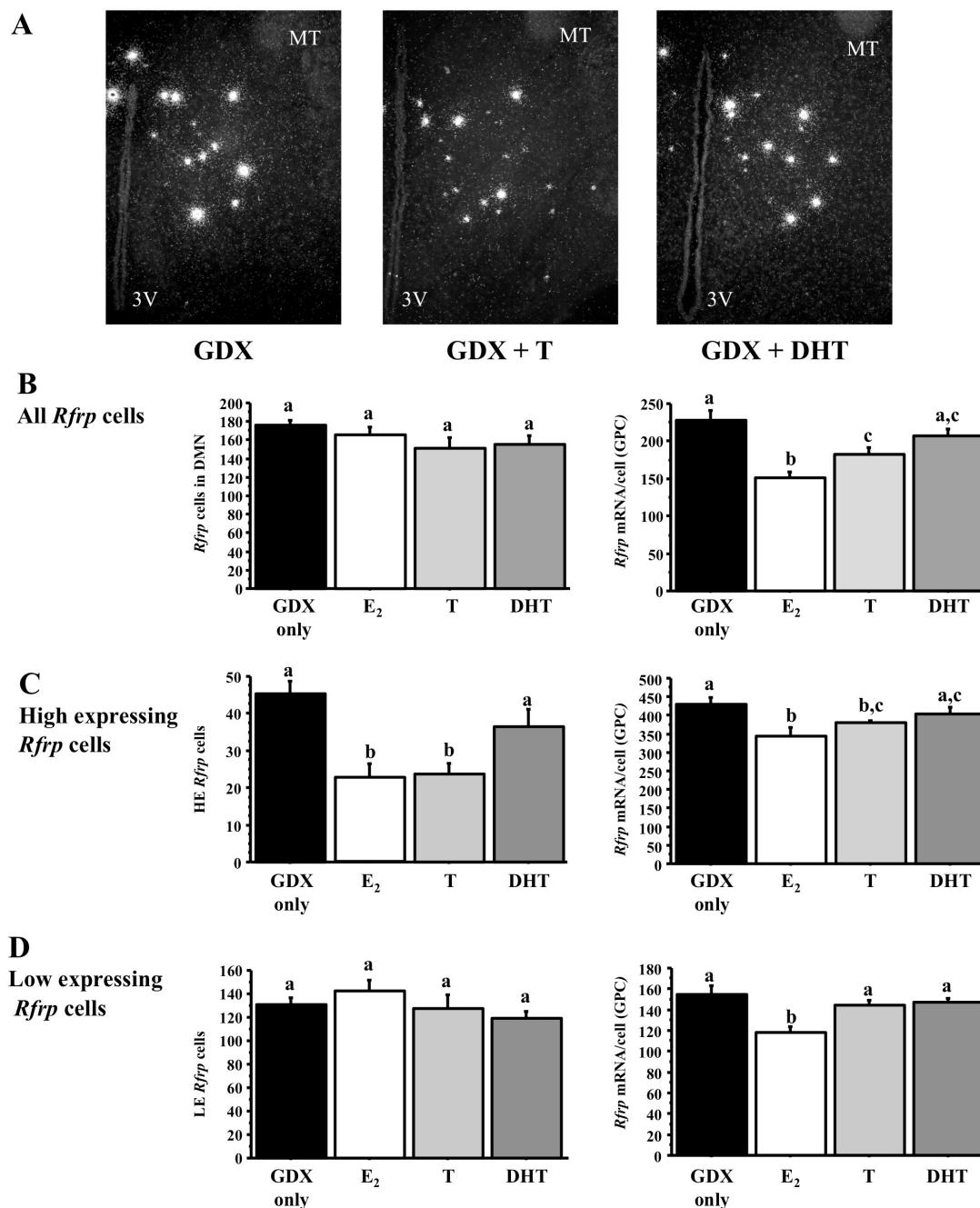


Figure 3.2. Changes in *Rfrp* expression with androgen treatment. [A] Representative photomicrographs of *Rfrp* expression between gonadectomized (GDX) and gonadectomized with testosterone replaced (GDX + T) and gonadectomized with dihydrotestosterone (GDX + DHT) replaced adult males. 3V, third ventricle. [B] Mean changes in the total number of *Rfrp* cells and *Rfrp* mRNA/cell of all cells. [C] Mean changes in the high-expressing (HE) *Rfrp* cells and *Rfrp* mRNA/HE cell. [D] Mean changes in the low-expressing (LE) *Rfrp* cells and *Rfrp* mRNA/LE cell. Bars labeled with different letters designate significantly different groups ($p < 0.05$).

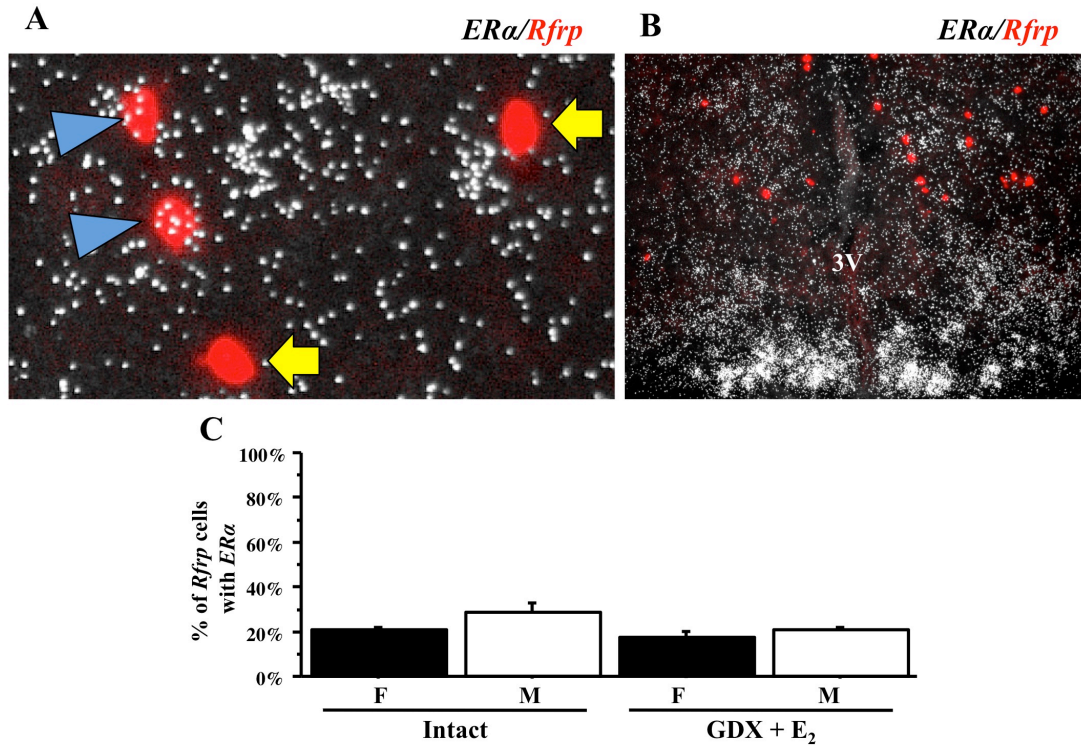


Figure 3.3. Expression of ER α in *Rfrp* neurons by double label *in-situ* hybridization. **[A]** Representative photomicrographs of double label *in-situ* hybridization of *Rfrp* (red fluorescence) and ER α (silver grains) in a diestrous female. *Rfrp* neurons co-expressing ER α (blue arrowhead) and *Rfrp* neurons with no co-expression of ER α (yellow arrows). 3V, third ventricle. **[B]** Low power magnification photomicrograph of extensive ER α expression (silver grains) in the arcuate nucleus, with red *Rfrp* neurons labeled in the DMN (same animal as [A]). **[C]** Quantification of the percent co-expression of ER α in *Rfrp* neurons between gonadally-intact females (F) and males (M), as well as in GDX + E₂ F and M. There were no significant differences in co-expression between any of the groups.

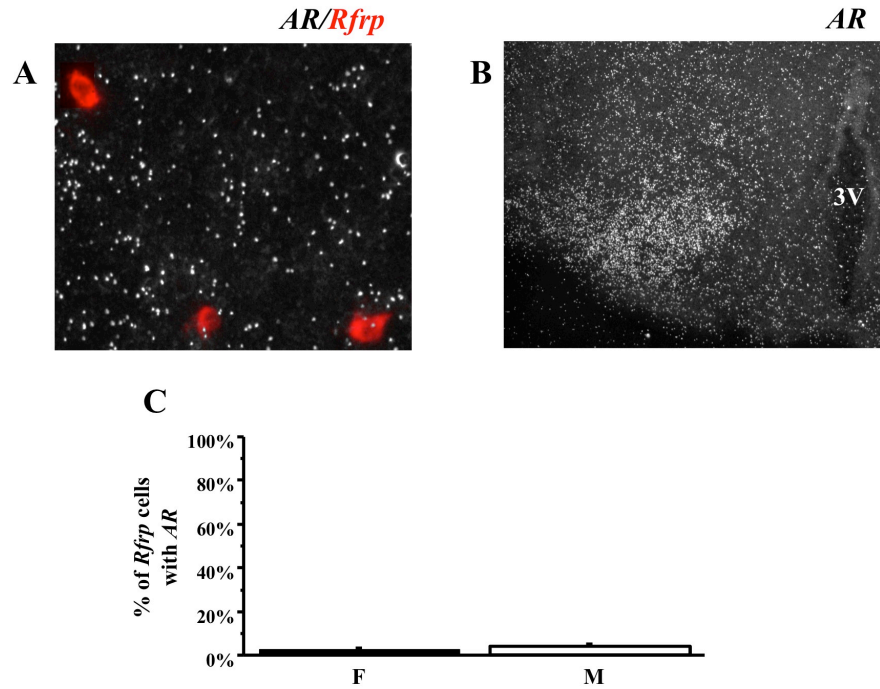


Figure 3.4. Expression of AR in *Rfrp* neurons by double label *in-situ* hybridization. [A] Representative photomicrographs of the lack of androgen receptor (*AR*) expression in *Rfrp* neurons. [B] Significant *AR* expression in the hypothalamic ventromedial nucleus of a male mouse from the same assay. [C] Quantification of the percent co-expression of *AR* in *Rfrp* neurons between females (F) and males (M).

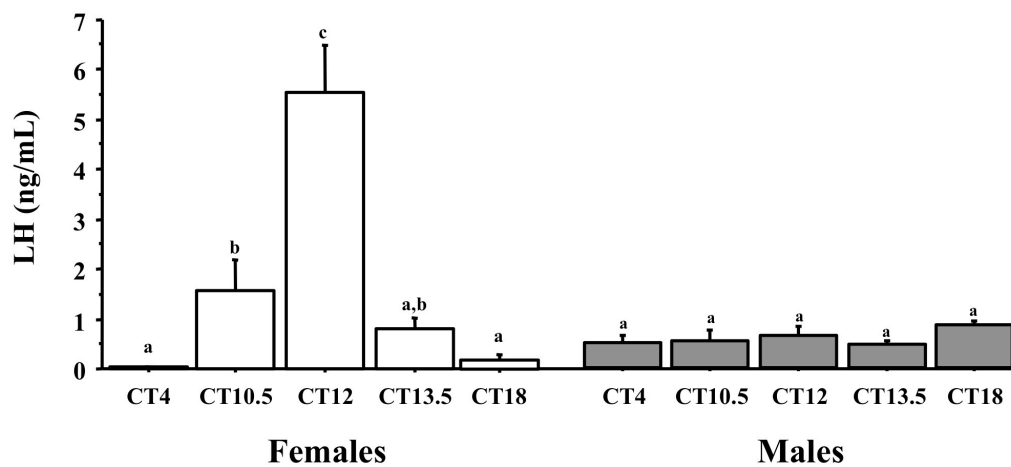


Figure 3.5. Serum LH of gonadectomized and estrogen replaced female and male mice. Female mice show statistically significant increase in serum LH, occurring shortly before and during the dark phase, while males show no differences in serum LH at any time. $p < 0.05$, different letters indicate significantly different groups.

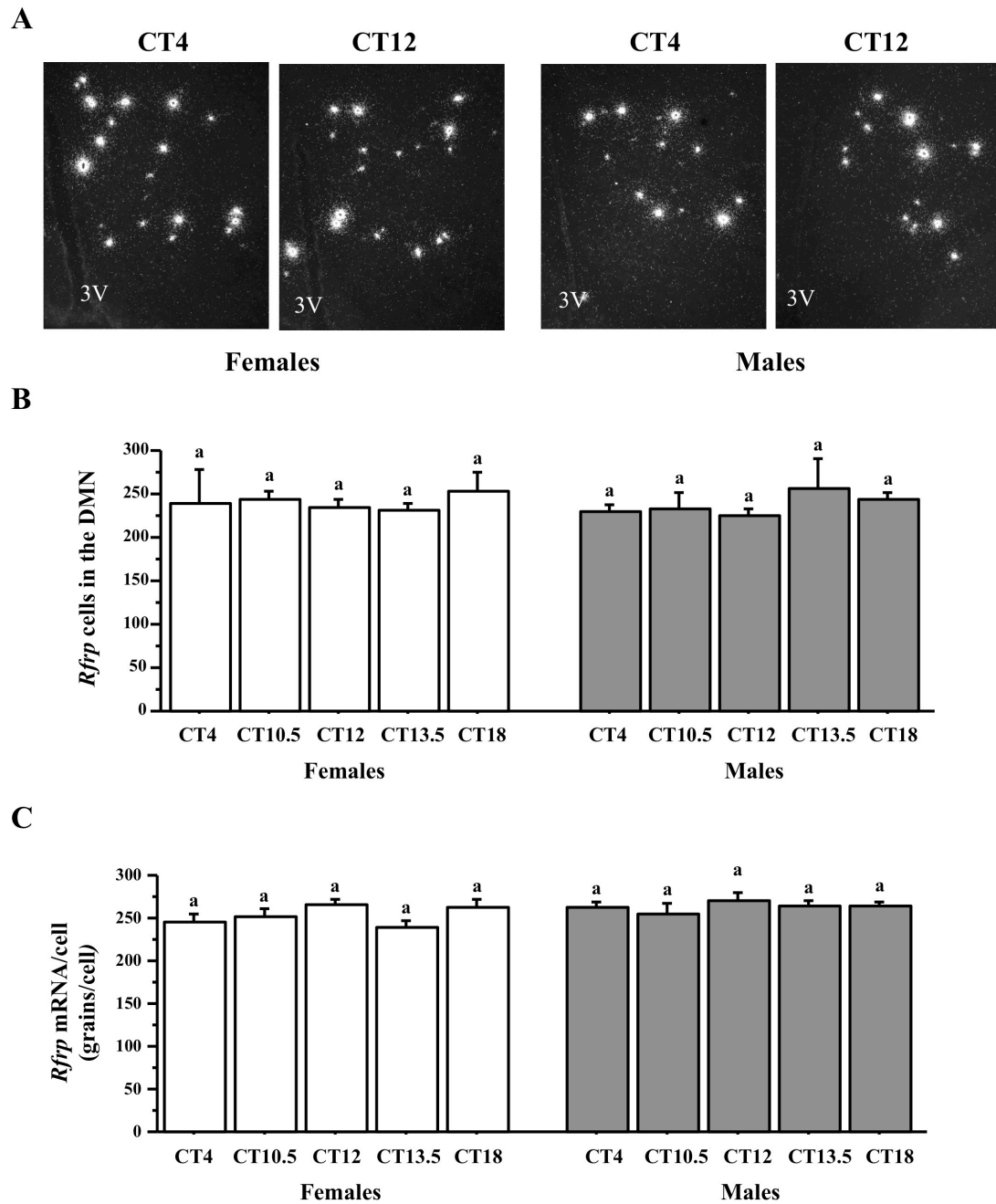


Figure 3.6. *In-situ* hybridization for *Rfrp* mRNA in the DMN during the time of the LH surge. **[A]** Representative photomicrographs of *Rfrp* mRNA in the DMN in both males and females at two time points. All animals are gonadectomized and estrogen replaced. 3V = third ventricle. **[B]** Quantification of the number of *Rfrp* neurons in the DMN. **[C]** Quantification of the grains per cell (a semi-quantitative measure of mRNA) of *Rfrp* neurons in the DMN. $p < 0.05$, different letters indicate significantly different groups.

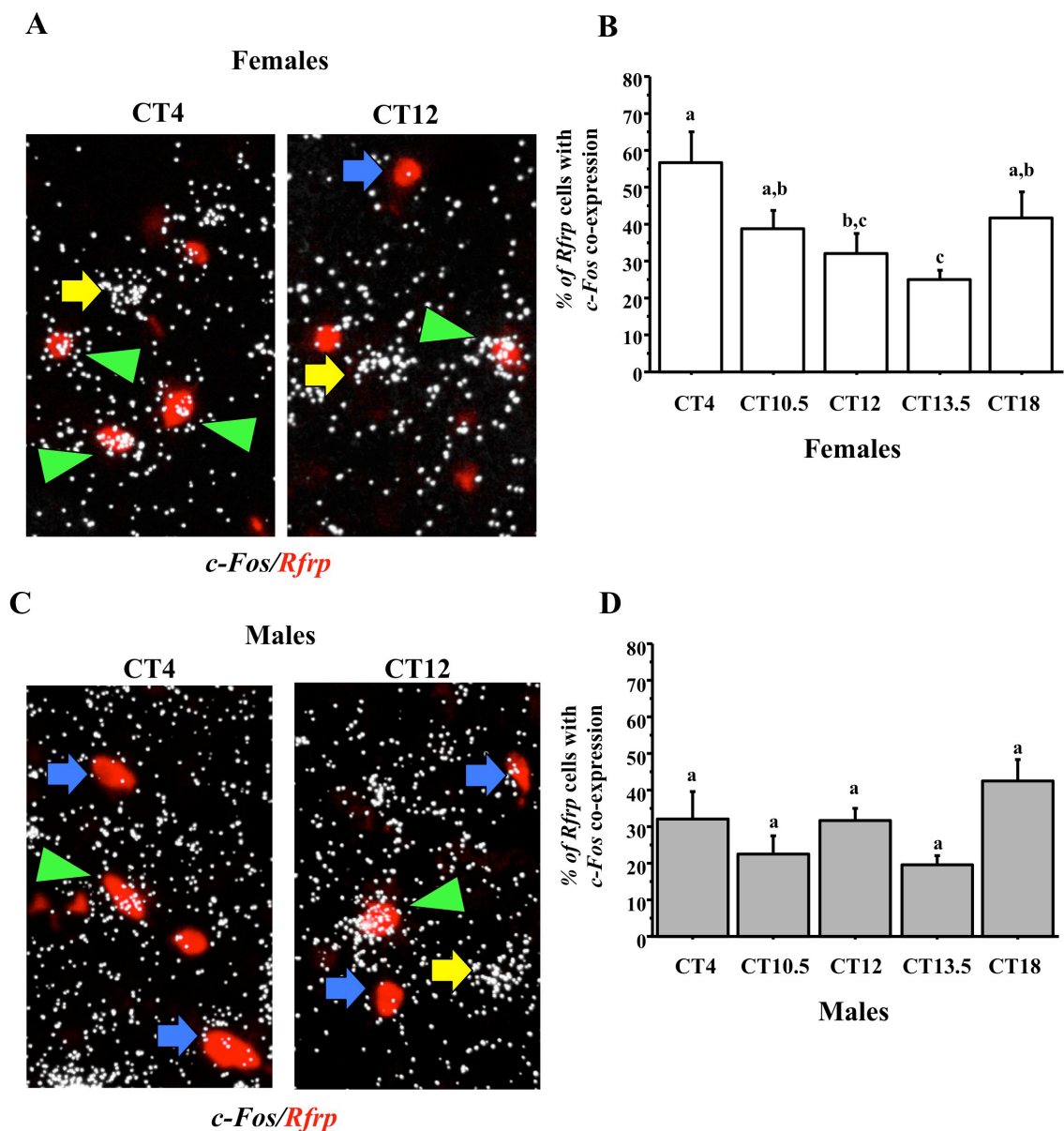


Figure 3.7. *In-situ* hybridization for *c-Fos* co-localization in *Rfrp* neurons during the time of the LH surge. **[A]** Representative photomicrographs of *c-Fos* (a marker of neuronal activation, silver grains) co-localizing with *Rfrp* neurons (red fluorescence) of female mice sacrificed at two time points, in the morning and during the LH surge. Female mice sacrificed at CT12 have less *c-Fos* co-localization than females sacrificed at CT4. **[B]** Quantification of *c-Fos* co-expression in *Rfrp* neurons of female mice before (CT4) and during the LH surge (CT12). **[C]** Representative photomicrographs of co-localizing with *Rfrp* neurons of male mice sacrificed at CT4 and CT12. Males have no noticeable differences in the degree of co localization. **[D]** Quantification of *c-Fos* co-expression in *Rfrp* neurons of male mice in the morning and evening. $p < 0.05$, different letters indicate significantly different groups.

CHAPTER 4: Changes in *Rfrp* expression and neuronal activation with metabolic and glucocorticoid-mediated stressors

Abstract

RFRP-3 may be a mediator of the metabolic or stress regulation systems that modulate reproductive function. To explore these possibilities, a series of experiments were conducted to characterize and begin teasing apart *Rfrp* neurons under stress conditions. Using double label ISH, *Rfrp* neurons appear to express glucocorticoid receptor, and a small subpopulation of *Rfrp* neurons co-express the leptin receptor, allowing for the possibility of direct glucocorticoid or leptin signaling in these cells. This finding is extended by the observation that adult Ob animals have less *Rfrp* expression, as determined by single label ISH, than their wildtype littermates. Surprisingly, *Rfrp* neurons in female and male mice appear to be resistant to short-term food deprivation, despite previous reports demonstrating effects of chronic food restriction on the activation of RFRP-3 neurons in other species. Finally, *Rfrp* expression and neuron activation are suppressed under various models of glucocorticoid-mediated stress, such as immobilization and corticosterone injections, which is in opposition with findings in other model species. Collectively, these data provide an insight into the role RFRP-3 may play in metabolic and glucocorticoid-mediated stressors.

Introduction

Various non-reproductive hormones input onto the reproductive axis, allowing modulation of the reproductive process during times of nutritional excess or limitations. Two of these hormones, leptin and corticosterone, have been studied extensively throughout reproductive biology but the mechanism of action for these two hormones on the reproductive system are not fully explored.

Leptin, a hormone secreted from adipocytes, has strong effects on hypothalamic regulation of satiety, energy expenditure, and body weight, not to mention a stimulatory (permissive) role in reproductive function. *Obese* mice (*Ob*) have a non-functional leptin gene and are morbidly overweight, hyperphagic, have low LH levels, and are infertile (145,146), illustrating the importance of leptin in maintenance of both energy homeostasis and reproduction. Leptin does not directly regulate GnRH neurons, as the long form of the leptin receptor (*LepRb*), which is responsible for signal transduction, is not expressed in GnRH neurons (147,148). Rather, leptin acts on GnRH neurons indirectly, through upstream intermediates that have yet to be fully identified. RFRP-3 neurons may be one potential relay system through which leptin signals are mediated, as the DMN (where RFRP-3 neurons reside) is a highly leptin-responsive brain region (149-151). Central injections of RFRP-3 not only inhibit LH secretion, but also stimulate feeding behavior (77,152). Moreover, RFRP-3 neurons are activated by chronic mild food restriction in hamsters (153), and RFRP-3's receptor, *Gpr147*, is required in mice to suppress LH secretion after acute food deprivation (89), suggesting that RFRP-3 plays a role in both energy balance and reproduction, as does leptin (154). Thus, it is possible that leptin might inhibit the production and/or secretion of RFRP-3 in order to facilitate reproductive function and/or suppress feeding behavior. Starvation activates gene programs in a variety of hypothalamic regions, including the DMN and has a potent suppressive effect on LH secretion (155,156). Increased *Rfrp* neuron activation is observed during caloric restriction in Syrian hamsters (153) and RFRP-3's potent

orexigenic effects (64,76,77) suggesting that *Rfrp* neurons would respond to short term food deprivation.

Corticosterone is a glucocorticoid steroid hormone secreted from the adrenal gland in response to various forms of physiological and psychological stress. High levels of corticosterone is know to inhibit reproductive function at the hypothalamic level, and is supported by evidence that glucocorticoids reduce the LH pulses pulse frequency in gonadectomized female rats as well as decrease the transcription of various reproductive hormones and their receptors (157-159). Because LH pulse frequency is modulated by GnRH release, it is thought that glucocorticoids suppress the frequency of GnRH pulses. The glucocorticoid receptor, GR, is expressed in various brain regions, including a number of nuclei of the hypothalamus (160) allowing for indirect neural targets by which glucocorticoids may modulate GnRH secretion or GnRH synthesis (158). Glucocorticoids may suppress GnRH and LH via direct actions upon the GnRH neuron itself, or through indirect mechanism via other neuronal cell types, such as RFRP-3 neurons. Immobilization stress, or restraint stress, is a common rodent model for increasing endogenous levels of glucocorticoids. LH secretion is suppressed in both male and female rodents by 90 minutes of restraint stress (157,161,162). RFRP-3 is hypothesized to mediate aspects of restraint stress as *Rfrp* expression is increased after 3 hours of immobility in male rats (163). Therefore, *Rfrp* expression, as well as *Rfrp* neuron activation, is hypothesized to be enhanced in restraint stressed mice.

This study sought to determine 1) what relevant metabolic and stress-related genes are expressed in *Rfrp* neurons of adult mice, 2) changes in *Rfrp* expression in Obese (Ob) animals, 3) changes in *Rfrp* expression and *Rfrp* neuron activation under food deprivation conditions, 4) the effect of glucocorticoid-mediated stress on *Rfrp* expression and *Rfrp* neuron activation male mice, as well as in female mice under LH surge conditions.

Methods

Animals, Gonadectomies, Tissue Collection, and in-situ hybridization

All experiments utilized C57BL6 mice, except experiment 2 which used mice from Ob strain (WT and Ob). Mice from the Ob line were purchased from Harlan Laboratories and maintained on a C57BL6 background in the lab. All animals were housed on a 12:12 light-dark cycle, with food and water available *ad libitum*, except where indicated in experiment 3. All experiments were conducted in accordance with the NIH Animal Care and Use Guidelines and with approval of the Animal Care and Use Committee of the University of California, San Diego.

C57BL6 mice were bilaterally gonadectomized (GDX), as previously described in this thesis. Gonadectomy was implemented to promote high levels of circulating LH for food restriction to inhibit, and to simultaneously control for differences in sex steroids between individuals since estradiol and testosterone can both mildly suppress *Rfrp* levels in mice of both sexes (124,137). For adult OB mice, 7-8 week old female or male WT or Ob mice were GDX (again, to control for sex steroids between genotypes and allow for maximal *Rfrp* expression levels in the absence of steroid inhibition) and then sacrificed 7 days later for blood and tissue collection.

For the restraint stress protocol, the animals are placed in ventilated tubes (Harvard Apparatus) that are small enough to restrain a mouse so that it is able to breathe but unable to move freely and have been used previously in this department (162). Experienced personnel continually observe mice during the 90-min restraint period. Mice were sacrificed immediately after completion of the restraint protocol.

For experiment 5, adult C57BL6 mice were housed on a 12-12 light-dark cycle (lights off at 1800h) with food and water available *ad libitum*. All mice were anesthetized with isoflurane and bilaterally gonadectomized and subcutaneously implanted with a SILASTIC capsules to

produce constant E₂ as previously described in Chapter 3. The corticosterone (50 mg/pellet) or cholesterol pellets were implanted at the same time as GDX.

For all experiments, five coronal series of 20 µm brain sections were cut on a cryostat, thaw-mounted onto Superfrost-plus slides, and stored at -80°C until use in *in-situ* hybridization. *In-situ* hybridization was performed for *Rfrp* (single label) or *Rfrp* and *NPY*, or *Rfrp* and *TRH*, *Rfrp* and *LepRb*, or *Rfrp* and *Mc4r*, *Rfrp* and *GR*, or *Rfrp* and *c-Fos* (double labels) as described in Chapter 1.

Blood from adult animals was collected by retro-orbital bleed. Serum luteinizing hormone (LH) was measured by the UVA Ligand Core (range 0.04 – 37.4 ng/mL). Serum corticosterone (CORT) was measured by UVA Ligand Core (range 15 – 2250 ng/mL). Serum leptin was measured using Quantikine Mouse Leptin ELISA kit (R&D Systems) following the manufacturer's protocol (range 1.25 ng/mL – 80 ng/mL).

All experiments were conducted in accordance with the NIH Animal Care and Use Guidelines and with approval of the Animal Care and Use Committee of the University of California, San Diego.

Statistical Analysis

All data are expressed as the mean ± SEM for each group. In all experiments, differences were analyzed by Student's t-test or by 2-way ANOVA, followed by post-hoc comparisons for individual sex/treatment groups or time points via Fisher's (protected) least significant difference. Statistical significance was set at $p < 0.05$. All analyses were performed in Statview 5.0.1 (SAS Institute, Cary, NC).

Experiment 1: What metabolic neuropeptides and receptors are expressed in Rfrp neurons?

The phenotypic identity of *Rfrp* neurons is virtually unknown. Besides estrogen receptor, other receptors or secreted co-factors, such as neurotransmitters or neuropeptides, have not been identified in *Rfrp* neuron. Any number of metabolic genes expressed in the DMN region may co-localize with *Rfrp*, and if so, would give valuable insight to the regulation and functions of RFRP-3 neurons. This experiment examined whether transcripts of important metabolic genes already known to be expressed in the DMN specifically co-localize with *Rfrp*. Adult C57BL6 mice of both sexes (females in diestrous) were sacrificed and their brains collected for double label ISH analyses. Using alternate series of coronal brain sections (encompassing the entire rostral to caudal span of the DMN) from each mouse, 5 separate assays were used to examine the co-expression of neuropeptide Y (*Npy*) (80-82), thyrotropin-releasing hormone (*Thr*) (119,164), leptin receptor long form (*LepRb*) (83), melanocortin receptor 4 (*Mc4r*) (84) and glucocorticoid receptor (*GR*) (160) in *Rfrp* neurons (n = 4-6 per sex).

Experiment 2: Is Rfrp expression altered in adult Ob animals?

Since Experiment 1 found that a subset of *Rfrp* neurons express *LepRb*, it was hypothesized that *Rfrp* expression may be leptin regulated. To determine if *Rfrp* levels are altered with chronic leptin deprivation, *Rfrp* neuron numbers and cellular *Rfrp* expression levels was measured using single label ISH in adult male and female GDX Ob mice (leptin deficient) and their WT GDX littermates (n = 5-7 animals per genotype per sex).

Experiment 3: Is Rfrp expression or neuron activity responsive to short-term metabolic challenge?

Given that RFRP-3 treatment increases food intake (64,76) and that a subset of *Rfrp* neurons express the leptin receptor (Experiment 1), it is possible that transiently diminished

serum leptin levels achieved via short-term food deprivation may alter *Rfrp* expression and/or *Rfrp* neuronal activation. Furthermore, a recent report demonstrated that LH secretion is not suppressed after 12 h of food deprivation (FD) in Gpr147 knockout mice, suggesting RFRP-3 is essential during the first 12 h of FD to suppress LH (89). To further examine this, adult C57BL6 female mice were first GDX (to equate sex steroids between groups, since E₂ can inhibit *Rfrp* levels) and were then later subjected to short-term (12-hour) FD or kept on *ad libitum* (*ad lib*) feeding (controls) (n = 7 per group). All food was removed from FD animals at lights off (1800 h) and all animals were sacrificed 12 h later at lights on (0600 h) the following morning. Cages of *ad lib* control mice were opened, but food was not removed. Brains and blood were collected immediately at the end of the 12 h FD or *ad lib* feeding period. *Rfrp* expression in the DMN was analyzed by single-label ISH and, in an alternate set of brain sections from the same animals, double-label ISH was performed for *Rfrp* and *c-Fos*, a marker of neuronal activation. Blood serum collected at the time of sacrifice was assayed for circulating LH, leptin and corticosterone.

A cohort of male mice was also subjected to short-term food deprivation. As male mice require longer durations of food deprivation before reproductive function is compromised (165), intact male mice were FD for 12 hours, 24 or 36 hours, or kept on *ad lib* feeding. All food was removed from FD animals at lights off (1800 h) and animals were sacrificed 12 h later at lights on (0600 h) or 24 h later at lights off (1800 h) or at 36 h later at lights on (0600 h) (n = 7 per group). A group of *ad lib* mice were sacrificed in parallel at every time point (n = 4 per group) and were pooled together *post hoc* after single label ISH found no difference in *Rfrp* expression between the various control groups (*data not shown*). Brains and blood were collected immediately at sacrifice. *Rfrp* expression in the DMN was analyzed by single-label ISH. Blood serum was assayed for circulating levels of corticosterone.

Experiment 4: Is Rfrp expression or neuron activity responsive to short-term restraint or glucocorticoid challenge?

A previous report in male rats demonstrated that RFRP-3 immunoreactivity and neuronal activation were increased after 180 minutes of restraint stress (163), a treatment that induces high levels of glucocorticoids. Experiment 3 demonstrated that food deprived animals also have high glucocorticoid levels, but with no changes in *Rfrp* expression, and therefore is in disagreement with the previous report in male rats. To clarify the issue, a similar restraint experiment was conducted in male mice to determine if *Rfrp* expression or neuronal activation is higher after restraint stress. Adult male mice were subjected to 180 minutes of restraint or allowed to remain in their home cages before sacrifice (n = 4-5 animals per group). This length of restraint stress is sufficient to suppress LH secretion in adult mice (157,161,162). At sacrifice, blood and brains were collected. *Rfrp* expression in the DMN was analyzed by single-label ISH and *Rfrp* and *c-Fos*, a marker of neuronal activation, was analyzed by double-label ISH. Blood serum was assayed for circulating levels of corticosterone.

In addition to testing the effects of glucocorticoids induced by restraint stress, adult male mice were subjected to high glucocorticoid levels pharmacologically via two intraperitoneal injections of corticosterone (50 µg of corticosterone dissolved in 200 µL of sesame oil) given 180 and 90 minutes prior to sacrifice. After each injection the mice were returned to their home cages. Brains and blood from a group of control mice that were injected twice with peanut oil only, 180 and 90 minutes prior to sacrifice, were also collected in parallel to the corticosterone treated animals. The brains were cryosectioned and stained for *Rfrp* by single label ISH, *c-Fos* and *Rfrp* by double label ISH. Blood serum was assayed for circulating levels of corticosterone (n = 4-5 animals per group).

Experiment 5: Is Rfrp expression or neuron activation altered during the LH surge when corticosterone is present?

Previous experiments have determined that *Rfrp* neuronal activation is suppressed during the peak of the preovulatory LH surge (Chapter 3). It is hypothesized that glucocorticoids would increase *Rfrp* neuronal activation, as seen in rats during restraint stress, and this glucocorticoid activation of *Rfrp* may counteract the suppression of *Rfrp* neuron activation seen during the LH surge. To test this possibility, adult female mice were gonadectomized and implanted with a E₂ capsule and a corticosterone pellet (50 mg/animal) or cholesterol pellet as described above. After 2 days of recovery, the mice were sacrificed at lights off (1800 h, the typical peak of the LH surge) and blood and the brain was collected from each animal. Brains were cryosectioned and stained for *Rfrp* by single label ISH, *c-Fos* and *Rfrp* by double label ISH. Blood serum was assayed for circulating levels of corticosterone and LH (n = 4 per treatment group).

Results

Experiment 1: A subset of Rfrp neurons express LepRb mRNA

Double label ISH was performed for energy balance-related genes known to be expressed in the DMN (80-84,119,164) to determine if they are co-expressed in *Rfrp* neurons of adult male or female mice. Virtually no *Rfrp* neurons co-expressed *Npy* or *Trh*, despite notable *Npy* and *Trh* expression in the same DMN region, often near *Rfrp* neurons (Figure 4.1; Table 4.1). Next, to assess the possibility that metabolic hormones/neuropeptides might directly regulate the RFRP-3 system, co-expression of several metabolic signaling factor receptors in *Rfrp* neurons was examined. Long form leptin receptor (*LepRb*) mRNA, which is strongly expressed in the rodent DMN, was found to be notably co-expressed in a subset of *Rfrp* neurons, suggesting that a proportion of adult *Rfrp* neurons may be leptin responsive. The degree of *LepRb-Rfrp* co-

expression was similar in both sexes (~ 15%, Figure 4.1). An even smaller subset of *Rfrp* neurons (~ 8%) in both sexes co-express the primary melanocortin receptor, *Mc4r* (Figure 4.1). On the contrary, the glucocorticoid receptor, *GR*, was found to be expressed in the vast majority of *Rfrp* neurons, with roughly ~ 86% of *Rfrp* neurons co-expressing the receptor in both sexes (Figure 4.1). *GR* is highly expressed in the DMN and is found in the majority of neurons in this region. A summary of the co-expression levels for each gene with *Rfrp* is in Table 4.1.

Experiment 2: Rfrp expression is decreased in adult Ob mice of both sexes.

This experiment assessed whether there are notable differences in *Rfrp* expression in adult Ob (leptin-deficient) and WT mice that were all GDX beforehand to remove any masking effects of circulating E_2 (which moderately decreases *Rfrp* expression). As expected, Ob animals of both sexes were significantly heavier, weighing almost twice as much, on average, than their WT counterparts ($p < 0.05$, *data not shown*). In the brain, the total number of detectable *Rfrp* neurons was not significantly different between Ob and WT mice in either sex (Figure 4.2A-B). However, using the HE and LE *Rfrp* cell criteria, there was a significant decrease in the number of HE *Rfrp* neurons in female Ob mice compared to female WTs (Figure 4A, $p < 0.05$), with no significant differences in the number of LE *Rfrp* cells between genotypes. Likewise, a similar reduction in the number of HE *Rfrp* neurons was detected in male Ob mice compared to WT male littermates (Figure 4.2C, $p < 0.05$). In addition to these changes in cell number, the total level of *Rfrp* mRNA in the DMN was significantly lower in both male and female Ob mice compared to their WT littermate controls (Figure 4.2A-C, $p < 0.05$).

Experiment 3: Rfrp neurons in mice appear unresponsive to 12-hour food deprivation

To test if energetic challenge induced by short-term food deprivation modifies *Rfrp* mRNA expression levels or the activity of RFRP-3 neurons, adult female mice were subjected to

short-term (12 h) food deprivation (12 h FD). Demonstrating the effectiveness of the energetic challenge, 12 h FD mice had a significant decrease in body weight (5.3%; $p < 0.05$) and significant decreases in serum LH and leptin relative to *ad lib* control females (Figure 4.3A-C, $p < 0.05$). However, despite this negative impact of 12 h FD on body weight and endocrine physiology, there were no significant differences in either the total number of *Rfrp* neurons or the total *Rfrp* mRNA between *ad lib* and FD animals (Figure 4.3D-F). Moreover, when *Rfrp* neurons were categorized as either HE or LE, there were no statistical differences between *ad lib* and FD animals (*data not shown*).

In addition to mRNA levels, double-label ISH was used to examine alterations in neuronal activation of RFRP-3 neurons in 12 h FD mice. As with the single label assay, the total number of *Rfrp* cells in this double-label assay did not differ between 12 h FD and *ad lib* mice (117 ± 8 cells versus 121 ± 8 cells, respectively). Moreover, there was no group difference in the percent of *Rfrp* neurons demonstrating recent neuronal activation, as measured by *c-Fos* mRNA co-expression in *Rfrp* neurons (Figure 4.3G-H).

As a follow-up experiment, male mice were also subjected to FD. However, male mice require a greater length of FD before demonstrating changes in reproductive function (165), therefore groups of males were subjected to 12, 24 and 36 hours of FD. This food deprivation periods lead to significant decreases in body weight in all deprived groups and significantly higher corticosterone levels than *ad lib* fed mice ($p < 0.05$, Figure 4.4A-B). Single label ISH for *Rfrp* was performed on DMN sections from these male mice, however no significant changes were found *Rfrp* cell number or the amount of mRNA per cell for any length of food deprivation (Figure 4.4C-E). Moreover, when *Rfrp* neurons were categorized as either HE or LE, there were no statistical differences between *ad lib* and FD animals (*data not shown*). A double label ISH for *c-Fos* and *Rfrp* co-expression was also performed, and found no differences in the degree of co-expression between any of the groups (*data not shown*).

Experiment 4: Restraint stress and glucocorticoid injections do not alter Rfrp expression but do suppress Rfrp neuronal activation.

To test the specific effects of glucocorticoid-mediated stress responses on the *Rfrp* system, adult male mice were subjected to restraint stress or injections of corticosterone. 180 minutes of restraint stress significantly increased serum corticosterone levels (Figure 4.5A, $p < 0.05$), but had no significant changes on *Rfrp* mRNA levels, as measured by total *Rfrp* cell number or mRNA per cell (Figure 4.5B-D). However, double label ISH for *c-Fos* co-expression in *Rfrp* neurons revealed a significant decrease in the number of *Rfrp* neurons expressing *c-Fos*, demonstrating suppression in their neuronal activity after 180 minutes of restraint (Figure 4.5E-F, $p < 0.05$).

The second experiment gave adult male mice two injections of corticosterone, 180 and 90 minutes prior to sacrifice, which significantly increased serum levels of corticosterone (Figure 4.6A, $p < 0.05$). This treatment had a minor effect on *Rfrp* expression, as the number of *Rfrp* neurons remained unchanged between corticosterone injected and vehicle treated animals (Figure 4.6B-C), but the amount of *Rfrp* mRNA per cell, as measured by grains per cell, was mildly but significantly greater in corticosterone treated animals, ($p < 0.05$, Figure 4.6D). The degree of *c-Fos* co-expression in *Rfrp* neurons, as determined using double label ISH, was lower in corticosterone-injected animals, suggested a suppression in their neuronal activity after CORT injection (Figure 4.6E-F, $p < 0.05$). For both sets of experiments, restraint and injections, subcategorizing *Rfrp* neurons as either HE or LE cell revealed no additional statistical differences between control and experimental animals (*data not shown*).

Experiment 5: Corticosterone is able to suppress Rfrp expression during the LH surge in female mice.

Glucocorticoids are known to suppress LH secretion and can effectively blunt the preovulatory LH surge. *Rfrp* neuronal activation is suppressed during the peak of the LH surge, but the activational effects of glucocorticoids on *Rfrp* neuron activity in male rats suggests that glucocorticoids may act to disinhibit *Rfrp* neurons that are normally suppressed during this event. Adult female mice were gonadectomized, estrogen replaced, and given an implant of corticosterone or cholesterol (control) and then assayed for *Rfrp* expression, neuronal activation, and serum hormones after two days of recovery. Animals receiving corticosterone implants had significantly lower LH and significantly higher serum corticosterone than their cholesterol treated counterparts (Figure 4.7A-B, $p < 0.05$), suggesting that the LH surge was successfully abolished in these mice. Single label ISH for *Rfrp* mRNA exposed a significant suppression of *Rfrp* expression, as measured by total cell number and *Rfrp* grains per cell (Figure 4.7C-E, $p < 0.05$). However, when examining *c-Fos* co-expression via double label ISH, there were was a trend for corticosterone treated mice having a higher degree of co-expression, but there was no significant effect of treatment between the two groups of female mice (Figure 4.7F-G, $p < 0.05$).

Discussion

The physiological roles RFRP-3 plays in mediated metabolic and stress responses still poorly understood. The current findings of this chapter show that a subset of RFRP-3 neurons express the long-form of the leptin receptor and that *Rfrp* mRNA expression is diminished in Ob (leptin deficient) animals of both sexes. However, *Rfrp* expression and neuronal activation appears unaltered during food deprivation in female and male mice. Furthermore, short term restraint or corticosterone injections are unable to alter *Rfrp* expression, but do modulated the basal activity of *Rfrp* neurons in male mice, and lastly several days of treatment with

corticosterone in female mice is able to suppress *Rfrp* expression during the preovulatory LH surge-like conditions.

Several studies have demonstrated an orexigenic effect of RFRP-3 (64,76,77), suggesting that RFRP-3 may be involved in receiving and/or transmitting energy balance signals. Both NPY and TRH are neuropeptide cell populations that reside, and are even expressed in a similar pattern as *Rfrp*, in the DMN (82,119). However *Rfrp* did not co-localize with either of these neuropeptides, demonstrating that it is a unique neuropeptide population within the DMN. A small subset of *Rfrp* neurons expressed each of these receptors, *LepRb* and *Mc4r*, with the leptin receptor being the more prominently expressed, suggesting that some *Rfrp* neurons may be a direct target of leptin signaling. However, most *Rfrp* neurons did not express *LepRb*, suggesting that any major effects of leptin signaling, or its absence, on *Rfrp* neurons may in fact be indirect. The co-expression of the glucocorticoid receptor, however, appears to be prevalent in the majority of *Rfrp* neurons of mice. This finding is consistent with previous reports in rats (163), which showed that the majority of RFRP-3 immunoreactive neurons co-expressed *GR*. It should be noted that this high degree co-expression is not specific to *Rfrp* neurons, as a large majority of DMN neurons express *GR* (as seen in Figure 4.1) and there are many hypothalamic regions that also express *GR* (160).

Ob mice are infertile due to a lack of gonadotropin secretion (154), and since RFRP-3 is known to inhibit LH secretion, and some *Rfrp* neurons express the leptin receptor. Therefore it was hypothesized that *Rfrp* expression would be higher in Ob mice. However, using GDX adult Ob males and females, opposite outcome was found: *Rfrp* expression is lower in adult Ob mice than their wildtype littermates. This was true for both sexes. While these experiments were being conducted, Rizwan et al. (166) published new data suggesting that RFRP-3 neurons are not regulated by leptin. That study's immunohistochemical data showed no difference between the number of RFRP-3-immunoreactive neurons in GDX, E₂-replaced Ob mice and WT littermates,

and minimal phosphorylation of signal transducer and activator of transcription 3 in RFRP-3 neurons after leptin injections. Those results suggest that RFRP-3 neurons are not directly regulated by leptin and that RFRP-3-immunoreactive levels are unaffected by leptin deficiency, differing from our present results in which *Rfrp* levels were diminished in Ob mice. It is possible that the exogenous E₂ replacement in the Rizwan study may have masked any difference between WT and Ob animals, as E₂ moderately represses *Rfrp* (124,137), and may have done so to equivalent levels in Ob and WT genotypes. In contrast, the present data quantifying gene expression (rather than protein) levels demonstrates that total *Rfrp* mRNA levels are significantly repressed in GDX Ob animals (no E₂ given, so *Rfrp* expression is not being inhibited by sex steroids). Additionally, in these Ob mice, there is a primary deficit in *Rfrp* expression specifically in the HE *Rfrp* cell population, which is a cellular distinction that has not yet been analyzed using IHC. The functional significance of the lower *Rfrp* levels in Ob mice is not yet known; it should be noted that RFRP-3 has proposed roles in several other physiological/behavioral systems beyond reproduction, such as feeding, stress, and anxiety, and the observed decreases in *Rfrp* levels in Ob mice may reflect RFRP-3's involvement in these processes rather than the impaired reproductive axis.

Although there is a notable decrease in overall *Rfrp* levels in adult Ob mice of both sexes, it remains unclear if this is due to changes in direct or indirect leptin signaling to RFRP-3 cells. Rizwan et al. showed minimal phosphorylation of STAT3 in RFRP-3 neurons after leptin treatment, ranging from ~ 3% in mice to 7-13% in rats, suggesting that any effects of leptin would likely be indirect. In the present study, using conventional double-label techniques, there is direct anatomical evidence for a slightly higher degree of *LepRb* expression in *Rfrp* neurons, 15-20% in female and male mice, suggesting that some effects of leptin could in fact be direct on a subset of *Rfrp* neurons. Yet, based on the overall low-to moderate percent of total *Rfrp* neurons expressing *LepRb*, it can be concluded, like Rizwan et al., that the majority of RFRP-3 neurons

are likely not directly responsive to leptin signaling. If so, the diminished *Rfrp* levels observed in Ob mice may reflect any of the following: 1) direct leptin signaling in only a small subset of *Rfrp* cells, causing only those cells to change gene expression, 2) indirect leptin signaling on upstream leptin-responsive circuits that themselves directly regulate RFRP-3 neurons, 3) influence of non-leptin metabolic signals that are secondarily altered in the obese state of Ob mice. This last possibility seems most likely, since *Rfrp* expression was normal in young juvenile Ob mice, in which leptin signaling is absent but obesity has yet to emerge (Chapter 5).

Central injections of RFRP-3 reportedly stimulate food intake (77,152), and RFRP-3 neurons are activated by chronic mild (20%) food restriction in hamsters (153). Moreover, a recent report demonstrated that LH secretion is not suppressed after 12 h of FD in *Gpr147* knockout mice (lacking the RFRP-3 receptor), suggesting that RFRP-3 is involved in the metabolic regulation of LH (89). Here *Rfrp*, expression levels or *Rfrp* neuronal activation were examined in adult female mice subjected to 12 h FD, and a cohort of male mice were subjected to 12 h, 24 h or 26 h of FD. This short-term FD had no effect on *Rfrp* expression or *Rfrp* neuronal activation. These results are surprising, as body weight and LH levels were all significantly lower after FD, reflecting successful metabolic challenge and inhibition of the reproductive system. Thus, the lower LH levels observed in our metabolically challenged females, which was hypothesized to be a direct or indirect effect of enhanced RFRP-3, appears to be induced by some other mechanism. The previously observed increase in *Rfrp* neuronal activation in hamsters that were food restricted to 80% of normal diet for much longer periods of time (8 days or more (153)) may suggest that metabolic alteration of *Rfrp* neurons may either be a part of chronic or mild nutritional stress, rather than acute, severe changes in energy availability, as in our 12 h FD paradigm.

In previous reports, *Rfrp* expression and/or neuronal activation is increased after glucocorticoid stimulation, either through endogenous secretion after immobilization, or

pharmacological treatment with corticosterone or GR agonists. *In-vitro* experiments using mouse immortalized cell lines have shown that GR agonists, such as dexamethasone, are able to increase *Rfrp* mRNA, through a GR-dependent mechanism (121). Similar experiments have been performed in rat immortalized cell lines, in which corticosterone was also able to upregulate *Rfrp* mRNA through GR binding to GR-specific response elements in the *Rfrp* promoter (122). Furthermore, corticosterone treatment upregulates *Rfrp* mRNA in male rats (163) and upregulates GnIH immunoreactivity in adult male rats and adult male Japanese quail *in-vivo* (122). However, these findings were not replicated in the present study in male mice. Both restraint stress and corticosterone injections failed to increase *Rfrp* mRNA and surprisingly showed a suppression of *Rfrp* neuronal activation. The reason for this discrepancy remains unclear. *Rfrp* neurons in mice do express GR, as in both rats and quails (122,163), so it is unlikely that glucocorticoids are unable to act on the murine *Rfrp* neuron. One possibility is the method of detection of the *Rfrp* mRNA. The radiolabeled *in-situ* hybridization used in these studies may have reached the maximum limit of detection and unable to discern higher levels of *Rfrp* mRNA. Another possibility is that unlike rats and quails, a longer duration of glucocorticoid exposure may be needed for changes in *Rfrp* expression to occur in mice. This theory is in agreement with the results of experiment 5, which showed that *Rfrp* mRNA per cell was lower in animals with corticosterone pellets when examined two days after being implanted. This longer time course, > 48 h, at supraphysiological levels, may be the only condition in which a major suppression of *Rfrp* mRNA may occur in response to glucocorticoids. However, this change in *Rfrp* expression is in the opposite direction of what would be predicted by published studies. Additional studies are needed to better understand how glucocorticoids may regulate *Rfrp* expression.

In conclusion, the data presented here provide further insight into the regulation and development of RFRP-3 neurons in mice. Although *Rfrp* neurons appears to be a distinct population of cells from NPY or TRH cells in the DMN, there does appear to be a small

subpopulation of *Rfrp* neurons that co-express *LepRb*, allowing for the possibility of direct leptin signaling in these cells. This finding is extended by the observation that adult Ob animals have less *Rfrp* expression than their WT littermates, though whether this decrease in *Rfrp* expression is due to direct or indirect effect of leptin signaling, or other metabolic cues associated with obesity, remains to be determined. Additionally, *Rfrp* neurons in female and male mice appear to be resistant to short-term food deprivation, despite previous reports demonstrating effects of chronic food restriction on the activation of RFRP-3 neurons in other species. Thus, the observed decrease in LH under short-term food deprivation in mice is unlikely to be due to changes in RFRP-3 neurons. Lastly, *Rfrp* expression and neuron activation are suppressed under various model of stress, such as immobilization and corticosterone treatments, and this may be a direct effect, as the majority of *Rfrp* neurons express *GR*.

Portions of this chapter are published in *Neuroendocrinology* (November 2014). The dissertation author was the primary investigator and author of this material. Morris Sheih, Nagambika Munaganuru, and Elena Luo were undergraduates in the lab who assisted in cyrosectioning and performing ISH. Alexander Kauffman supervised the project and provided advice.

Portions of this chapter are in preparation for publication. The dissertation author was the primary investigator and author of this material. Elena Luo assisted in animal preparation, tissue collection, cyrosectioning and performing ISH. Kellie Breen-Church and Alexander Kauffman supervised the project and provided advice.

Table 4.1. Summary of four double label *in-situ* hybridization assays for metabolic-related genes in the DMN co-expressed with *Rfrp* neurons. Adult diestrous (DE) females and intact male mice were assayed for neuropeptide Y (NPY), thyrotropin-releasing hormone (TRH), long form leptin receptor (LepRb), melanocortin receptor 4 (Mc4r), or glucocorticoid receptor (GR) mRNA in *Rfrp* cells in the DMN. Values are average percent co-expression with \pm SEM. n = 4-6 animals per sex.

	<u>Intact Males</u>	<u>DE Females</u>
NPY/Rfrp	1.5 \pm 0.7%	3.0 \pm 1.5%
TRH/Rfrp	1.1 \pm 0.5%	1.6 \pm 0.8%
LepRb/Rfrp	16.9 \pm 1.6%	13.0 \pm 1.6%
Mc4r/Rfrp	6.9 \pm 1.0%	8.7 \pm 0.7%
GR/Rfrp	87.0 \pm 4.9%	86.2 \pm 2.9%

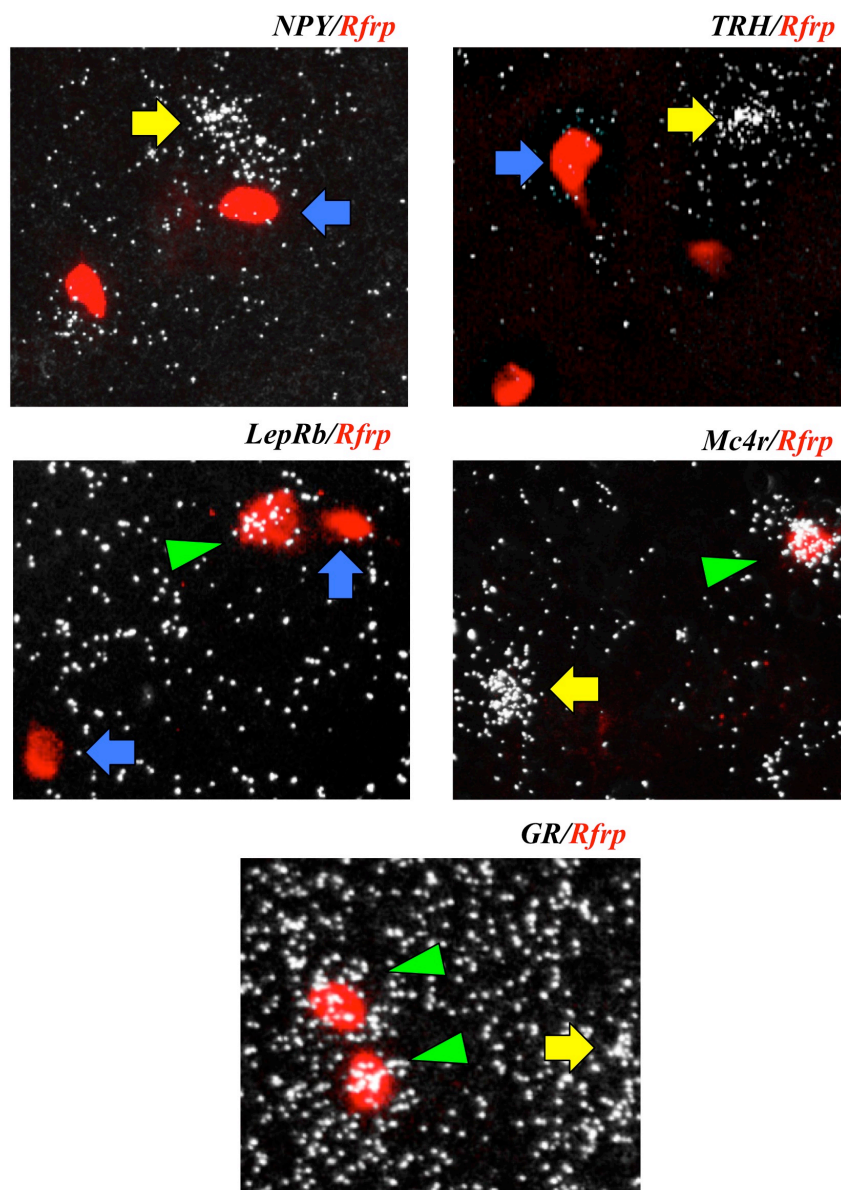


Figure 4.1. Expression of hypothalamic energy balance genes in the dorsal-medial hypothalamus. Representative photomicrographs of double label *in-situ* hybridization of neuropeptide Y (*NPY*), thyrotropin-releasing hormone (*TRH*), long form leptin receptor (*LepRb*) or melanocortin receptor 4 (*Mc4r*) or glucocorticoid receptor (*GR*) (silver grains) in *Rfrp* neurons (red fluorescence). Single labeled *Rfrp* neurons are identified with blue arrows and single labeled *NPY*, *TRH*, *LepRb*, *Mc4r*, or *GR* neurons are marked with yellow arrows. Double labeled *LepRb/Rfrp* and double labeled *Mc4r/Rfrp* neurons are marked with a green arrowheads.

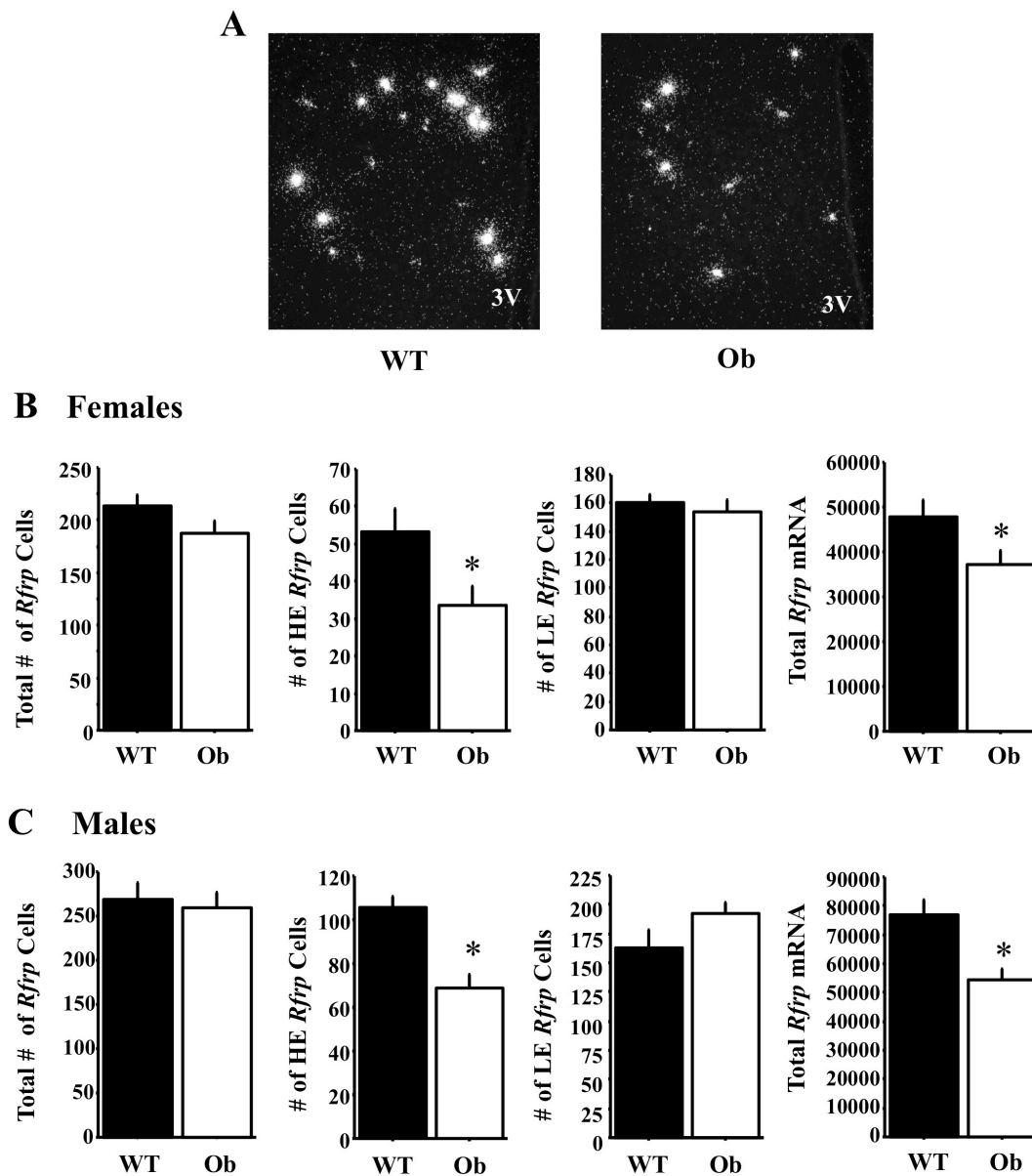


Figure 4.2. *Rfrp* expression in obese (Ob) male and female gonadectomized (GDX) mice. [A] Representative photomicrographs of single label *in-situ* hybridization for *Rfrp* mRNA in wildtype (WT) and Ob female GDX mice. 3V = third ventricle [B] Quantification of total *Rfrp* neurons, high expressing (HE) *Rfrp* neurons, low expressing (LE) *Rfrp* neurons, and total *Rfrp* mRNA from single label ISH in female GDX mice. The number of HE cells and the total *Rfrp* mRNA was significantly less in Ob females than WT littermates ($p < 0.05$). There were no significant differences between the total number of *Rfrp* neurons or number of LE cells. [C] Quantification of total *Rfrp* neurons, HE *Rfrp* neurons, LE *Rfrp* neurons, and total *Rfrp* mRNA from single label ISH in male GDX mice. The number of HE cells and the total *Rfrp* mRNA was significantly less in Ob males than WT littermates ($p < 0.05$). There were no significant differences between the total number of *Rfrp* neurons or number of LE cells.

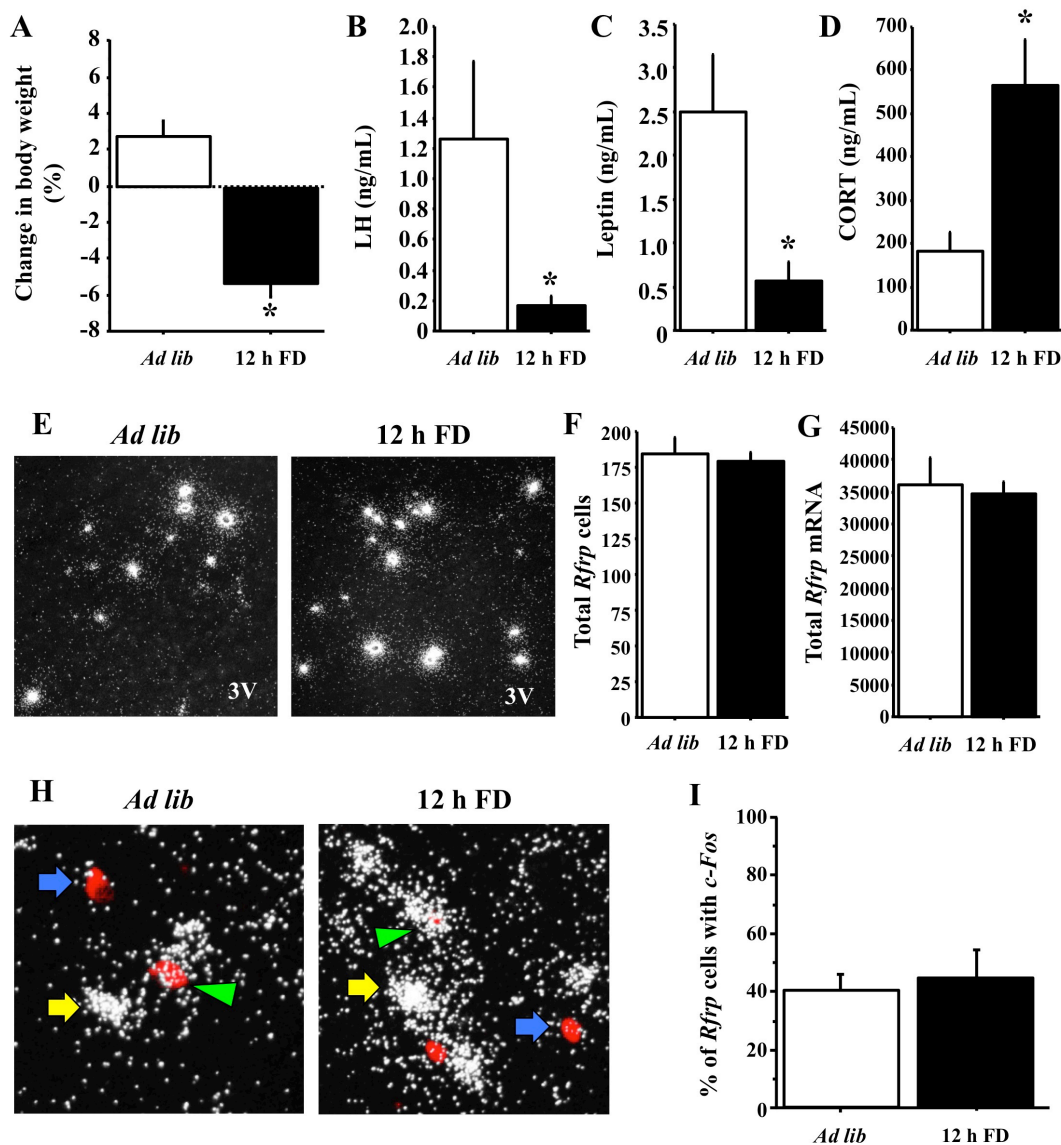


Figure 4.3. Effects of food deprivation on *Rfrp* expression and *Rfrp* neuron activation in gonadectomized (GDX) female mice. [A] The percent change in body weight after 12 hours of food deprivation (12 h FD) or *ad-libitum* access to food (*Ad lib*). Food deprivation had a significant effect on the change in body weight ($p < 0.05$). [B] Serum luteinizing hormone (LH) is significantly less in 12 h FD GDX animals than *Ad lib* animals ($p < 0.05$). [C] Serum leptin is significantly less in 12 h FD GDX animals than *Ad lib* animals ($p < 0.05$). [D] Serum corticosterone (CORT) is significantly higher in 12 h FD than *Ad lib* animals ($p < 0.05$). [E] Representative photomicrographs of single label *in-situ* hybridization (ISH) for *Rfrp* mRNA in *Ad lib* and 12 h FD mice. 3V = third ventricle. [F] Quantification of single label ISH for *Rfrp* expressing cells; *Rfrp* neurons number is not significantly different between *Ad lib* and 12 h FD animals. [G] Quantification of total *Rfrp* mRNA from single label ISH. There is no significant difference between *Ad lib* and 12 h FD animals. [H] Representative photomicrographs of double label ISH for *c-Fos* and *Rfrp* mRNAs. Double labeled *c-Fos* and *Rfrp* (green arrowhead) and single labeled *c-Fos* cells (yellow arrow) and single labeled *Rfrp* neurons (blue arrow) are shown. [I] Quantification of double label ISH. There was no significant difference between groups.

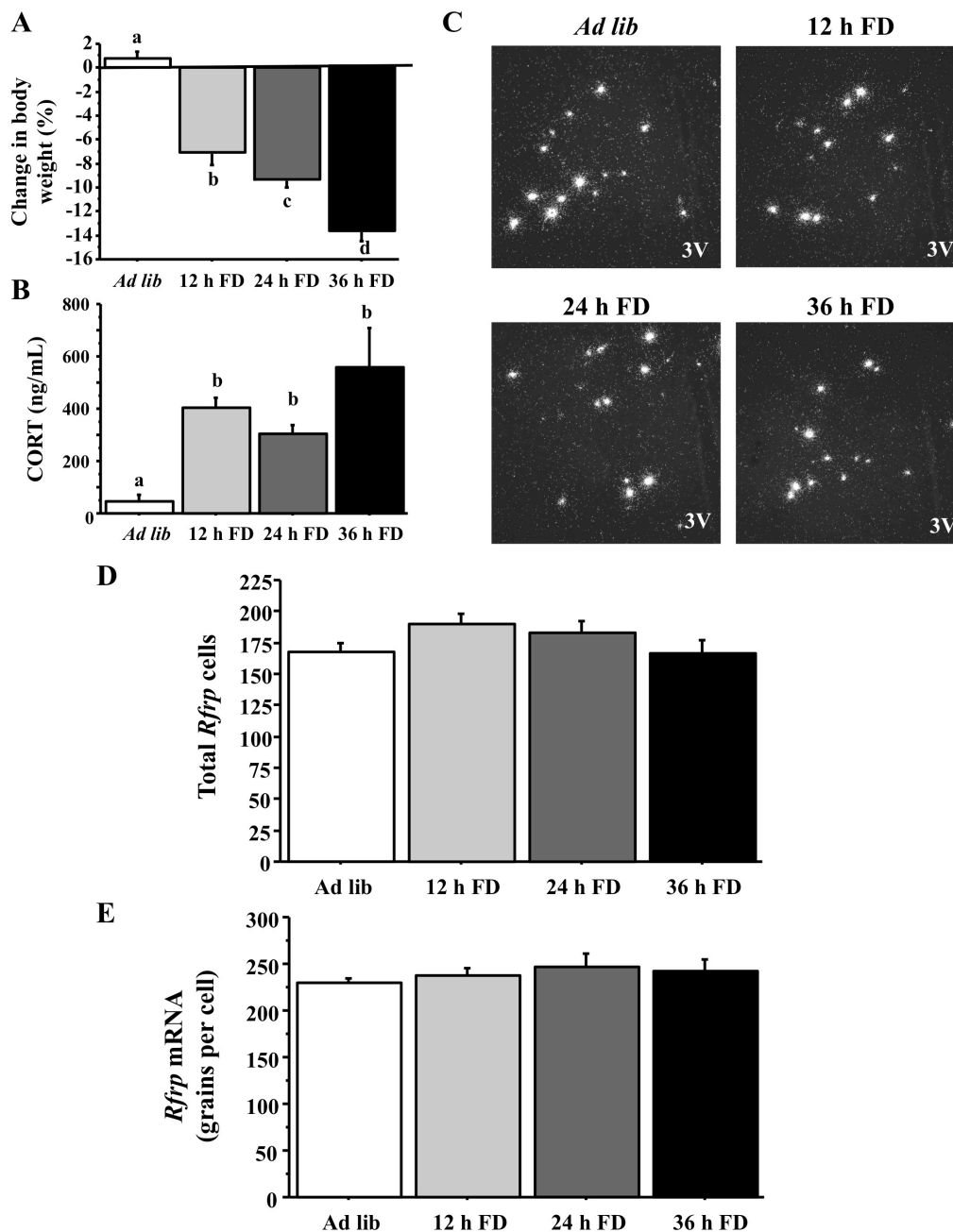


Figure 4.4. Effects of food deprivation on *Rfrp* expression and *Rfrp* neuron activation in intact male mice. **[A]** The percent change in body weight after 12 hours (12 h FD), 24 hours (24 h FD), or 36 hours of food deprivation (36 h FD) or *ad-libitum* access to food (*Ad lib*). Food deprivation had a significant effect on body weight ($p < 0.05$). Different letters indicated significantly different groups. **[B]** Corticosterone (CORT) is significantly higher in food-deprived groups than the *Ad lib* group. Different letters indicated significantly different groups ($p < 0.05$). **[C]** Representative photomicrographs of single label ISH for *Rfrp* mRNA in *Ad lib* and food deprived male mice. 3V = third ventricle. **[D]** Quantification of single label ISH for *Rfrp* expressing cells; the total number of *Rfrp* neurons is not significantly different. **[E]** Quantification of *Rfrp* mRNA per neuron, as measured by grains per cell, is not significantly different between groups.

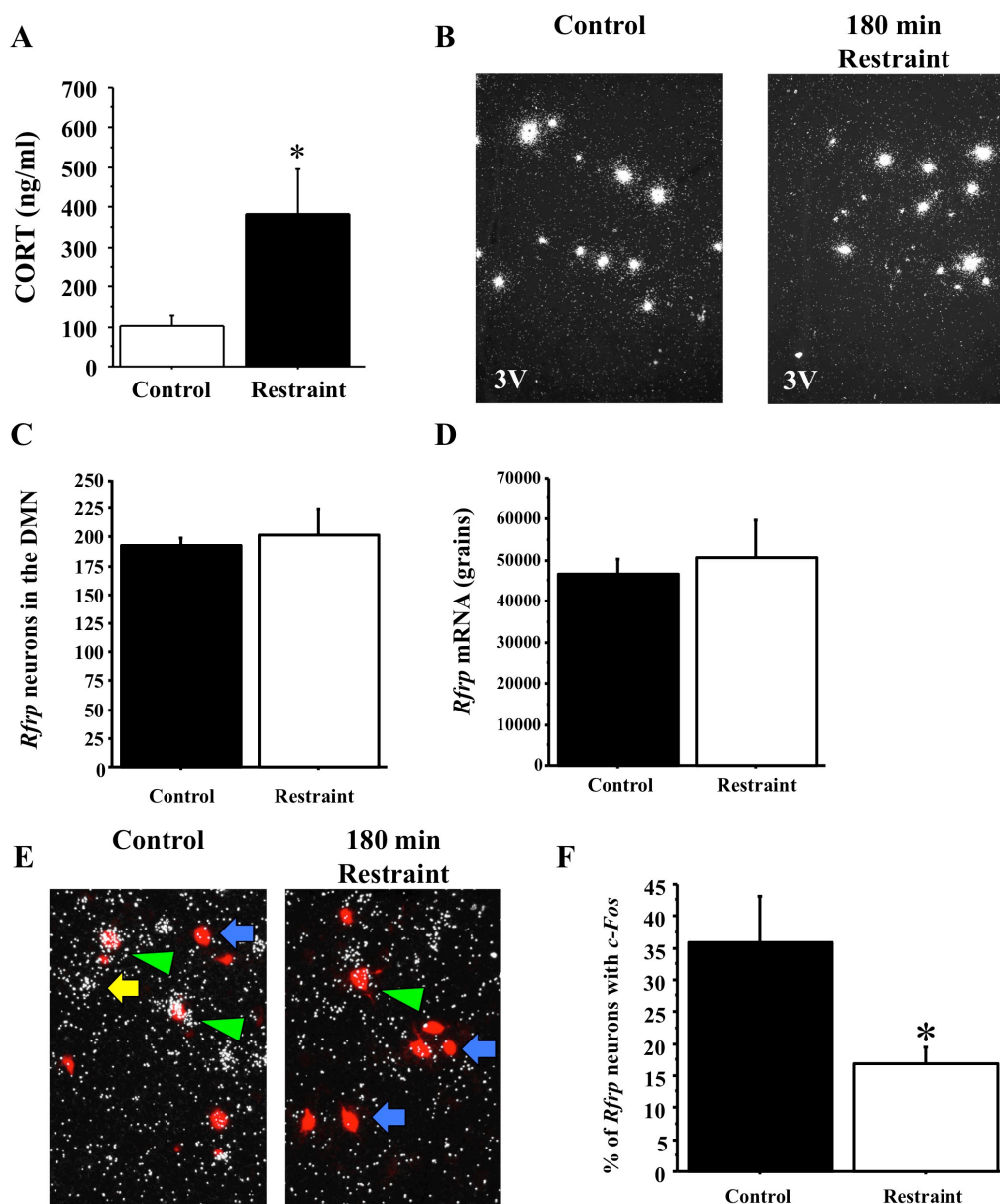


Figure 4.5. Effects of immobilization restraint on *Rfrp* expression and *Rfrp* neuron activation in intact male mice. **[A]** Serum corticosterone (CORT) is significantly higher in animals after 180 minutes of restraint stress than animals that had no restraint (control) ($p < 0.05$) **[B]** Representative photomicrographs of single label ISH for *Rfrp* mRNA in control and 180-minute restraint treated mice. 3V = third ventricle. **[C]** Quantification of single label ISH for *Rfrp* expressing cells; the total number of *Rfrp* neurons is not significantly different. **[D]** Quantification of total *Rfrp* mRNA from single label ISH; the amount of *Rfrp* mRNA per neuron, as measured by grains per cell, is not significantly different. **[E]** Representative photomicrographs of double label ISH for *c-Fos* and *Rfrp* mRNAs in control and 180 minute restraint stressed mice. Double labeled *c-Fos* and *Rfrp* (green arrowhead) and single labeled *c-Fos* cells (yellow arrow) and single labeled *Rfrp* neurons (blue arrow) are shown. **[F]** Quantification of percent *c-Fos* and *Rfrp* co-expression between control and 180-minute restrained mice. There was a significant decrease in *c-Fos* co-expression in the restrained mice ($p < 0.05$).

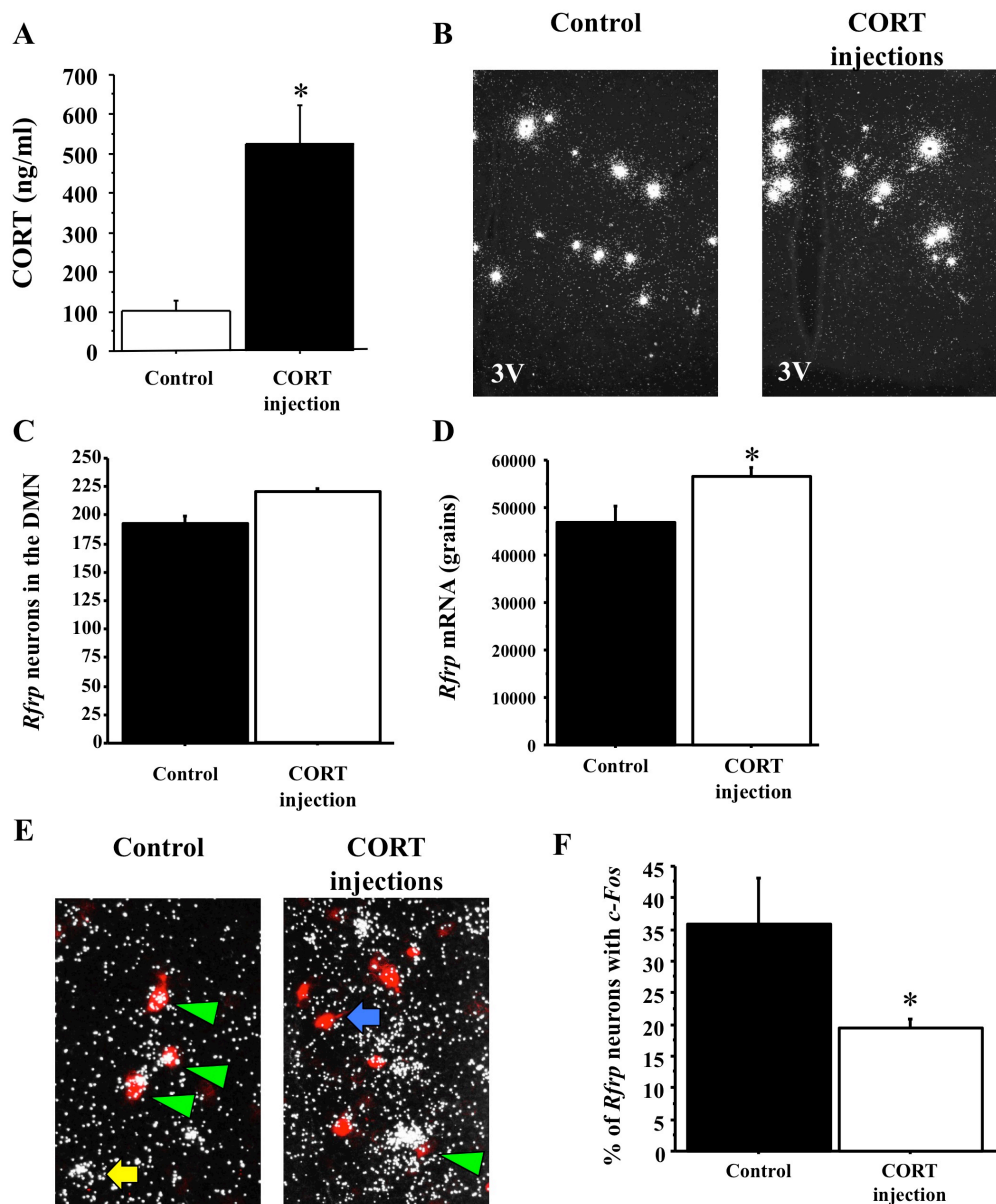


Figure 4.6. Effects of corticosterone injections on *Rfrp* expression and *Rfrp* neuron activation in intact male mice. **[A]** Serum corticosterone (CORT) is significantly higher after corticosterone injection vehicle injections (control) ($p < 0.05$) **[B]** Representative photomicrographs of single label ISH for *Rfrp* mRNA in control and corticosterone injected mice. 3V = third ventricle. **[C]** Quantification of single label ISH for *Rfrp* expressing cells; the total number of *Rfrp* neurons is not significantly different between groups. **[D]** Quantification of total *Rfrp* mRNA from single label ISH; the amount of *Rfrp* mRNA per neuron, as measured by grains per cell was significantly greater in the corticosterone treated groups ($p < 0.05$). **[E]** Representative photomicrographs of double label ISH for *c-Fos* and *Rfrp* mRNAs in control and corticosterone injected mice. Double labeled *c-Fos* and *Rfrp* (green arrowhead) and single labeled *c-Fos* cells (yellow arrow) and single labeled *Rfrp* neurons (blue arrow) are shown. **[F]** Quantification of percent *c-Fos* and *Rfrp* co-expression between control and corticosterone injected male mice. There was a significant decrease in *c-Fos* co-expression in the corticosterone treated mice ($p < 0.05$).

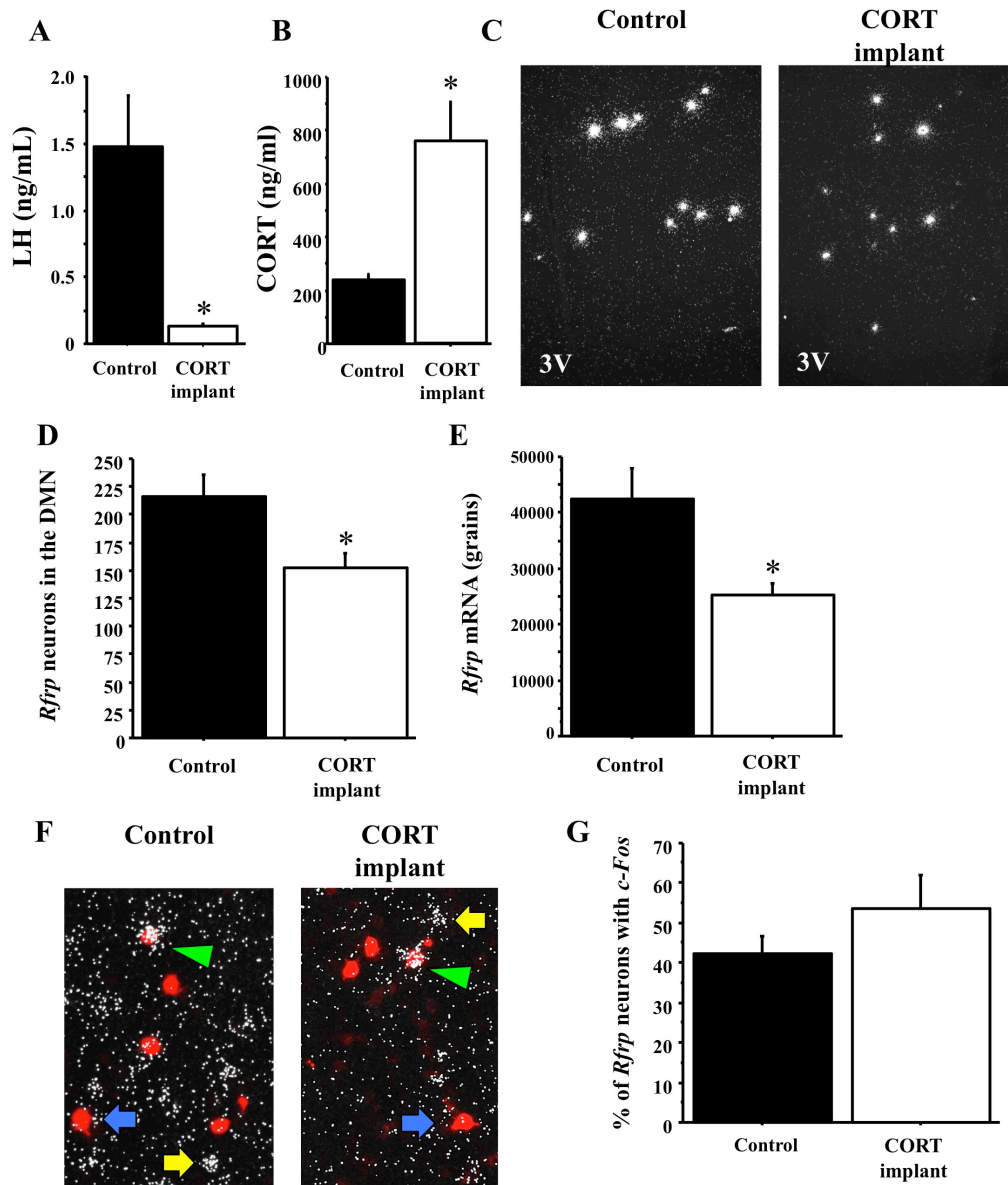


Figure 4.7. Effects of corticosterone implants on *Rfrp* expression and *Rfrp* neuron activation during the LH surge in gonadectomized and estrogen replaced female mice. **[A]** Serum luteinizing hormone (LH) is significantly lower in female mice with a corticosterone (CORT) implant than those receiving cholesterol implant (control) ($p < 0.05$). **[B]** Serum CORT is significantly higher in animals receiving CORT implant than control animals ($p < 0.05$). **[C]** Representative photomicrographs of single label ISH for *Rfrp* mRNA in control and CORT implanted female mice. 3V = third ventricle. **[D]** Quantification of single label ISH for *Rfrp* expressing cells; total number of *Rfrp* neurons is significantly less in CORT-implanted animals ($p < 0.05$). **[E]** Quantification of total *Rfrp* mRNA from single label ISH; the amount of *Rfrp* mRNA per neuron, as measured by grains per cell, is significantly less in CORT-implanted animals ($p < 0.05$). **[F]** Representative photomicrographs of double label ISH for *c-Fos* and *Rfrp* mRNAs. Double labeled *c-Fos* and *Rfrp* (green arrowhead) and single labeled *c-Fos* cells (yellow arrow) and single labeled *Rfrp* neurons (blue arrow) are shown. **[G]** Quantification of percent *c-Fos* and *Rfrp* co-expression groups. There was a no significant change in *c-Fos*.

CHAPTER 5: *Rfrp* expression during postnatal development and the postnatal leptin surge

Abstract

RFRP-3's potent inhibition of the reproductive system has been hypothesized to be a mechanism in which the under developed prepubertal neuroendocrine axis is suppressed prior to puberty. In order to test this hypothesis, *in-situ* hybridization (ISH) was used to measure changes in *Rfrp*-expressing neurons in mice of both sexes during development. There are two interspersed subpopulations of *Rfrp* cells (high *Rfrp*-expressing, HE; low *Rfrp*-expressing, LE), which have unique developmental characteristics. The number of LE cells robustly decreases during postnatal development, while HE cell number increases significantly before puberty. BAX knockout were used to determine that BAX-dependent apoptosis is not responsible for the dramatic developmental decrease in LE *Rfrp* cell. Since apoptosis does not regulate the development *Rfrp* neuronal population, leptin was examined next due to its know effects on the maturation of the DMN. *Rfrp* gene expression was examined over a higher resolution throughout juvenile development and this correlating with the timing of the juvenile "leptin surge." However, the dramatic developmental changes in juvenile *Rfrp* expression did not appear to be leptin-driven, as the pattern and timing of *Rfrp* neuron development were unaltered in Ob juveniles. Overall, these experiments provide a foundation for the developmental regulation of the RFRP-3 neuropeptide system.

Introduction

Early experiments in this lab uncovered a dramatic decrease in the number of *Rfrp* neurons between birth and adulthood. Furthermore, the adult *Rfrp* population can be grouped as high expressing (HE) and low expressing (LE) neurons, and the vast majority of *Rfrp* neurons are LH cells at birth. Other investigators have determined that in rodents, *Rfrp* neurons in the DMN are born embryonically (167) and total *Rfrp* mRNA levels, quantified with qPCR, increase in juvenile rats before puberty and then subsequently decrease after puberty (66,117). Similar data obtained by quantifying RFRP-3-ir in male mice showed a decrease in RFRP-3-ir cell number after sexual maturation (115,116), but developmental changes in *Rfrp* mRNA were not measured in mice, nor were females studied. Additionally, it is unknown what mechanism regulates these developmental changes. Programmed cell death, termed apoptosis, is dependent on Bcl-2 associated protein X (BAX) and the BAX KO mouse line is a powerful tool to determine if apoptosis is responsible for the maturation of a specific neural population (168). Moreover, to date, sex differences in developmental changes in *Rfrp* expression have not been directly assessed in any species.

Leptin has strong effects on hypothalamic regulation of metabolism and reproductive function (Chapter 4). In addition to its roles in adulthood, leptin has important developmental effects on the hypothalamus. During the second week of postnatal life, serum leptin levels increase drastically and transiently in a postnatal leptin “surge” (169). This temporary increase in juvenile leptin levels regulates the development of axonal projections from the arcuate nucleus to the DMN, as well as other brain regions (85,170). Based on previous data demonstrating that DMN *Rfrp* expression, as measured by cell number and *Rfrp* mRNA levels per cell, is dramatically higher in juveniles on postnatal day 10 than at birth (124), it has been hypothesized that this developmental difference is caused, fully or in part, by the juvenile leptin surge.

Another study within this lab discovered a significant decrease in *Rfrp* neuronal activation, as measured by *c-Fos* between PND 15 and PND 21 (171). This decrease during the second postnatal week is hypothesized to be permissive to allow puberty to commence. A previous study in male rats utilized small interfering RNA to knockdown *Rfrp* expression in prepubertal male rats (152). While this knockdown was successful in decrease RFRP-3 immunoreactivity and increasing serum LH, there were no significant effect on the timing of puberty in these male rats. Similar experiments have not been performed in mice or in females, which complete puberty earlier than males.

These experiments sought to answer the following questions 1) what is the developmental profile of *Rfrp* expression in postnatal/prepubertal mice, 2) is the developmental pattern of *Rfrp* neurons affected by BAX-mediated apoptosis, 3) do changes in *Rfrp* expression over development coincide with leptin secretion, 4) is *Rfrp* maturation dependent on leptin signaling, 5) is RFRP-3 sufficient to delay puberty in female mice.

Methods

Animals, Tissue Collection, ELISA, and in-situ hybridization

All experiments used C57BL6 mice, except experiment 2 which utilized brain sections collected from adult BAX knockout (KO) mice from a previous study (106), and experiment 4 which used mice from Ob strain (WT and Ob). Mice from the Ob line were purchased from Harlan Laboratories and maintained on a C57BL6 background in the lab. All animals were housed on a 12:12 light-dark cycle, lights off at 1800, with food and water available *ad libitum*.

Developmental experiments used infantile and juvenile pups generated by C57BL6 breeder pairs or heterozygous Ob breeder pairs (producing WT, Ob and heterozygous littermates). The date of birth was designated as postnatal day (PND) 1. Newborn and juvenile pups of various ages were anesthetized with isoflurane, weighed, and rapidly decapitated. Trunk blood was

collected from each animal to measure serum leptin levels. For mice of the OB strain, tail samples were taken postmortem to determine the Ob genotype. Note that the obesity phenotype in Ob mice is not present until 4 weeks of age or later (145,146). All experiments were conducted in accordance with the NIH Animal Care and Use Guidelines and with approval of the Animal Care and Use Committee of the University of California, San Diego.

Serum leptin was measured using Quantikine Mouse Leptin ELISA kit (R&D Systems) following the manufacturer's protocol (range 1.25 ng/mL – 80 ng/mL).

For all experiments, five coronal series of 20 μ m brain sections were cut on a cryostat, thaw-mounted onto Superfrost-plus slides, and stored at -80°C until use in *in-situ* hybridization. *In-situ* hybridization was performed for *Rfrp* (single label) or *Rfrp* and *LepRb* (double label) as described in Chapter 1.

Statistical Analysis

All data are expressed as the mean \pm SEM for each group. In all experiments, differences were analyzed by Student's t-test or by 2-way ANOVA, followed by post-hoc comparisons for individual genotype/treatments groups or time points via Fisher's (protected) least significant difference. Completion of vaginal opening was plotted on a Kaplan–Meier survival plot and analyzed by logrank (Mantel-Cox) test. Statistical significance was set at $p < 0.05$. All analyses were performed in Statview 5.0.1 (SAS Institute, Cary, NC).

Experiment 1: Assessment of the pattern of Rfrp mRNA expression during postnatal and prepubertal development in mice of both sexes

The developmental pattern of *Rfrp* expression in male and female mice during postnatal and peripubertal development is not well characterized. This first experiment determined if and

when *Rfrp* expression changes during postnatal development in mice of both sexes at ages PND 1, PND 10, PND 20 and adulthood (7-9 wks; females in diestrous). Brains from mice at these ages were assayed for *Rfrp* mRNA expression, including number of *Rfrp*-expressing cells and relative *Rfrp* mRNA/cell, using single-label ISH (n = 6-7 animals/group/sex).

Experiment 2: Assessment of BAX-dependent apoptosis regulation of Rfrp neuron development

Experiment 1 identified a significant decrease in total *Rfrp* cell number, primarily due to a robust decrease in LE cells, between birth and adulthood. Apoptosis (programmed cell death) was hypothesized to be responsible for this developmental decrease in *Rfrp* cells. To test this, brain sections from gonadectomized adult BAX knockout (KO) males (which lack BAX-mediated apoptosis) were assayed and compared to wildtypes (WT) using single-label ISH for *Rfrp* expression (n = 7-8 animals/genotype).

Experiment 3: Does Rfrp expression during postnatal development coincide with serum leptin levels?

Chapter 4 demonstrated that adult Ob mice display altered *Rfrp* expression, suggesting that leptin may regulate RFRP-3 neurons. In development, there is a large transient rise in serum leptin that occurs during the second week of life in mice. Around this same age, *Rfrp* expression is significantly higher than on the day of birth (124). In order to see if the juvenile leptin surge coincides with developmental changes in *Rfrp* neurons, C57BL6 breeder pairs were allowed to deliver pups naturally and the day of birth (postnatal day 1; PND 1) was noted for each litter (only litters of 4-8 pups were used). Pups were sacrificed by rapid decapitation on PND 1, 3, 6, 8, 10, 12, 14, and 16 (n = 5-9 animals per age, per sex). Trunk blood was collected for serum hormone analysis, and brains were collected and frozen on dry ice. For each sex, brain slices

containing the entire DMN were assayed and analyzed for *Rfrp* expression by single-label ISH, using the HE and LE *Rfrp* cell criteria described previously; each sex was assayed independently. Serum leptin was measured by ELISA. Along with the postnatal mice, cohorts of control adult diestrous female or male mice were simultaneously assayed for *Rfrp* expression and serum leptin levels.

To determine if the long form leptin receptor is expressed in juvenile *Rfrp* neurons at different developmental stages, an alternate set of brain slides from female PND 1, 10 and 12 mice (along with adult diestrous female controls) was assayed for *LepRb* co-expression in *Rfrp* neurons using double label ISH (n = 6-7 animals per age group).

Experiment 4: Are the juvenile changes in Rfrp expression during development dependent on leptin?

Given the synchronous developmental changes in juvenile *Rfrp* expression and postnatal leptin secretion observed in Experiment 5, it was hypothesized that this specifically-timed developmental changes in *Rfrp* neurons may be leptin dependent. To test this, experiment 5 was repeated using heterozygous *Ob* breeding pairs to produce WT, *Ob*, and heterozygous pups. Brains, trunk blood, and tail snips for genotyping were collected on PND 1, 6, 10, 12, and 16. Only litters of 4-8 pups were used. Brains from WT and *Ob* males of these various postnatal ages were analyzed for *Rfrp* mRNA expression levels via single-label ISH (n = 5-9 animals per age per genotype). Serum leptin for each animal was measured via ELISA to confirm the presence or absence of circulating leptin.

Results

Experiment 1: Expression of Rfrp changes dramatically in both sexes during postnatal and prepubertal development

This experiment determined the developmental profile of *Rfrp* expression in the DMN of both sexes. *Rfrp* mRNA levels showed significant developmental changes between birth and adulthood in both males and females. In both sexes, total DMN *Rfrp* mRNA levels increased during early postnatal life and then decreased between PND 20 and adulthood (*data not shown*). However, the total number of *Rfrp* cells significantly decreased between birth and adulthood, dropping nearly two-fold in both sexes, whereas the overall relative amount of *Rfrp* mRNA per cell significantly increased between birth and adulthood, rising more than 3-fold (Figure 5.1A-B, $p < 0.05$). Specifically, the number of *Rfrp* cells was significantly lower on PND 10 than PND 1, did not differ between PND 10 and PND 20, and dropped significantly again between PND 20 and adulthood (Figure 5.1B). Conversely, the relative *Rfrp* mRNA/cell significantly increased at each subsequent age examined, except between PND 20 and adults (Figure 5.1B). Overall, males and females showed the same general developmental pattern in total *Rfrp* cell number, relative *Rfrp* mRNA/cell, and total *Rfrp* mRNA.

The developmental pattern of *Rfrp* expression in the HE and LE *Rfrp* subpopulations were analyzed. At all ages, and in both sexes, there were more LE cells than HE cells. Interestingly, there were virtually no HE cells detected on PND 1 in either sex. A dramatic increase in the number of HE cells occurred between PND 1 and PND 10 and PND 20 ($p < 0.05$, Figure 5.1C). The number of HE cells then decreased significantly between PND 20 and adulthood. In both sexes, the *Rfrp* mRNA levels of HE cells increased over development, being significantly higher in PND 20 and adult mice than PND 1 mice (Figure 5.1C, $p < 0.05$).

LE *Rfrp* cells displayed a different developmental pattern than HE cells. The number of LE cells mirrored the total *Rfrp* cell population, decreasing steadily and significantly from PND 1 through adulthood (Figure 5.1D). In both sexes, there were significantly more LE cells on PND 1 than other ages, with each older age group having fewer LE cells than previous ages (Figure 5.1D, $p < 0.05$). While there was a small sex difference in the number of LE cells on PND 1 ($p < 0.05$), there were no sex differences at other ages. Similar to HE cells, the relative amount of *Rfrp* mRNA of LE cells increased during development in both males and females, being significantly lower on PND 1 than older ages (Figure 5.1D, $p < 0.05$).

Experiment 2: BAX-dependent apoptosis moderately affects Rfrp neurons development

Experiment 1 revealed a dramatic decrease in the total number of *Rfrp* cells, and LE cells, between birth and adulthood. Here BAX KO and WT mice were used to determine whether BAX-mediated apoptosis (cell death) underlies the robust developmental decrease in *Rfrp* cells. BAX KO mice have a small but significant increase in the total number of *Rfrp* cells compared to WT mice (Figure 5.2B, $p < 0.05$). The same general pattern was observed in both HE and LE *Rfrp* subpopulations, but only the number of LE cells was statistically different between BAX KOs and WTs (Figure 5.2D, $p < 0.05$). There was no significant difference in *Rfrp* mRNA/cell between WT and KO mice in either subpopulation (*data not shown*). While there are fewer *Rfrp* cells in WT than BAX KO animals, the observed difference in cell number (~ 17% decrease) was not nearly as great as the difference seen between PND 1 and adult mice (> 55% decrease, Figure 5.1), suggesting that BAX-mediated apoptosis is not fully responsible for the developmental decline in *Rfrp* cells.

Experiment 3: Changes in Rfrp expression over postnatal development correlate with the leptin surge

Chapter 4 demonstrated that *Rfrp* expression is significantly altered in adult Ob animals of both sexes. The juvenile leptin surge (169) might govern the developmental changes in *Rfrp* expression. To test this hypothesis, possible correlation between juvenile leptin levels and postnatal developmental changes in *Rfrp* expression was examined. C57BL6 mice of both sexes were sacrificed on PND 1, 3, 6, 8, 10, 12, 14, 16 and their brains assayed for *Rfrp* expression (Figure 5.3) and compared to serum leptin levels at each age. The total number of detectable *Rfrp* neurons was highest at birth and was significantly lower at later postnatal ages, with the lowest number of *Rfrp* neurons in adulthood (diestrous females) (Figure 5.4A). However, the amount of *Rfrp* being expressed per cell was notably lowest at birth and increased substantially with age. Indeed, the total amount of *Rfrp* mRNA in the DMN increased with postnatal development, beginning to rise around PND 6 and peaking at PND 12 before dropping again at subsequent older ages (Figure 5.4B, $p < 0.05$). This robust increase in total *Rfrp* mRNA during the second week of postnatal life appears to reflect a large increase in the number of HE *Rfrp* cells, which are virtually absent at birth but substantially increase in abundance beginning around PND 6, peaking at maximal levels at PND 12 before dropping slightly at subsequent older ages (Figures 5.4C, $p < 0.05$). Unlike HE *Rfrp* cells, the number of LE cells decreases slowly and steadily throughout these postnatal ages, with the lowest number of LE cells in adulthood (Figure 5.4D, $p < 0.05$). Virtually identical results were found in similarly-aged male mice (*data not shown*).

Serum leptin levels were measured in each animal to see if they correlated with *Rfrp* levels. For both sexes, mean serum leptin levels were essentially undetectable at birth (PND 1) and on PND 3, and were first readily detectable at PND 6. Leptin levels increased robustly during the second week of life, peaking at PND 10 and 12 (the leptin surge), and subsequently began to fall on PNDs 14 and 16, being low again in adult animals (Figure 5.4E, $p < 0.05$). Leptin levels

were significantly higher than adult female (diestrous) levels at all postnatal ages examined, except for PND 1 and 3 ($p < 0.05$). Interestingly, these postnatal changes in leptin levels, reflective of the leptin surge, appeared to correlate well with the observed increases in the number of HE *Rfrp* cells and total *Rfrp* mRNA, with both starting to increase around PND 6 and both reaching maximal levels around PND 10 and PND 12 (Figure 5.4).

The dramatic developmental increase in HE *Rfrp* neurons and total *Rfrp* mRNA observed around PND 10 and 12 correlates with the zenith of the juvenile leptin surge, suggesting that the two events may be related. To test this possibility, double label ISH was performed to determine if *Rfrp* neurons co-express *LepRb* during specific postnatal ages. In postnatal brains examined for *Rfrp/LepRb* co-expression, a subset of *Rfrp* cells clearly co-expressed notable *LepRb* mRNA (Figure 5.5A); the degree of co-expression did not vary with age, being 15-20% from birth through adulthood (Figure 5.5B).

Experiment 4: Juvenile Rfrp expression is not dependent on leptin during development

To determine if leptin signaling is required, directly or indirectly, for the normal pattern of *Rfrp* neuron development in juveniles, female Ob and WT brains were analyzed for *Rfrp* expression on PND 1, 6, 10, 12 and 16 (Figure 5.6, 5.7). Despite the strong correlation between developmental *Rfrp* and leptin changes observed in normal mice, there were no significant differences in the number of *Rfrp* neurons, total amount of *Rfrp* mRNA, or the number of HE and LE *Rfrp* cells between Ob and WT mice at any developmental age (Figure 5.7A-D). The same developmental pattern in *Rfrp* expression seen in Experiment 5 was observed in both genotypes, with identical magnitude increases detected in total *Rfrp* mRNA and the number of HE cells. Moreover, all *Rfrp* expression increases occurred at the same specific postnatal ages, regardless of genotype. Confirming the genotypes and leptin milieu, serum leptin was significantly elevated

between PND 6 and 12 (representing the leptin surge), and lower on PND 16 than 12 in WT animals ($p < 0.05$) but remained undetectable in Ob animals at all ages (Figure 5.7E).

Discussion

The developmental profile for *Rfrp* is remarkably unique. At birth, there are primarily only LE cells, which gradually decrease over time while there is an increase in HE cells beginning around PND 6-10. This change in *Rfrp* cell number is not solely reflective of BAX-mediated apoptosis or the effects of leptin on hypothalamic development, despite the correlation of the leptin surge and *Rfrp* expression.

Total *Rfrp* mRNA levels rise similarly in both sexes during postnatal/prepubertal development and then decline again between PND 20 and adulthood. This pattern is consistent with qPCR findings in developing rats (66,117), and may possibly reflect a developmental mechanism that restrains activation of the reproductive axis before puberty and then reduces inhibition of GnRH neurons by RFRP-3 during the pubertal transition. However, subsequent analysis of *Rfrp* cell number and relative *Rfrp* expression per cell, in both the total *Rfrp* population and the HE and LE subpopulations, uncovered divergent and unique patterns not previously detected using just qPCR. Intriguingly, the HE and LE cells showed dramatically different developmental patterns in cell number, though both sub-populations increased their cellular *Rfrp* levels throughout with age. The significance of these specific developmental changes is currently unknown. Although there are dramatic developmental decreases in the total number of *Rfrp* cells (specifically, LE cells) in both sexes, this change is likely not primarily due to BAX-dependent apoptosis, the main mechanism of neuronal cell death (168). Although BAX-mediated apoptosis regulates *Rfrp* cell development to a minor degree (~ 17% change in cell number), this small change cannot fully explain the dramatic (> 55%) developmental decrease in

Rfrp cells. Whether transcriptional and/or epigenetic changes underlie the observed decrease in *Rfrp* cells is currently unknown.

In the second set of experiments, using a more detailed time-line during the first two weeks of life in C57BL6 mice, the developmental increase in HE *Rfrp* cells and total *Rfrp* mRNA appears around PND 6-8, with a peak in these measures around PND 12. This was in striking synchronous alignment with the occurrence of the postnatal leptin surge. However, using Ob mice, neither the timing nor magnitude of this developmental pattern of the *Rfrp* population is leptin dependent. The developmental changes observed in *Rfrp* expression may be due to other metabolic hormones, such as ghrelin or insulin (172-174), or reproductive hormones from maturing gonads (175-178), all of which have been shown to modify gene expression in the developing hypothalamus. Identifying the cause of the dramatic *Rfrp* changes during development, and just as importantly, the functional significance of such changes, will be an important avenue of future inquiry.

Rfrp neuronal activation decreases significantly prior to pubertal development (171) and this removal of an inhibitory neuropeptide may allow puberty to occur. However, RFRP-3 add back during PND 21-28 was ineffective at delaying pubertal advancement as there were no differences in the completion of VO with either administration method (mini-osmotic pumps or daily injections, *data not shown*). It is also possible that RFRP-3 does not regulate pubertal development. Small interfering RNA knockdown RFRP-3 of was unable to advance or delay pubertal advancement (152) and Gpr147 knockout mice, which are unresponsive to RFRP-3, have no changes in the timing of vaginal opening (89). However, RFRP-3 may still have a role in prepubertal mice controlling LH secretion, but not the timing of puberty. Prepubertal Gpr147 KO male mice have higher LH levels than their wildtype counterparts, but this difference normalizes after puberty (89). RFRP-3 may not have a role in the timing of puberty, but still may act to suppress LH secretion prior to puberty.

The developmental pattern of *Rfrp* expression in the rodent brain during infantile and juvenile life is incredibly unique, not an apoptotic mechanism, and though this pattern correlates with leptin levels, it does not appear to be dependent on leptin signaling. The mechanism and physiological significance of this dramatic *Rfrp* changes during juvenile development remains to be determined. These findings establish that RFRP-3 may have a role in regulating reproductive function prior to puberty, and the sets a precedent for examine RFRP-3 during puberty.

Portions of this chapter are published in *Endocrinology* (April 2012). The dissertation author was the primary investigator and author of this material. Josh Kim and Sangeeta Dhamija provided support with brain cyrosectioning and performing ISH. Alexander Kauffman supervised the project and provided advice.

Portions of this chapter are published in *Neuroendocrinology* (November 2014). The dissertation author was the primary investigator and author of this material. Morris Sheih, Nagambika Munaganuru, and Elena Luo were undergraduates in the lab who assisted in cyrosectioning and performing ISH. Alexander Kauffman supervised the project and provided advice.

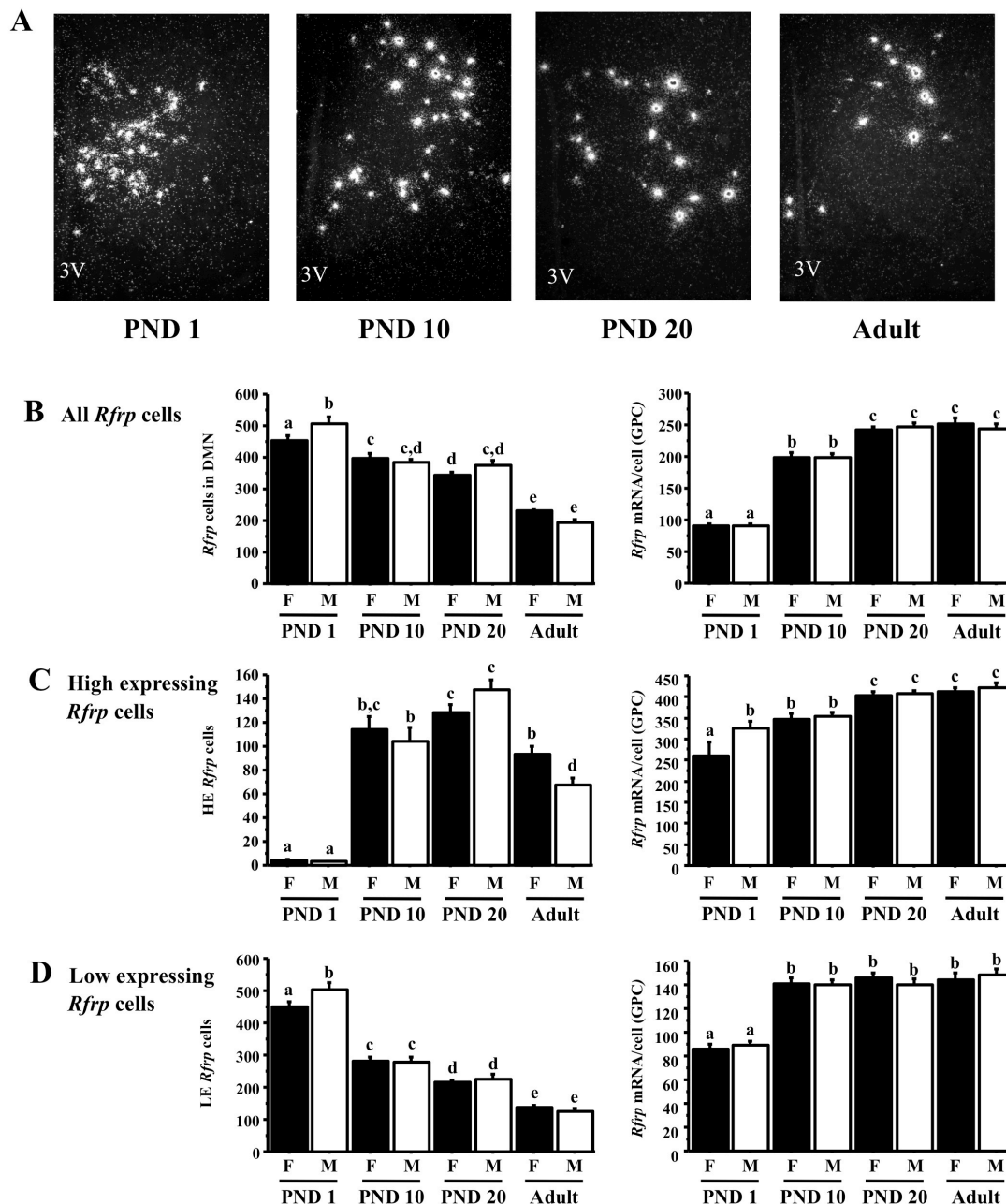


Figure 5.1. Changes in *Rfrp* expression in male and female mice over postnatal development. **[A]** Representative photomicrographs of *Rfrp* expression on postnatal day (PND) 1, PND 10, PND 20, and adult male mice. 3V = third ventricle. **[B]** Mean changes in the total number of *Rfrp* cells and *Rfrp* mRNA/cell (determined by silver grains/cell) of all cells in males (M) and females (F) over development. **[C]** Mean changes in the high-expressing (HE) *Rfrp* cells and *Rfrp* mRNA/HE cell in M and F over development. **[D]** Mean changes in the low-expressing (LE) *Rfrp* cells and *Rfrp* mRNA/LE cell in M and F over development. Bars labeled with different letters differ significantly from each other ($p < 0.05$).

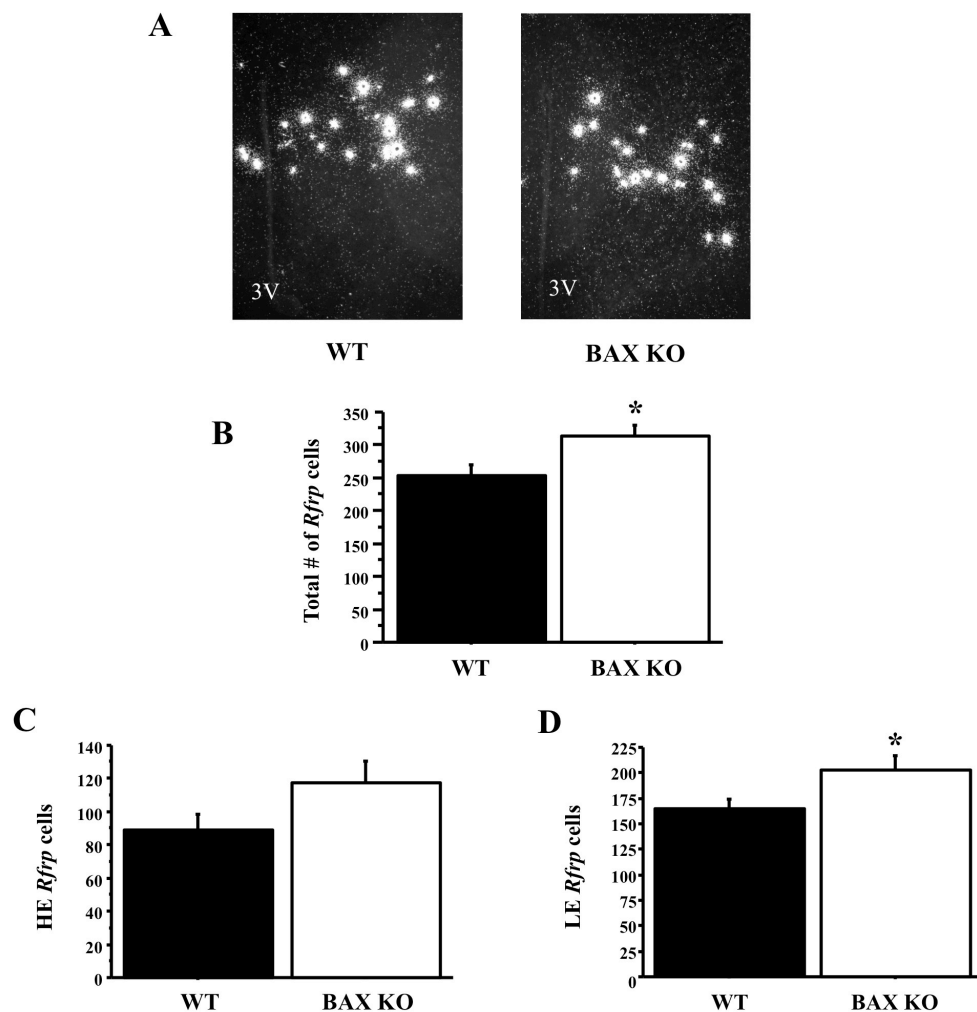


Figure 5.2. Maturation of *Rfrp* neurons in BAX knockout mice. **[A]** Representative photomicrographs of *Rfrp* expression in adult-gonadectomized wildtype (WT) and BAX knockout (KO) male mice. 3V = third ventricle. **[B]** Mean number of total *Rfrp* cells between WT and KO animals is significantly different ($p < 0.05$). **[C]** Mean number of high-expressing (HE) *Rfrp* cells between WT and KO animals. There was no significant difference between genotypes. **[D]** Mean number of low-expressing (LE) *Rfrp* cells between WT and KO animals. There were significantly more LE cells in BAX KO than WT animals ($p < 0.05$).

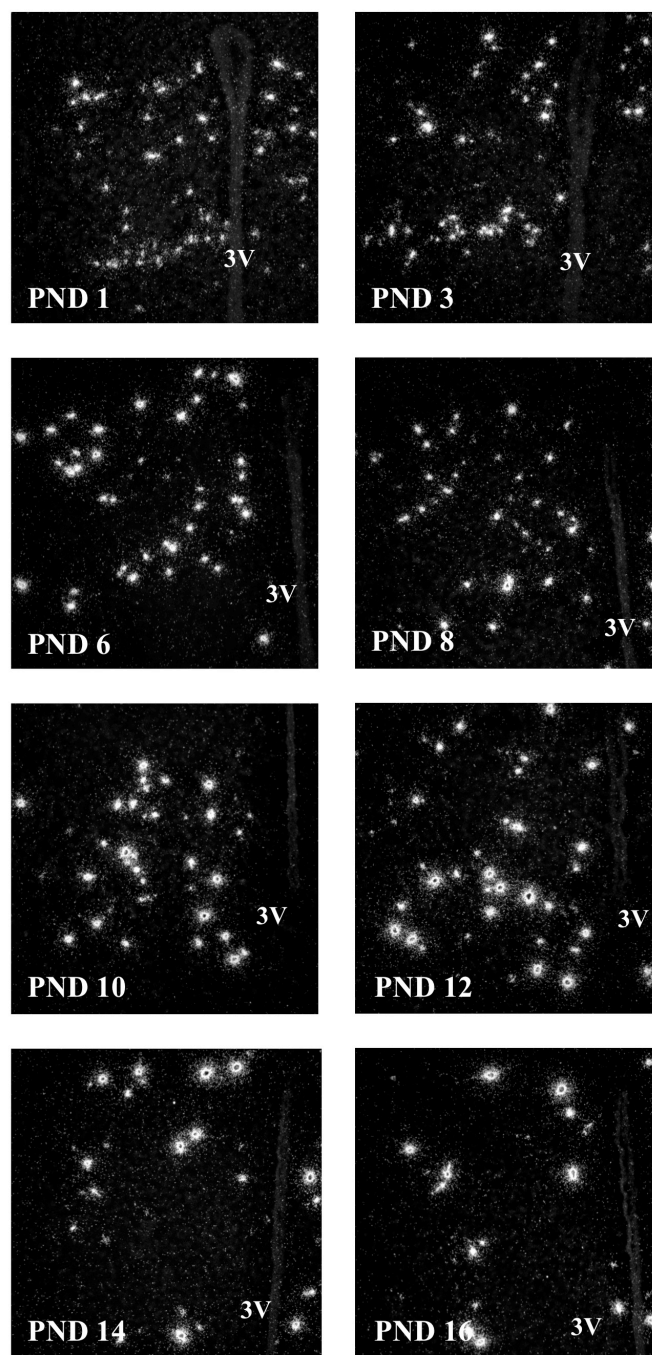


Figure 5.3 *Rfrp* expression over the first 16 days of postnatal life. Representative photomicrographs of single label *in-situ* hybridization for *Rfrp* mRNA on postnatal days (PND) 1, 3, 6, 8, 10, 12, 14, 16 in female mice. Day of birth is designated PND 1. 3V = third ventricle.

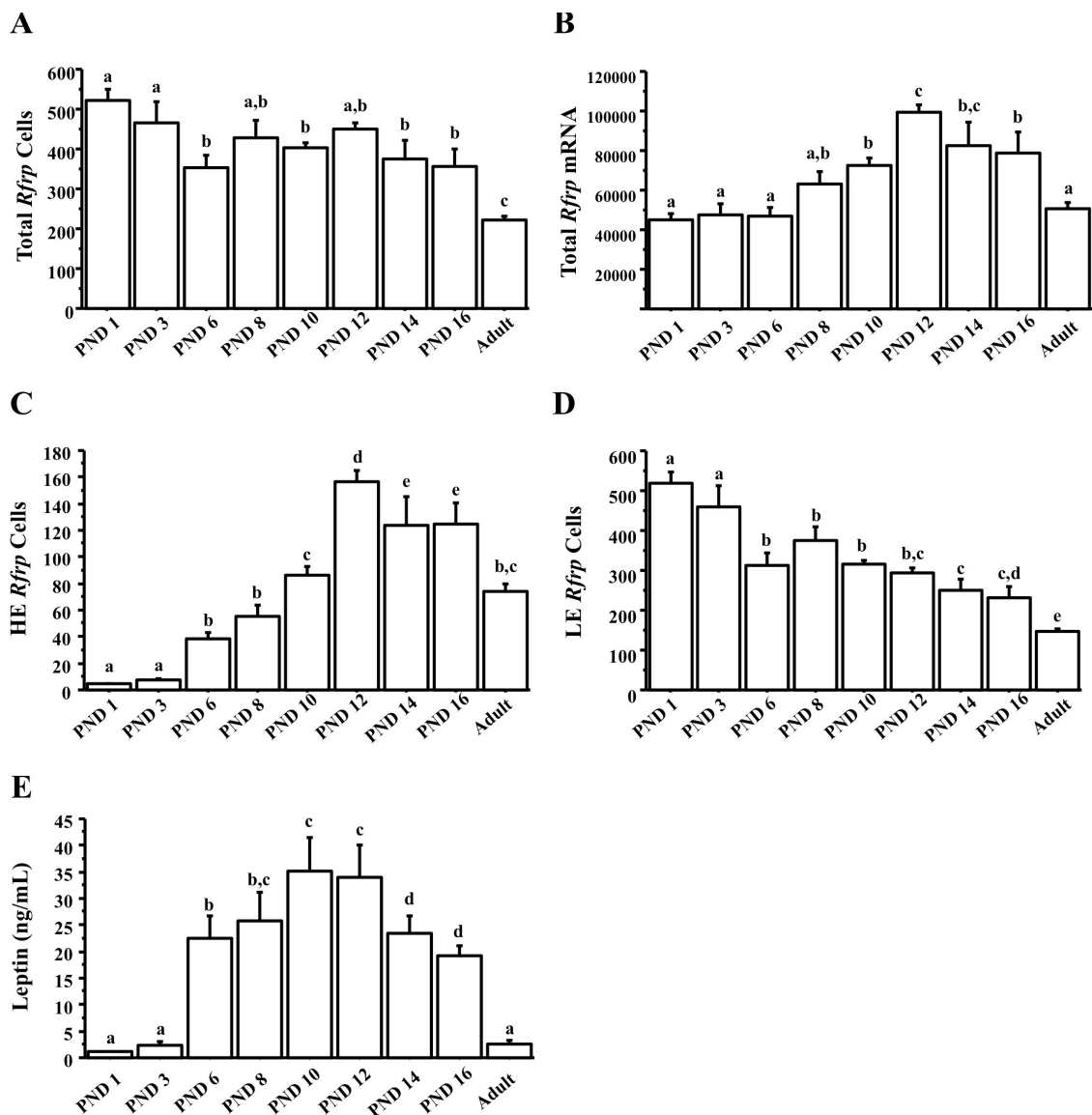


Figure 5.4. Summary of changes in *Rfrp* expression over the first 16 days of postnatal life in female mice from single label *in-situ* hybridization. *Rfrp* mRNA was quantified on postnatal days (PND) 1, 3, 6, 8, 10, 12, 14, 16 and diestrous female adult mice. **[A]** Quantification of total number of *Rfrp* neurons during the first two weeks of life. Different letters indicate significantly different groups ($p < 0.05$). **[B]** Quantification of total *Rfrp* mRNA during the first two weeks of life. Different letters indicate significantly different groups ($p < 0.05$). **[C]** Quantification of the number of high expressing (HE) *Rfrp* neurons during the first two weeks of life. Different letters indicate significantly different groups ($p < 0.05$). **[D]** Quantification of the number of low expressing (LE) *Rfrp* neurons during the first two weeks of life. Different letters indicate significantly different groups ($p < 0.05$). **[E]** Average serum leptin levels of mice sacrificed across development on PND 1, 3, 6, 8, 10, 12, 14, 16 and a cohort of diestrous female adult mice. Different letters indicate significantly different groups ($p < 0.05$).

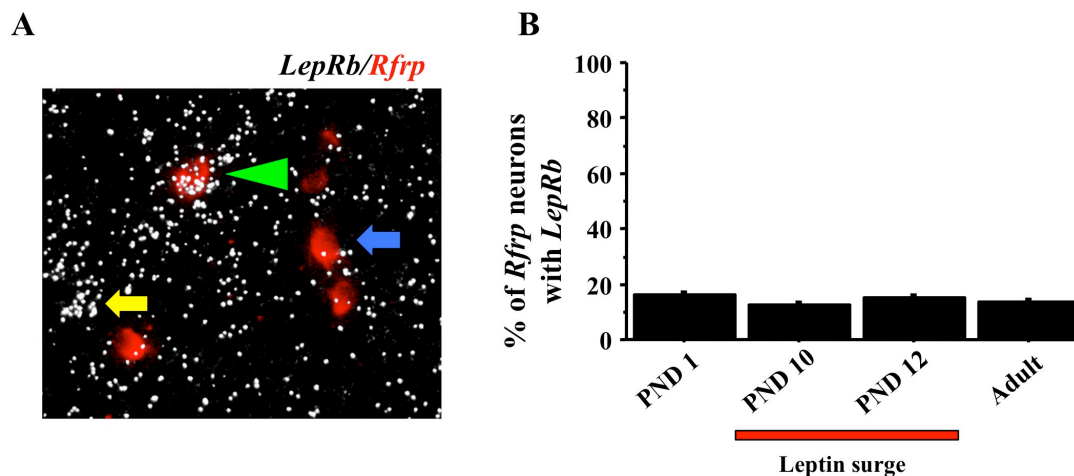


Figure 5.5. Long-form leptin receptor (*LepRb*) expression in some *Rfrp* neurons during postnatal life. **[A]** Representative photomicrographs of double label *in-situ* hybridization *LepRb* (silver grains) in *Rfrp* neurons (red fluorescence) in the DMN region. A single labeled *Rfrp* neurons is identified with a blue arrows and a single labeled *LepRb* neuron is marked with a yellow arrow. Double labeled *LepRb/Rfrp* is marked with a green arrowhead. 3V = third ventricle. **[B]** Quantification of the percent co-expression of *LepRb* and *Rfrp* during postnatal development. Animals sacrificed on postnatal days (PND) 1, 10, 12 and a cohort of adult diestrous females were assayed. No significant differences were seen between ages. The leptin surge peaks around PND 10 and 12, as indicated by the red bar.

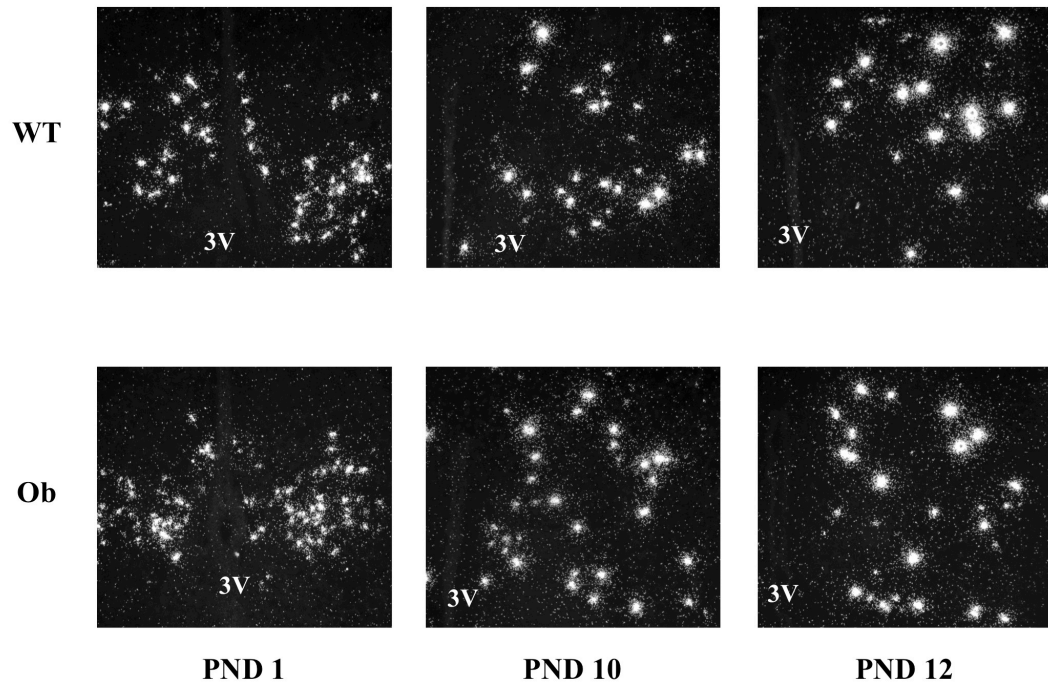


Figure 5.6. *Rfrp* expression over postnatal life in female Obese (Ob) and wildtype (WT) littermates. Representative photomicrographs of single label *in-situ* hybridization for *Rfrp* mRNA on postnatal days (PND) 1, 10, and 12 are shown. 3V = third ventricle.

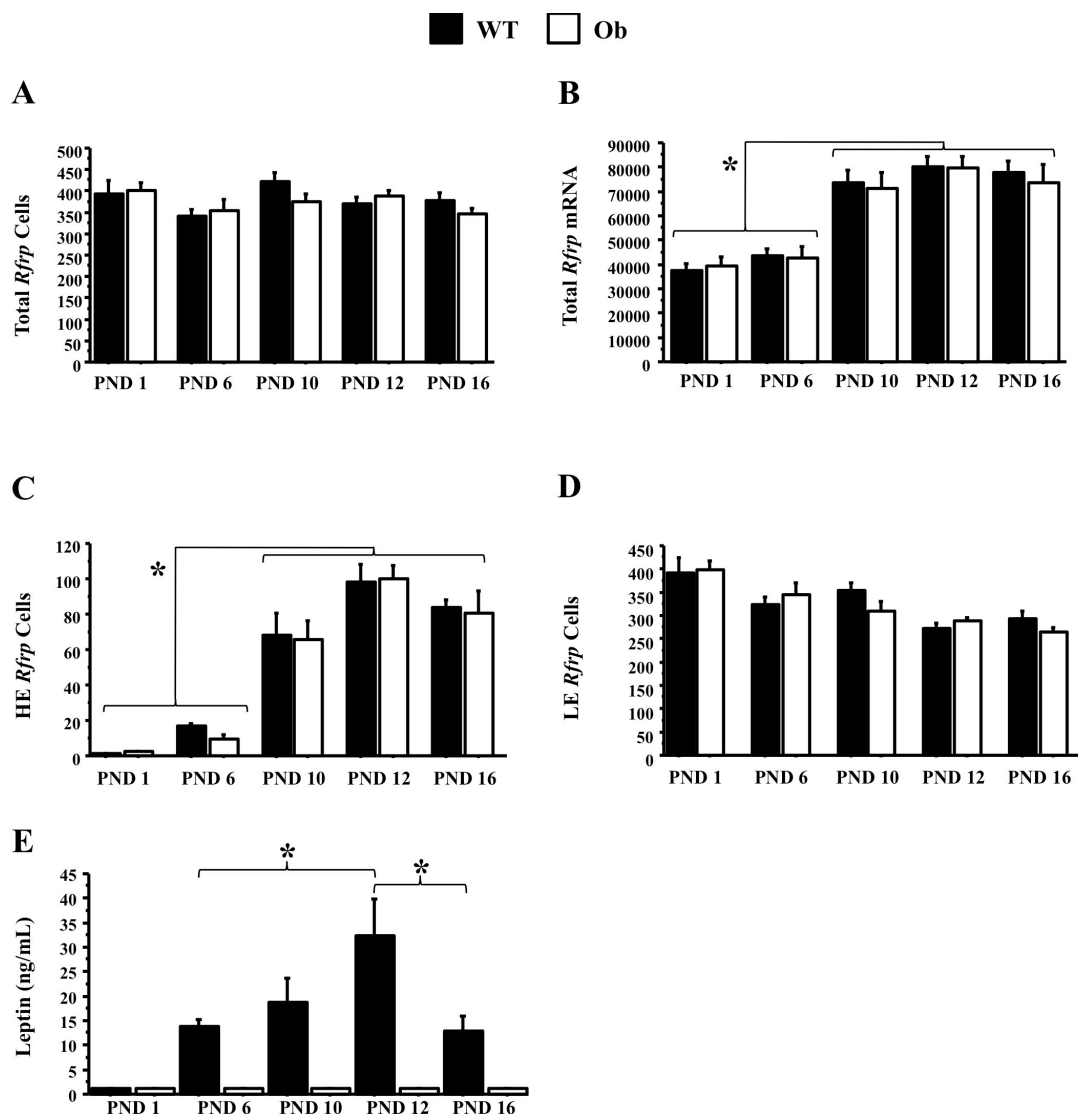


Figure 5.7. Summary of changes in *Rfrp* expression on postnatal days (PND) 1, 6, 10, 12, and 16 in female Obese (Ob) and wildtype (WT) animals. **[A]** Quantification of total number of *Rfrp* neurons during the leptin surge. There were no significant changes between genotypes. **[B]** Quantification of total *Rfrp* mRNA during the leptin surge. *Rfrp* expression is significantly higher on postnatal (PND) 10, 12, and 16 than on PND 1 or PND 6 ($p < 0.05$). **[C]** Quantification of the number of high expressing (HE) *Rfrp* neurons during the leptin surge. The number of *Rfrp* neurons is significantly higher on PND 10, 12, and 16 than on PND 1 or PND 6 ($p < 0.05$). **[D]** Quantification of the number of low expressing (LE) *Rfrp* neurons during the leptin surge. Different letters indicate significantly different groups ($p < 0.05$). **[E]** Serum leptin concentration in Ob and WT female mice as measured by ELISA. Leptin is highest on postnatal days 10 and 12, dropping on 16, demonstrating the postnatal leptin surge. Leptin concentration in WT mice were significantly elevated between PND 6 and PND 16, peaking around PND 12 ($p < 0.05$). Leptin was not detectable on the day of birth in WT mice or in Ob animals at any age.

CONCLUSIONS

This thesis investigated the following questions: how does RFRP-3 effect hormone levels, where is RFRP-3 and its receptors found within the mouse brain, how does RFRP-3 interface with the kisspeptin system, is RFRP-3 regulated by sex steroids, does the RFRP-3 system respond to metabolic or glucocorticoid stressors, and how does RFRP-3 change during prepubertal development. These six studies, while being independent lines of investigation, all contribute to our understanding of the neuroendocrine system and how RFRP-3 fits into the reproductive system.

RFRP-3 gained notoriety as the mammalian ortholog of the avian gonadotropin-inhibiting hormone. In avian neuroendocrinology, the discovery of GnIH was a major advancement in the understanding of the bird reproductive system, as the role of several neuropeptide systems are not conserved between mammals and birds. Since GnIH has very potent and clear-cut effects on the avian pituitary, mammalian reproductive biologist hoped a similar pharmacological effect would be observed in mammalian models. Additionally, the term “gonadotropin inhibiting hormone,” which is a clear opposite term of “gonadotropin releasing hormone,” promotes exaggeration of peptide’s role in normal physiology. As this thesis and other publications have shown, RFRP-3 treatment has a clear effect on LH secretion, but still lacks an obvious identified role in mouse reproduction. The majority of GnRH neurons lack Gpr147, which is also absent from the pituitary and the majority of kisspeptin neurons. RFRP-3 neurons do not appear to be major mediators or sex steroid negative feedback, or relay metabolic challenges or glucocorticoid responses, although minor effects have been observed. There is suppression of *Rfrp* neuronal activity during the LH surge, which suggests RFRP-3 has a role in that event. Lastly, *Rfrp* expression, and neuronal morphology/distribution changes dramatically during postnatal development, but is not associated with changes in leptin. While this is a nowhere near exhaustive list of possible roles

for RFRP-3 in reproductive biology, RFRP-3 does not seem to fall neatly in any of these major categories.

Of the experiments presented here, the suppression of *Rfrp* expression by E_2 and the decrease in activity during the LH surge provides the best hint as to the possible function of RFRP-3 in mouse reproduction; the mechanism in which the LH surge is halted. The LH surge is a positive feedback event that promotes ovulation, the physical ejection of matured follicles from the ovarian body. After ovulation, E_2 levels drop, GnRH neuronal activity decreases, and gonadotropin secretion ceases, but the mechanism that returns GnRH neurons to their basal level of activity is unknown. This transition could be mediated by RFRP-3, which acts as the brake to slow GnRH secretion, and is supported by 1) RFRP-3 suppresses GnRH neuron firing, 2) RFRP-3 expression is suppressed by E_2 , therefore gating this inhibitor until after all follicles are liberated from the ovary, and 3) the temporal decrease in RFRP-3 neuronal activity during the LH surge in female rodents, which keeps GnRH/LH secretion high until ovulation is complete. Given these three facts, RFRP-3 may prove to be a part of the unknown neural mechanism that dictates the LH surge.

The relevance of RFRP-3 in human reproduction is unknown. Mutations in *GPR54* and *KISS1* in humans have profound effects on reproduction, causing complete infertility and absent puberty (17,18), and these discoveries generated an entire new sub-discipline of reproductive endocrinology. Similar findings regarding *Rfrp* do not exist, as there are currently no studies examining humans with mutations to *RFRP* or *GPR147*. The absence of this data from the literature could be explained by either a subtle or lack of phenotype in human subjects with these mutations, and therefore they are not identified, or human patients with reproductive, or other phenotypes, have not been screened for mutations in these genes. Until such a study is published, it is difficult to determine the significance of RFRP-3 or GPR147 in human reproduction.

Currently, there is only one knockout animal model examining RFRP-3 biology, the Gpr147 KO mouse (89). As stated earlier, the Gpr147 KO mouse has no impairments in fertility, has normal LH secretion in adulthood, and normal pubertal progression. A minor phenotype was found in LH secretion prior to puberty, and there was a significant effect on LH secretion after food deprivation. However, neither of these outcomes are a striking reproductive phenotype. Surprisingly, there is still no *Rfrp* knockout mouse, which is the opposite and essential animal model that needs to be generated. The reason for the absence of an *Rfrp* knockout mouse is unclear, but is possibly due to the speculative concern that there may be no obvious reproductive phenotype and this would limit the experimental potential of this mouse model.

The studies presented here were inherently biased in their design in which a role in reproduction was assumed. This has pigeonholed RFRP-3 as a reproductive peptide, when in fact it may have interesting and clinically relevant roles in other physiological or behavior systems. There are a number of studies in rodents demonstrating the RFRP-3, and other RFamide peptides, have effects on body temperature (73,93), nociception (32,60,73,94), feeding behavior (64,77,179) and anxiety behaviors (95). RFRP-3 may have an essential role in any of these systems, or another aspect of mammalian physiology or behavior that has yet to be explored.

To advance the understanding of RFRP-3, and address methodological limitations, our lab has developed two new unbiased models to explore RFRP-3 biology utilizing Cre/loxP technology. Collaborators at Harvard University have developed a *Rfrp*-cre (RC) mouse line which allows for investigators to selectively knock-in or knock-out genes in RFRP-3 producing cells. The first of these models is a RC ROSA-tdTomato mouse line that produces mice that express the red fluorescent recombination protein tdTomato in RFRP-3 neurons. Using established flow cytometry protocols, hypothalami from these mice are dissociated and sorted for these fluorescent cells. After sorting, RNA can be extracted from the cells to be used for

downstream applications, such as qPCR or next generation RNA-sequencing. After acquiring the sequencing results and bioinformatics analysis, the expression profile of *Rfrp* neurons will be known and directed studies can be designed.

The second of these RC mouse models is a selective ablation mouse line using the diphtheria toxin receptor (ROSA-iDTR). Mice from this line have the diphtheria toxin receptor knocked into *Rfrp* expressing cells that allows them to be sensitively ablated using diphtheria toxin. This model has experimental advantage over traditional gene knockout studies in that the toxin can be administered to the animals in adulthood, therefore eliminating the issue of developmental compensation, or administered after a specific experimental treatment allowing for animals to be “paired” against themselves (i.e. sex steroid regulation before and after cell ablation). A concern for this series of experiments is that the toxin needs to be administered centrally, as pilot experiments demonstrated that peripheral injections of the toxin were ineffective. Also, as the toxin eliminates the entire neuron, including all other neuropeptides and transmitters synthesized by that neuron, in addition to removing RFRP-3, any interesting phenotype may be due to the loss of RFRP-3, or another gene product produced by those neurons.

In conclusion, RFRP-3 is an interesting neuropeptide that can elicit inhibitory effects on the reproductive system in rodents, similar to its avian counterpart, although the exact mechanism in which RFRP-3 fits into *in vivo* reproductive biology remains unclear. RFRP-3 appears to be an independent neuropeptide system originating in the DMN of the hypothalamus that regulates GnRH secretion, directly and indirectly, is perhaps a component of the LH surge neural network, and exhibits a unique developmental gene expression profile, the functional significance of which remains to be elucidated.

REFERNCES

1. Herbison AE. Physiology of the Gonadotropin-Releasing Hormone Neuronal Network. In: Neill JD, ed. *Knobil and Neill's Physiology of Reproduction*. Vol 2. 3rd ed. St. Louis: Elsevier; 2006.
2. Dode C, Hardelin JP. Clinical genetics of Kallmann syndrome. *Annales d'endocrinologie*. 2010;71(3):149-157.
3. Plant TM. The male monkey as a model for the study of the neurobiology of puberty onset in man. *Mol Cell Endocrinol*. 2006;254-255:97-102.
4. Bourguignon JP, Franchimont P. Puberty-related increase in episodic LHRH release from rat hypothalamus in vitro. *Endocrinology*. 1984;114(5):1941-1943.
5. Urbanski HF, Ojeda SR. Activation of luteinizing hormone-releasing hormone release advances the onset of female puberty. *Neuroendocrinology*. 1987;46(3):273-276.
6. Gottsch ML, Cunningham MJ, Smith JT, Popa SM, Acohido BV, Crowley WF, Seminara S, Clifton DK, Steiner RA. A role for kisspeptins in the regulation of gonadotropin secretion in the mouse. *Endocrinology*. 2004;145(9):4073-4077.
7. Roa J, Herbison AE. Direct regulation of GnRH neuron excitability by arcuate nucleus POMC and NPY neuron neuropeptides in female mice. *Endocrinology*. 2012;153(11):5587-5599.
8. True C, Verma S, Grove KL, Smith MS. Cocaine- and amphetamine-regulated transcript is a potent stimulator of GnRH and kisspeptin cells and may contribute to negative energy balance-induced reproductive inhibition in females. *Endocrinology*. 2013;154(8):2821-2832.
9. Selvage DJ, Johnston CA. Interaction between norepinephrine, oxytocin, and nitric oxide in the stimulation of gonadotropin-releasing hormone release from proestrous rat basal hypothalamus explants. *J Neuroendocrinol*. 2004;16(10):819-824.
10. Virmani MA, Stojilkovic SS, Catt KJ. Stimulation of luteinizing hormone release by gamma-aminobutyric acid (GABA) agonists: mediation by GABAA-type receptors and activation of chloride and voltage-sensitive calcium channels. *Endocrinology*. 1990;126(5):2499-2505.
11. Kalra SP, Crowley WR. Norepinephrine-like effects of neuropeptide Y on LH release in the rat. *Life Sci*. 1984;35(11):1173-1176.
12. Sahu A, Crowley WR, Tatemoto K, Balasubramaniam A, Kalra SP. Effects of neuropeptide Y, NPY analog (norleucine4-NPY), galanin and neuropeptide K on LH release in ovariectomized (ovx) and ovx estrogen, progesterone-treated rats. *Peptides*. 1987;8(5):921-926.

13. Ducret E, Anderson GM, Herbison AE. RFamide-related peptide-3, a mammalian gonadotropin-inhibitory hormone ortholog, regulates gonadotropin-releasing hormone neuron firing in the mouse. *Endocrinology*. 2009;150(6):2799-2804.
14. Gamba M, Pralong FP. Control of GnRH neuronal activity by metabolic factors: the role of leptin and insulin. *Mol Cell Endocrinol*. 2006;254-255:133-139.
15. Moenter SM. Identified GnRH neuron electrophysiology: a decade of study. *Brain Res*. 2010;1364:10-24.
16. Yeo SH. Neuronal circuits in the hypothalamus controlling gonadotrophin-releasing hormone release: the neuroanatomical projections of kisspeptin neurons. *Experimental physiology*. 2013;98(11):1544-1549.
17. de Roux N, Genin E, Carel JC, Matsuda F, Chaussain JL, Milgrom E. Hypogonadotropic hypogonadism due to loss of function of the KiSS1-derived peptide receptor GPR54. *Proc Natl Acad Sci U S A*. 2003;100(19):10972-10976.
18. Seminara SB, Messenger S, Chatzidaki EE, Thresher RR, Acierno JS, Jr., Shagoury JK, Bo-Abbas Y, Kuohung W, Schwinof KM, Hendrick AG, Zahn D, Dixon J, Kaiser UB, Slaugenhaupt SA, Gusella JF, O'Rahilly S, Carlton MB, Crowley WF, Jr., Aparicio SA, Colledge WH. The GPR54 gene as a regulator of puberty. *N Engl J Med*. 2003;349(17):1614-1627.
19. Tsutsui K, Saigoh E, Ukena K, Teranishi H, Fujisawa Y, Kikuchi M, Ishii S, Sharp PJ. A novel avian hypothalamic peptide inhibiting gonadotropin release. *Biochem Biophys Res Commun*. 2000;275(2):661-667.
20. Kriegsfeld LJ, Mei DF, Bentley GE, Ubuka T, Mason AO, Inoue K, Ukena K, Tsutsui K, Silver R. Identification and characterization of a gonadotropin-inhibitory system in the brains of mammals. *Proc Natl Acad Sci U S A*. 2006;103(7):2410-2415.
21. Tsutsui K, Bentley GE, Kriegsfeld LJ, Osugi T, Seong JY, Vaudry H. Discovery and evolutionary history of gonadotrophin-inhibitory hormone and kisspeptin: new key neuropeptides controlling reproduction. *J Neuroendocrinol*. 2010;22(7):716-727.
22. Simonin F. Neuropeptide FF receptors as therapeutic targets. *Drugs of the Future*. 2006.
23. Bonini JA, Jones KA, Adham N, Forray C, Artymyshyn R, Durkin MM, Smith KE, Tamm JA, Boteju LW, Lakhani PP, Raddatz R, Yao WJ, Ogozalek KL, Boyle N, Kouranova EV, Quan Y, Vaysse PJ, Wetzel JM, Branchek TA, Gerald C, Borowsky B. Identification and characterization of two G protein-coupled receptors for neuropeptide FF. *J Biol Chem*. 2000;275(50):39324-39331.
24. Yoshida H, Habata Y, Hosoya M, Kawamata Y, Kitada C, Hinuma S. Molecular properties of endogenous RFamide-related peptide-3 and its interaction with receptors. *Biochim Biophys Acta*. 2003;1593(2-3):151-157.
25. Orsini MJ, Klein MA, Beavers MP, Connolly PJ, Middleton SA, Mayo KH. Metastin (KiSS-1) mimetics identified from peptide structure-activity relationship-derived

- pharmacophores and directed small molecule database screening. *J Med Chem.* 2007;50(3):462-471.
26. Oishi S, Misu R, Tomita K, S. S, Masuda R, Ohno H, Naniwa Y, Ieda N, Inoue N, Satoshi O, Uenoyama Y, Tsukamura H, Maeda K, Hirasawa A, Tsujimoto G, Fujii N. Activation of Neuropeptide FF Receptors by Kisspeptin Receptor Ligands. *ACS Medicinal Chemistry Letters.* 2011;2:53-57.
 27. Hinuma S, Habata Y, Fujii R, Kawamata Y, Hosoya M, Fukusumi S, Kitada C, Masuo Y, Asano T, Matsumoto H, Sekiguchi M, Kurokawa T, Nishimura O, Onda H, Fujino M. A prolactin-releasing peptide in the brain. *Nature.* 1998;393(6682):272-276.
 28. Lee DK, Nguyen T, Lynch KR, Cheng R, Vanti WB, Arkhitko O, Lewis T, Evans JF, George SR, O'Dowd BF. Discovery and mapping of ten novel G protein-coupled receptor genes. *Gene.* 2001;275(1):83-91.
 29. Ohtaki T, Shintani Y, Honda S, Matsumoto H, Hori A, Kanehashi K, Terao Y, Kumano S, Takatsu Y, Masuda Y, Ishibashi Y, Watanabe T, Asada M, Yamada T, Suenaga M, Kitada C, Usuki S, Kurokawa T, Onda H, Nishimura O, Fujino M. Metastasis suppressor gene KiSS-1 encodes peptide ligand of a G-protein-coupled receptor. *Nature.* 2001;411(6837):613-617.
 30. Tomita K, Niida A, Oishi S, Ohno H, Cluzeau J, Navenot JM, Wang ZX, Peiper SC, Fujii N. Structure-activity relationship study on small peptidic GPR54 agonists. *Bioorg Med Chem.* 2006;14(22):7595-7603.
 31. Lyubimov Y, Engstrom M, Wurster S, Savola JM, Korpi ER, Panula P. Human kisspeptins activate neuropeptide FF2 receptor. *Neuroscience.* 2010;170(1):117-122.
 32. Elhabazi K, Humbert JP, Bertin I, Schmitt M, Bihel F, Bourguignon JJ, Bucher B, Becker JA, Sorg T, Meziane H, Petit-Demouliere B, Ilien B, Simonin F. Endogenous mammalian RF-amide peptides, including PrRP, kisspeptin and 26RFa, modulate nociception and morphine analgesia via NPF receptors. *Neuropharmacology.* 2013;75:164-171.
 33. Funes S, Hedrick JA, Vassileva G, Markowitz L, Abbondanzo S, Golovko A, Yang S, Monsma FJ, Gustafson EL. The KiSS-1 receptor GPR54 is essential for the development of the murine reproductive system. *Biochem Biophys Res Commun.* 2003;312(4):1357-1363.
 34. Messenger S, Chatzidaki EE, Ma D, Hendrick AG, Zahn D, Dixon J, Thresher RR, Malinge I, Lomet D, Carlton MB, Colledge WH, Caraty A, Aparicio SA. Kisspeptin directly stimulates gonadotropin-releasing hormone release via G protein-coupled receptor 54. *Proc Natl Acad Sci U S A.* 2005;102(5):1761-1766.
 35. Lapatto R, Pallais JC, Zhang D, Chan YM, Mahan A, Cerrato F, Le WW, Hoffman GE, Seminara SB. Kiss1^{-/-} mice exhibit more variable hypogonadism than Gpr54^{-/-} mice. *Endocrinology.* 2007;148(10):4927-4936.
 36. d'Anglemont de Tassigny X, Fagg LA, Dixon JP, Day K, Leitch HG, Hendrick AG, Zahn D, Franceschini I, Caraty A, Carlton MB, Aparicio SA, Colledge WH. Hypogonadotropic

- hypogonadism in mice lacking a functional Kiss1 gene. *Proc Natl Acad Sci U S A*. 2007;104(25):10714-10719.
37. Clarkson J, d'Anglemont de Tassigny X, Moreno AS, Colledge WH, Herbison AE. Kisspeptin-GPR54 signaling is essential for preovulatory gonadotropin-releasing hormone neuron activation and the luteinizing hormone surge. *J Neurosci*. 2008;28(35):8691-8697.
 38. Mayer C, Boehm U. Female reproductive maturation in the absence of kisspeptin/GPR54 signaling. *Nat Neurosci*. 2011;14(6):704-710.
 39. Kauffman AS, Park JH, McPhie-Lalmansingh AA, Gottsch ML, Bodo C, Hohmann JG, Pavlova MN, Rohde AD, Clifton DK, Steiner RA, Rissman EF. The kisspeptin receptor GPR54 is required for sexual differentiation of the brain and behavior. *J Neurosci*. 2007;27(33):8826-8835.
 40. Kinoshita M, Tsukamura H, Adachi S, Matsui H, Uenoyama Y, Iwata K, Yamada S, Inoue K, Ohtaki T, Matsumoto H, Maeda K. Involvement of central metastin in the regulation of preovulatory luteinizing hormone surge and estrous cyclicity in female rats. *Endocrinology*. 2005;146(10):4431-4436.
 41. Navarro VM, Castellano JM, Fernandez-Fernandez R, Tovar S, Roa J, Mayen A, Barreiro ML, Casanueva FF, Aguilar E, Dieguez C, Pinilla L, Tena-Sempere M. Effects of KiSS-1 peptide, the natural ligand of GPR54, on follicle-stimulating hormone secretion in the rat. *Endocrinology*. 2005;146(4):1689-1697.
 42. Navarro VM, Castellano JM, Fernandez-Fernandez R, Tovar S, Roa J, Mayen A, Nogueiras R, Vazquez MJ, Barreiro ML, Magni P, Aguilar E, Dieguez C, Pinilla L, Tena-Sempere M. Characterization of the potent luteinizing hormone-releasing activity of KiSS-1 peptide, the natural ligand of GPR54. *Endocrinology*. 2005;146(1):156-163.
 43. Irwig MS, Fraley GS, Smith JT, Acohido BV, Popa SM, Cunningham MJ, Gottsch ML, Clifton DK, Steiner RA. Kisspeptin activation of gonadotropin releasing hormone neurons and regulation of KiSS-1 mRNA in the male rat. *Neuroendocrinology*. 2004;80(4):264-272.
 44. Han SK, Gottsch ML, Lee KJ, Popa SM, Smith JT, Jakawich SK, Clifton DK, Steiner RA, Herbison AE. Activation of gonadotropin-releasing hormone neurons by kisspeptin as a neuroendocrine switch for the onset of puberty. *J Neurosci*. 2005;25(49):11349-11356.
 45. Pielecka-Fortuna J, Chu Z, Moenter SM. Kisspeptin acts directly and indirectly to increase gonadotropin-releasing hormone neuron activity and its effects are modulated by estradiol. *Endocrinology*. 2008;149(4):1979-1986.
 46. d'Anglemont de Tassigny X, Fagg LA, Carlton MB, Colledge WH. Kisspeptin can stimulate gonadotropin-releasing hormone (GnRH) release by a direct action at GnRH nerve terminals. *Endocrinology*. 2008;149(8):3926-3932.

47. Clarkson J, Herbison AE. Postnatal development of kisspeptin neurons in mouse hypothalamus; sexual dimorphism and projections to gonadotropin-releasing hormone neurons. *Endocrinology*. 2006;147(12):5817-5825.
48. Yeo SH, Herbison AE. Projections of arcuate nucleus and rostral periventricular kisspeptin neurons in the adult female mouse brain. *Endocrinology*. 2011;152(6):2387-2399.
49. Lehman MN, Merkley CM, Coolen LM, Goodman RL. Anatomy of the kisspeptin neural network in mammals. *Brain Res*. 2010;1364:90-102.
50. Yeo SH, Clarkson J, Herbison AE. Kisspeptin-gpr54 signaling at the GnRH neuron is necessary for negative feedback regulation of luteinizing hormone secretion in female mice. *Neuroendocrinology*. 2014;100(2-3):191-197.
51. Gutierrez-Pascual E, Martinez-Fuentes AJ, Pinilla L, Tena-Sempere M, Malagon MM, Castano JP. Direct pituitary effects of kisspeptin: activation of gonadotrophs and somatotrophs and stimulation of luteinising hormone and growth hormone secretion. *J Neuroendocrinol*. 2007;19(7):521-530.
52. Smith JT, Rao A, Pereira A, Caraty A, Millar RP, Clarke IJ. Kisspeptin is present in ovine hypophysial portal blood but does not increase during the preovulatory luteinizing hormone surge: evidence that gonadotropes are not direct targets of kisspeptin in vivo. *Endocrinology*. 2008;149(4):1951-1959.
53. Kadokawa H, Suzuki S, Hashizume T. Kisspeptin-10 stimulates the secretion of growth hormone and prolactin directly from cultured bovine anterior pituitary cells. *Anim Reprod Sci*. 2008;105(3-4):404-408.
54. Suzuki S, Kadokawa H, Hashizume T. Direct kisspeptin-10 stimulation on luteinizing hormone secretion from bovine and porcine anterior pituitary cells. *Anim Reprod Sci*. 2008;103(3-4):360-365.
55. Ubuka T, Ukena K, Sharp PJ, Bentley GE, Tsutsui K. Gonadotropin-inhibitory hormone inhibits gonadal development and maintenance by decreasing gonadotropin synthesis and release in male quail. *Endocrinology*. 2006;147(3):1187-1194.
56. Osugi T, Ukena K, Bentley GE, O'Brien S, Moore IT, Wingfield JC, Tsutsui K. Gonadotropin-inhibitory hormone in Gambel's white-crowned sparrow (*Zonotrichia leucophrys gambelii*): cDNA identification, transcript localization and functional effects in laboratory and field experiments. *J Endocrinol*. 2004;182(1):33-42.
57. Ubuka T, Kim S, Huang YC, Reid J, Jiang J, Osugi T, Chowdhury VS, Tsutsui K, Bentley GE. Gonadotropin-inhibitory hormone neurons interact directly with gonadotropin-releasing hormone-I and -II neurons in European starling brain. *Endocrinology*. 2008;149(1):268-278.
58. Yin H, Ukena K, Ubuka T, Tsutsui K. A novel G protein-coupled receptor for gonadotropin-inhibitory hormone in the Japanese quail (*Coturnix japonica*): identification, expression and binding activity. *J Endocrinol*. 2005;184(1):257-266.

59. Hinuma S, Shintani Y, Fukusumi S, Iijima N, Matsumoto Y, Hosoya M, Fujii R, Watanabe T, Kikuchi K, Terao Y, Yano T, Yamamoto T, Kawamata Y, Habata Y, Asada M, Kitada C, Kurokawa T, Onda H, Nishimura O, Tanaka M, Iбата Y, Fujino M. New neuropeptides containing carboxy-terminal RFamide and their receptor in mammals. *Nat Cell Biol.* 2000;2(10):703-708.
60. Liu Q, Guan XM, Martin WJ, McDonald TP, Clements MK, Jiang Q, Zeng Z, Jacobson M, Williams DL, Jr., Yu H, Bomford D, Figueroa D, Mallee J, Wang R, Evans J, Gould R, Austin CP. Identification and characterization of novel mammalian neuropeptide FF-like peptides that attenuate morphine-induced antinociception. *J Biol Chem.* 2001;276(40):36961-36969.
61. Yano T, Iijima N, Kakihara K, Hinuma S, Tanaka M, Iбата Y. Localization and neuronal response of RFamide related peptides in the rat central nervous system. *Brain Res.* 2003;982(2):156-167.
62. Ukena K, Tsutsui K. Distribution of novel RFamide-related peptide-like immunoreactivity in the mouse central nervous system. *Neurosci Lett.* 2001;300(3):153-156.
63. Gibson EM, Humber SA, Jain S, Williams WP, 3rd, Zhao S, Bentley GE, Tsutsui K, Kriegsfeld LJ. Alterations in RFamide-related peptide expression are coordinated with the preovulatory luteinizing hormone surge. *Endocrinology.* 2008;149(10):4958-4969.
64. Johnson MA, Tsutsui K, Fraley GS. Rat RFamide-related peptide-3 stimulates GH secretion, inhibits LH secretion, and has variable effects on sex behavior in the adult male rat. *Horm Behav.* 2007;51(1):171-180.
65. Rizwan MZ, Poling MC, Corr M, Cornes PA, Augustine RA, Quennell JH, Kauffman AS, Anderson GM. RFamide-Related Peptide-3 Receptor Gene Expression in GnRH and Kisspeptin Neurons and GnRH-Dependent Mechanism of Action. *Endocrinology.* 2012;153(8):3770-3779.
66. Quennell JH, Rizwan MZ, Relf HL, Anderson GM. Developmental and steroidogenic effects on the gene expression of RFamide related peptides and their receptor in the rat brain and pituitary gland. *J Neuroendocrinol.* 2010;22(4):309-316.
67. Pineda R, Garcia-Galiano D, Sanchez-Garrido MA, Romero M, Ruiz-Pino F, Aguilar E, Dijcks FA, Blomenrohr M, Pinilla L, van Noort PI, Tena-Sempere M. Characterization of the inhibitory roles of RFRP3, the mammalian ortholog of GnIH, in the control of gonadotropin secretion in the rat: in vivo and in vitro studies. *Am J Physiol Endocrinol Metab.* 2010;299(1):E39-46.
68. Pineda R, Garcia-Galiano D, Sanchez-Garrido MA, Romero M, Ruiz-Pino F, Aguilar E, Dijcks FA, Blomenrohr M, Pinilla L, van Noort PI, Tena-Sempere M. Characterization of the potent gonadotropin-releasing activity of RF9, a selective antagonist of RF-amide-related peptides and neuropeptide FF receptors: physiological and pharmacological implications. *Endocrinology.* 2010;151(4):1902-1913.

69. Wu M, Dumalska I, Morozova E, van den Pol AN, Alreja M. Gonadotropin inhibitory hormone inhibits basal forebrain vGluT2-gonadotropin-releasing hormone neurons via a direct postsynaptic mechanism. *J Physiol*. 2009;587(Pt 7):1401-1411.
70. Rizwan MZ, Porteous R, Herbison AE, Anderson GM. Cells expressing RFamide-related peptide-1/3, the mammalian gonadotropin-inhibitory hormone orthologs, are not hypophysiotropic neuroendocrine neurons in the rat. *Endocrinology*. 2009;150(3):1413-1420.
71. Son YL, Ubuka T, Millar RP, Kanasaki H, Tsutsui K. Gonadotropin-inhibitory hormone inhibits GnRH-induced gonadotropin subunit gene transcriptions by inhibiting AC/cAMP/PKA-dependent ERK pathway in LbetaT2 cells. *Endocrinology*. 2012;153(5):2332-2343.
72. Mollereau C, Mazarguil H, Marcus D, Quelven I, Kotani M, Lannoy V, Dumont Y, Quirion R, Dethieux M, Parmentier M, Zajac JM. Pharmacological characterization of human NPFF(1) and NPFF(2) receptors expressed in CHO cells by using NPY Y(1) receptor antagonists. *Eur J Pharmacol*. 2002;451(3):245-256.
73. Quelven I, Roussin A, Zajac JM. Comparison of pharmacological activities of Neuropeptide FF1 and Neuropeptide FF2 receptor agonists. *Eur J Pharmacol*. 2005;508(1-3):107-114.
74. Gouarderes C, Mazarguil H, Mollereau C, Chartrel N, Leprince J, Vaudry H, Zajac JM. Functional differences between NPFF1 and NPFF2 receptor coupling: high intrinsic activities of RFamide-related peptides on stimulation of [³⁵S]GTPgammaS binding. *Neuropharmacology*. 2007;52(2):376-386.
75. Talmont F, Mouldous L, Piedra-Garcia L, Schmitt M, Bihel F, Bourguignon JJ, Zajac JM, Mollereau C. Pharmacological characterization of the mouse NPFF2 receptor. *Peptides*. 2010;31(2):215-220.
76. Murakami M, Matsuzaki T, Iwasa T, Yasui T, Irahara M, Osugi T, Tsutsui K. Hypophysiotropic role of RFamide-related peptide-3 in the inhibition of LH secretion in female rats. *J Endocrinol*. 2008;199(1):105-112.
77. Clarke IJ, Smith JT, Henry BA, Oldfield BJ, Stefanidis A, Millar RP, Sari IP, Chng K, Fabre-Nys C, Caraty A, Ang BT, Chan L, Fraley GS. Gonadotropin-inhibitory hormone is a hypothalamic peptide that provides a molecular switch between reproduction and feeding. *Neuroendocrinology*. 2012;95(4):305-316.
78. Fu LY, van den Pol AN. Kisspeptin directly excites anorexigenic proopiomelanocortin neurons but inhibits orexigenic neuropeptide Y cells by an indirect synaptic mechanism. *J Neurosci*. 2010;30(30):10205-10219.
79. Bellinger LL, Bernardis LL. The dorsomedial hypothalamic nucleus and its role in ingestive behavior and body weight regulation: lessons learned from lesioning studies. *Physiol Behav*. 2002;76(3):431-442.

80. Sahu A, Kalra PS, Kalra SP. Food deprivation and ingestion induce reciprocal changes in neuropeptide Y concentrations in the paraventricular nucleus. *Peptides*. 1988;9(1):83-86.
81. Chan YY, Steiner RA, Clifton DK. Regulation of hypothalamic neuropeptide-Y neurons by growth hormone in the rat. *Endocrinology*. 1996;137(4):1319-1325.
82. Li C, Chen P, Smith MS. The acute suckling stimulus induces expression of neuropeptide Y (NPY) in cells in the dorsomedial hypothalamus and increases NPY expression in the arcuate nucleus. *Endocrinology*. 1998;139(4):1645-1652.
83. Elmquist JK, Bjorbaek C, Ahima RS, Flier JS, Saper CB. Distributions of leptin receptor mRNA isoforms in the rat brain. *J Comp Neurol*. 1998;395(4):535-547.
84. Kishi T, Aschkenasi CJ, Lee CE, Mountjoy KG, Saper CB, Elmquist JK. Expression of melanocortin 4 receptor mRNA in the central nervous system of the rat. *J Comp Neurol*. 2003;457(3):213-235.
85. Bouret SG, Draper SJ, Simerly RB. Formation of projection pathways from the arcuate nucleus of the hypothalamus to hypothalamic regions implicated in the neural control of feeding behavior in mice. *J Neurosci*. 2004;24(11):2797-2805.
86. Elmquist JK, Ahima RS, Elias CF, Flier JS, Saper CB. Leptin activates distinct projections from the dorsomedial and ventromedial hypothalamic nuclei. *Proc Natl Acad Sci U S A*. 1998;95(2):741-746.
87. Singru PS, Fekete C, Lechan RM. Neuroanatomical evidence for participation of the hypothalamic dorsomedial nucleus (DMN) in regulation of the hypothalamic paraventricular nucleus (PVN) by alpha-melanocyte stimulating hormone. *Brain Res*. 2005;1064(1-2):42-51.
88. Soga T, Kitahashi T, Clarke IJ, Parhar IS. Gonadotropin-inhibitory hormone promoter-driven enhanced green fluorescent protein expression decreases during aging in female rats. *Endocrinology*. 2014;155(5):1944-1955.
89. Leon S, Garcia-Galiano D, Ruiz-Pino F, Barroso A, Manfredi-Lozano M, Romero-Ruiz A, Roa J, Vazquez MJ, Gaytan F, Blomenrohr M, van Duin M, Pinilla L, Tena-Sempere M. Physiological Roles of Gonadotropin-Inhibitory Hormone Signaling in the Control of Mammalian Reproductive Axis: Studies in the NPFF1 Receptor Null Mouse. *Endocrinology*. 2014:en20141030.
90. Anderson GM, Relf HL, Rizwan MZ, Evans JJ. Central and peripheral effects of RFamide-related peptide-3 on luteinizing hormone and prolactin secretion in rats. *Endocrinology*. 2009;150(4):1834-1840.
91. Ubuka T, Morgan K, Pawson AJ, Osugi T, Chowdhury VS, Minakata H, Tsutsui K, Millar RP, Bentley GE. Identification of human GnIH homologs, RFRP-1 and RFRP-3, and the cognate receptor, GPR147 in the human hypothalamic pituitary axis. *PLoS One*. 2009;4(12):e8400.

92. Smith JT, Shahab M, Pereira A, Pau KY, Clarke IJ. Hypothalamic expression of KISS1 and gonadotropin inhibitory hormone genes during the menstrual cycle of a non-human primate. *Biol Reprod.* 2010;83(4):568-577.
93. Mouldous L, Barthas F, Zajac JM. Opposite control of body temperature by NPFF1 and NPFF2 receptors in mice. *Neuropeptides.* 2010;44(5):453-456.
94. Mouldous L, Mollereau C, Zajac JM. Opioid-modulating properties of the neuropeptide FF system. *Biofactors.* 2010;36(6):423-429.
95. Kaewwongse M, Takayanagi Y, Onaka T. Effects of RFamide-related peptide (RFRP)-1 and RFRP-3 on oxytocin release and anxiety-related behaviour in rats. *J Neuroendocrinol.* 2011;23(1):20-27.
96. Ubuka T, Inoue K, Fukuda Y, Mizuno T, Kazyoshi U, Kriegsfeld LJ, Tsutsui K. Identification, Expression, and Physiological Functions of Siberian Hamster Gonadotropin-Inhibitory Hormone. *Endocrinology.* 2012;153:In Press.
97. Mellon PL, Windle JJ, Goldsmith PC, Padula CA, Roberts JL, Weiner RI. Immortalization of hypothalamic GnRH neurons by genetically targeted tumorigenesis. *Neuron.* 1990;5(1):1-10.
98. Clarke IJ, Sari IP, Qi Y, Smith JT, Parkington HC, Ubuka T, Iqbal J, Li Q, Tilbrook A, Morgan K, Pawson AJ, Tsutsui K, Millar RP, Bentley GE. Potent action of RFamide-related peptide-3 on pituitary gonadotropes indicative of a hypophysiotropic role in the negative regulation of gonadotropin secretion. *Endocrinology.* 2008;149(11):5811-5821.
99. Anderson GM, Augustine RA, Rizwan MZ, Cornes PA. RFamide-related peptide-3 (RFRP-3) regulates LH secretion exclusively via a GnRH-dependent mechanism in the rat. *Neuroscience* 2011; 2011; Washington D.C.
100. Thomas P, Mellon PL, Turgeon J, Waring DW. The L beta T2 clonal gonadotrope: a model for single cell studies of endocrine cell secretion. *Endocrinology.* 1996;137(7):2979-2989.
101. Smith JT, Cunningham MJ, Rissman EF, Clifton DK, Steiner RA. Regulation of Kiss1 gene expression in the brain of the female mouse. *Endocrinology.* 2005;146(9):3686-3692.
102. Smith JT, Dungan HM, Stoll EA, Gottsch ML, Braun RE, Eacker SM, Clifton DK, Steiner RA. Differential regulation of Kiss-1 mRNA expression by sex steroids in the brain of the male mouse. *Endocrinology.* 2005;146(7):2976-2984.
103. Finn PD, Steiner RA, Clifton DK. Temporal patterns of gonadotropin-releasing hormone (GnRH), c-fos, and galanin gene expression in GnRH neurons relative to the luteinizing hormone surge in the rat. *J Neurosci.* 1998;18(2):713-719.
104. Kauffman AS, Gottsch ML, Roa J, Byquist AC, Crown A, Clifton DK, Hoffman GE, Steiner RA, Tena-Sempere M. Sexual differentiation of Kiss1 gene expression in the brain of the rat. *Endocrinology.* 2007;148(4):1774-1783.

105. Robertson JL, Clifton DK, de la Iglesia HO, Steiner RA, Kauffman AS. Circadian regulation of Kiss1 neurons: implications for timing the preovulatory gonadotropin-releasing hormone/luteinizing hormone surge. *Endocrinology*. 2009;150(8):3664-3671.
106. Semaan SJ, Murray EK, Poling MC, Dhamija S, Forger NG, Kauffman AS. BAX-dependent and BAX-independent regulation of Kiss1 neuron development in mice. *Endocrinology*. 2010;151(12):5807-5817.
107. Chowen JA, Clifton DK. Semiquantitative analysis of cellular somatostatin mRNA levels by in situ hybridization histochemistry. *Method Neurosci*. 1991;5:137-158.
108. Kauffman AS, Navarro VM, Kim J, Clifton D, Steiner RA. Sex Differences in the Regulation of Kiss1/NKB Neurons in Juvenile Mice: Implications for the Timing of Puberty. *Am J Physiol Endocrinol Metab*. 2009:00461.02009.
109. Kim J, Semaan SJ, Clifton DK, Steiner RA, Dhamija S, Kauffman AS. Regulation of Kiss1 expression by sex steroids in the amygdala of the rat and mouse. *Endocrinology*. 2011;152(5):2020-2030.
110. Gouarderes C, Puget A, Zajac JM. Detailed distribution of neuropeptide FF receptors (NPFF1 and NPFF2) in the rat, mouse, octodon, rabbit, guinea pig, and marmoset monkey brains: a comparative autoradiographic study. *Synapse*. 2004;51(4):249-269.
111. Gouarderes C, Kieffer BL, Zajac JM. Opposite alterations of NPFF1 and NPFF2 neuropeptide FF receptor density in the triple MOR/DOR/KOR-opioid receptor knockout mouse brains. *J Chem Neuroanat*. 2004;27(2):119-128.
112. Todaro GJ, Green H. Successive Transformations of an Established Cell Line by Polyoma Virus and Sv40. *Science*. 1965;147(3657):513-514.
113. Semaan SJ, Kauffman AS. Sexual differentiation and development of forebrain reproductive circuits. *Curr Opin Neurobiol*. 2010;20(4):424-431.
114. Ancel C, Bentsen AH, Sebert ME, Tena-Sempere M, Mikkelsen JD, Simonneaux V. Stimulatory effect of RFRP-3 on the gonadotrophic axis in the male Syrian hamster: the exception proves the rule. *Endocrinology*. 2012;153(3):1352-1363.
115. Sethi S, Tsutsui K, Chaturvedi CM. Temporal phase relation of circadian neural oscillations alters RFamide-related peptide-3 and testicular function in the mouse. *Neuroendocrinology*. 2009;91(2):189-199.
116. Sethi S, Tsutsui K, Chaturvedi CM. Age-dependent variation in the RFRP-3 neurons is inversely correlated with gonadal activity of mice. *Gen Comp Endocrinol*. 2010;168(3):326-332.
117. Iwasa T, Matsuzaki T, Murakami M, Kinouchi R, Osugi T, Gereltsetseg G, Yoshida S, Irahara M, Tsutsui K. Developmental changes in the mammalian gonadotropin-inhibitory hormone (GnIH) ortholog RFamide-related peptide (RFRP) and its cognate receptor GPR147 in the rat hypothalamus. *Int J Dev Neurosci*. 2011;In Press.

118. Smith JT, Coolen LM, Kriegsfeld LJ, Sari IP, Jaafarzadehshirazi MR, Maltby M, Bateman K, Goodman RL, Tilbrook AJ, Ubuka T, Bentley GE, Clarke IJ, Lehman MN. Variation in kisspeptin and RFamide-related peptide (RFRP) expression and terminal connections to gonadotropin-releasing hormone neurons in the brain: a novel medium for seasonal breeding in the sheep. *Endocrinology*. 2008;149(11):5770-5782.
119. Sugrue ML, Vella KR, Morales C, Lopez ME, Hollenberg AN. The thyrotropin-releasing hormone gene is regulated by thyroid hormone at the level of transcription in vivo. *Endocrinology*. 2010;151(2):793-801.
120. Simonin F, Schmitt M, Laulin JP, Laboureyras E, Jhamandas JH, MacTavish D, Matifas A, Mollereau C, Laurent P, Parmentier M, Kieffer BL, Bourguignon JJ, Simonnet G. RF9, a potent and selective neuropeptide FF receptor antagonist, prevents opioid-induced tolerance associated with hyperalgesia. *Proc Natl Acad Sci U S A*. 2006;103(2):466-471.
121. Gojska NM, Belsham DD. Glucocorticoid receptor-mediated regulation of Rfrp (GnIH) and Gpr147 (GnIH-R) synthesis in immortalized hypothalamic neurons. *Mol Cell Endocrinol*. 2014;384(1-2):23-31.
122. Son YL, Ubuka T, Narihiro M, Fukuda Y, Hasunuma I, Yamamoto K, Belsham DD, Tsutsui K. Molecular basis for the activation of gonadotropin-inhibitory hormone gene transcription by corticosterone. *Endocrinology*. 2014;155(5):1817-1826.
123. Sukhbaatar U, Kanasaki H, Mijiddorj T, Oride A, Miyazaki K. Expression of gonadotropin-inhibitory hormone receptors in mouse pituitary gonadotroph LbetaT2 cells and hypothalamic gonadotropin-releasing hormone-producing GT1-7 cells. *Endocr J*. 2014;61(1):25-34.
124. Poling MC, Kim J, Dhamija S, Kauffman AS. Development, Sex Steroid Regulation, and Phenotypic Characterization of RFamide-Related Peptide (Rfrp) Gene Expression and RFamide Receptors in the Mouse Hypothalamus. *Endocrinology*. 2012;153(4):1827-1840.
125. Mercer JG, Hoggard N, Williams LM, Lawrence CB, Hannah LT, Trayhurn P. Localization of leptin receptor mRNA and the long form splice variant (Ob-Rb) in mouse hypothalamus and adjacent brain regions by in situ hybridization. *FEBS Lett*. 1996;387(2-3):113-116.
126. Poling MC, Shieh MP, Munaganuru N, Luo E, Kauffman AS. Examination of the Influence of Leptin and Acute Metabolic Challenge on RFRP-3 Neurons of Mice in Development and Adulthood. *Neuroendocrinology*. 2014.
127. Navarro VM, Gottsch ML, Chavkin C, Okamura H, Clifton DK, Steiner RA. Regulation of GnRH secretion by kisspeptin/dynorphin/neurokinin B neurons in the arcuate nucleus of the mouse. *J Neurosci*. 2009;29(38):11859-11866.
128. Lee DK, Nguyen T, O'Neill GP, Cheng R, Liu Y, Howard AD, Coulombe N, Tan CP, Tang-Nguyen AT, George SR, O'Dowd BF. Discovery of a receptor related to the galanin receptors. *FEBS Lett*. 1999;446(1):103-107.

129. Allen Mouse Brain Atlas Resources [Internet]. Allen Institute for Brain Science; 2009. <http://www.brain-map.org>.
130. Rance NE, Bruce TR. Neurokinin B gene expression is increased in the arcuate nucleus of ovariectomized rats. *Neuroendocrinology*. 1994;60(4):337-345.
131. Navarro VM, Castellano JM, McConkey SM, Pineda R, Ruiz-Pino F, Pinilla L, Clifton DK, Tena-Sempere M, Steiner RA. Interactions between kisspeptin and neurokinin B in the control of GnRH secretion in the female rat. *Am J Physiol Endocrinol Metab*. 2011;300(1):E202-210.
132. Krajewski SJ, Burke MC, Anderson MJ, McMullen NT, Rance NE. Forebrain projections of arcuate neurokinin B neurons demonstrated by anterograde tract-tracing and monosodium glutamate lesions in the rat. *Neuroscience*. 2010;166(2):680-697.
133. Marksteiner J, Sperk G, Krause JE. Distribution of neurons expressing neurokinin B in the rat brain: immunohistochemistry and in situ hybridization. *J Comp Neurol*. 1992;317(4):341-356.
134. Smith JT, Young IR, Veldhuis JD, Clarke IJ. Gonadotropin-inhibitory hormone (GnIH) secretion into the ovine hypophyseal portal system. *Endocrinology*. 2012;153(7):3368-3375.
135. Khan AR, Kauffman AS. The Role of Kisspeptin and RFRP-3 Neurons in the Circadian-Timed Preovulatory Luteinizing Hormone Surge. *J Neuroendocrinol*. 2012;24(1):131-143.
136. Clarkson J, d'Anglemont de Tassigny X, Colledge WH, Caraty A, Herbison AE. Distribution of kisspeptin neurones in the adult female mouse brain. *J Neuroendocrinol*. 2009;21(8):673-682.
137. Molnar CS, Kallo I, Liposits Z, Hrabovszky E. Estradiol down-regulates RF-amide-related peptide (RFRP) expression in the mouse hypothalamus. *Endocrinology*. 2011;152(4):1684-1690.
138. Caligaris L, Astrada JJ, Taleisnik S. Release of luteinizing hormone induced by estrogen injection into ovariectomized rats. *Endocrinology*. 1971;88(4):810-815.
139. Legan SJ, Coon GA, Karsch FJ. Role of estrogen as initiator of daily LH surges in the ovariectomized rat. *Endocrinology*. 1975;96(1):50-56.
140. Dror T, Franks J, Kauffman AS. Analysis of multiple positive feedback paradigms demonstrates a complete absence of LH surges and GnRH activation in mice lacking kisspeptin signaling. *Biol Reprod*. 2013;88(6):146.
141. Christian CA, Mobley JL, Moenter SM. Diurnal and estradiol-dependent changes in gonadotropin-releasing hormone neuron firing activity. *Proc Natl Acad Sci U S A*. 2005;102(43):15682-15687.

142. Rizwan MZ, Bergin DB, Grattan DR, Anderson GM. Evidence that hypothalamic rfamide related peptide-3 (rfrp-3) neurons act as a conduit between prolactin and the stress axis. Poster presented at Neuroscience 2011; 2011; Washington D.C.
143. Poling MC, Quennell JH, Anderson GM, Kauffman AS. Kisspeptin neurones do not directly signal to RFRP-3 neurones but RFRP-3 may directly modulate a subset of hypothalamic kisspeptin cells in mice. *J Neuroendocrinol.* 2013;25(10):876-886.
144. Bailey M, Silver R. Sex differences in circadian timing systems: implications for disease. *Front Neuroendocrinol.* 2014;35(1):111-139.
145. Ingalls AM, Dickie MM, Snell GD. Obese, a new mutation in the house mouse. *J Hered.* 1950;41(12):317-318.
146. Zhang Y, Proenca R, Maffei M, Barone M, Leopold L, Friedman JM. Positional cloning of the mouse obese gene and its human homologue. *Nature.* 1994;372(6505):425-432.
147. Quennell JH, Mulligan AC, Tups A, Liu X, Phipps SJ, Kemp CJ, Herbison AE, Grattan DR, Anderson GM. Leptin indirectly regulates gonadotropin-releasing hormone neuronal function. *Endocrinology.* 2009;150(6):2805-2812.
148. Louis GW, Greenwald-Yarnell M, Phillips R, Coolen LM, Lehman MN, Myers MG, Jr. Molecular mapping of the neural pathways linking leptin to the neuroendocrine reproductive axis. *Endocrinology.* 2011;152(6):2302-2310.
149. Elmquist JK, Ahima RS, Maratos-Flier E, Flier JS, Saper CB. Leptin activates neurons in ventrobasal hypothalamus and brainstem. *Endocrinology.* 1997;138(2):839-842.
150. Oliveira VX, Jr., Fazio MA, Miranda MT, da Silva JM, Bittencourt JC, Elias CF, Miranda A. Leptin fragments induce Fos immunoreactivity in rat hypothalamus. *Regul Pept.* 2005;127(1-3):123-132.
151. Myers MG, Jr., Munzberg H, Leininger GM, Leshan RL. The geometry of leptin action in the brain: more complicated than a simple ARC. *Cell Metab.* 2009;9(2):117-123.
152. Johnson MA, Fraley GS. Rat RFRP-3 alters hypothalamic GHRH expression and growth hormone secretion but does not affect KiSS-1 gene expression or the onset of puberty in male rats. *Neuroendocrinology.* 2008;88(4):305-315.
153. Klingerman CM, Williams WP, 3rd, Simberlund J, Brahme N, Prasad A, Schneider JE, Kriegsfeld LJ. Food Restriction-Induced Changes in Gonadotropin-Inhibiting Hormone Cells are Associated with Changes in Sexual Motivation and Food Hoarding, but not Sexual Performance and Food Intake. *Front Endocrinol (Lausanne).* 2012;2:101.
154. Swerdloff RS, Batt RA, Bray GA. Reproductive hormonal function in the genetically obese (ob/ob) mouse. *Endocrinology.* 1976;98(6):1359-1364.
155. Bronson FH, Marsteller FA. Effect of short-term food deprivation on reproduction in female mice. *Biol Reprod.* 1985;33(3):660-667.

156. Swart I, Jahng JW, Overton JM, Haupt TA. Hypothalamic NPY, AGRP, and POMC mRNA responses to leptin and refeeding in mice. *Am J Physiol Regul Integr Comp Physiol.* 2002;283(5):R1020-1026.
157. Li XF, Edward J, Mitchell JC, Shao B, Bowes JE, Coen CW, Lightman SL, O'Byrne KT. Differential effects of repeated restraint stress on pulsatile luteinizing hormone secretion in female Fischer, Lewis and Wistar rats. *J Neuroendocrinol.* 2004;16(7):620-627.
158. Gore AC, Attardi B, DeFranco DB. Glucocorticoid repression of the reproductive axis: effects on GnRH and gonadotropin subunit mRNA levels. *Mol Cell Endocrinol.* 2006;256(1-2):40-48.
159. Briski KP, Vogel KL, McIntyre AR. The antiglucocorticoid, RU486, attenuates stress-induced decreases in plasma-luteinizing hormone concentrations in male rats. *Neuroendocrinology.* 1995;61(6):638-645.
160. Cintra A, Solfrini V, Bunnemann B, Okret S, Bortolotti F, Gustafsson JA, Fuxe K. Prenatal development of glucocorticoid receptor gene expression and immunoreactivity in the rat brain and pituitary gland: a combined in situ hybridization and immunocytochemical analysis. *Neuroendocrinology.* 1993;57(6):1133-1147.
161. Rivier C, Rivier J, Vale W. Stress-induced inhibition of reproductive functions: role of endogenous corticotropin-releasing factor. *Science.* 1986;231(4738):607-609.
162. Breen KM, Thackray VG, Hsu T, Mak-McCully RA, Coss D, Mellon PL. Stress Levels of Glucocorticoids Inhibit LHBeta-Subunit Gene Expression in Gonadotrope Cells. *Mol Endocrinol.* 2012.
163. Kirby ED, Geraghty AC, Ubuka T, Bentley GE, Kaufer D. Stress increases putative gonadotropin inhibitory hormone and decreases luteinizing hormone in male rats. *Proc Natl Acad Sci U S A.* 2009;106(27):11324-11329.
164. Lechan RM, Jackson IM. Immunohistochemical localization of thyrotropin-releasing hormone in the rat hypothalamus and pituitary. *Endocrinology.* 1982;111(1):55-65.
165. Bergendahl M, Perheentupa A, Huhtaniemi I. Effect of short-term starvation on reproductive hormone gene expression, secretion and receptor levels in male rats. *J Endocrinol.* 1989;121(3):409-417.
166. Rizwan MZ, Harbid AA, Inglis MA, Quennell JH, Anderson GM. Evidence That Hypothalamic RFamide Related Peptide-3 Neurones are not Leptin-Responsive in Mice and Rats. *J Neuroendocrinol.* 2014;26(4):247-257.
167. Legagneux K, Bernard-Franchi G, Poncet F, La Roche A, Colard C, Fellmann D, Pralong F, Risold PY. Distribution and genesis of the RFRP-producing neurons in the rat brain: comparison with melanin-concentrating hormone- and hypocretin-containing neurons. *Neuropeptides.* 2009;43(1):13-19.

168. White FA, Keller-Peck CR, Knudson CM, Korsmeyer SJ, Snider WD. Widespread elimination of naturally occurring neuronal death in Bax-deficient mice. *J Neurosci*. 1998;18(4):1428-1439.
169. Ahima RS, Prabakaran D, Flier JS. Postnatal leptin surge and regulation of circadian rhythm of leptin by feeding. Implications for energy homeostasis and neuroendocrine function. *J Clin Invest*. 1998;101(5):1020-1027.
170. Bouret SG, Draper SJ, Simerly RB. Trophic action of leptin on hypothalamic neurons that regulate feeding. *Science*. 2004;304(5667):108-110.
171. Semaan SJ, Kauffman AS. Daily successive changes in reproductive gene expression and neuronal activation in the brains of pubertal female mice. *Mol Cell Endocrinol*. 2015;401:84-97.
172. Bouret SG. Organizational actions of metabolic hormones. *Front Neuroendocrinol*. 2013;34(1):18-26.
173. Hayashida T, Nakahara K, Mondal MS, Date Y, Nakazato M, Kojima M, Kangawa K, Murakami N. Ghrelin in neonatal rats: distribution in stomach and its possible role. *J Endocrinol*. 2002;173(2):239-245.
174. Steculorum SM, Bouret SG. Maternal diabetes compromises the organization of hypothalamic feeding circuits and impairs leptin sensitivity in offspring. *Endocrinology*. 2011;152(11):4171-4179.
175. Mannan MA, O'Shaughnessy PJ. Ovarian steroid metabolism during post-natal development in the normal mouse and in the adult hypogonadal (hpg) mouse. *J Reprod Fertil*. 1988;82(2):727-734.
176. Simerly RB. Wired for reproduction: organization and development of sexually dimorphic circuits in the mammalian forebrain. *Annu Rev Neurosci*. 2002;25:507-536.
177. Scott HM, Mason JI, Sharpe RM. Steroidogenesis in the fetal testis and its susceptibility to disruption by exogenous compounds. *Endocr Rev*. 2009;30(7):883-925.
178. Poling MC, Kauffman AS. Organizational and activational effects of sex steroids on kisspeptin neuron development. *Front Neuroendocrinol*. 2013;34(1):3-17.
179. Maletinska L, Ticha A, Nagelova V, Spolcova A, Blechova M, Elbert T, Zelezna B. Neuropeptide FF analog RF9 is not an antagonist of NPF receptor and decreases food intake in mice after its central and peripheral administration. *Brain Res*. 2013;1498:33-40.